Non-Separability Indicators for Quantum Optical Fields Involving Intensity Correlation Measurements

A thesis presented for the degree of Doctor of Philosophy

Bianka Wołoncewicz

Supervisor: **Prof. Marek Żukowski**

Faculty of Mathematics, Physics and Informatics

University of Gdańsk

Poland

Acknowledgements

First, I would like to thank my supervisor Marek Żukowski for all his support and the wisdom that he shared with me during my PhD studies. Marek, you are a great supervisor! Also, big thanks to all my co-authors and members of Multiphoton Quantum Optics group. Especially, I thank: Tamoghna Das, Marcin Markiewicz and Konrad Schlichtholtz. Thanks to Mahasweta Pandit, Palash Pandya, Ricard Ravell Rodríguez, Marcin Wieśniak and Marek Winczewski for mind-opening conversations. Discussing, studying, writing and solving all kind of problems together was a beautiful experience. I thank Joanna Dawidowska whose presence and friendly help allowed me to go smoothly through my bachelors studies and consider further scientific development. I thank Adrian Kołodziejski for sharing his scientific knowledge and practical information concerning PhD survival. Thanks to Tomasz Młynik and Dorota Wejer for protips, discussions and all the time spent together. I thank Omer, the love of my life, who lifts me up when I fall down. Finally, I thank my Mum, who made a great effort to provide me with good educational opportunities that was extremely challenging to obtain in post-communist Poland for a visually impaired kid.

Streszczenie

Wraz z rozwojem kuantowych technologii, technik eksperymentalnych i postępem technologicznym w ogóle splątanie kwantowego światła jest (i najprawdopodobniej będzie również w przyszłości) bardzo aktualnym zagadnieniem badawczym. Taka jest również tematyka niniejszej rozprawy doktorskiej, w skład której wchodzą cztery artykuły naukowe (wymienione w bibliografii PhD Series) opatrzone wstępem. Wstęp zawiera zwięzły opis badań przeprowadzonych w czasie studiów doktoranckich, których wyniki zostały umieszczone w wyżej wspomnianych publikacjach. Przeprowadzone badania dotyczą nieklasycznych korelacji kwantowych stanów optycznych o nieustalonej ilości cząstek analizowanych za pomocą pomiarów intensywności w kontekście polaryzacji i pomiaru homodynowego. Publikacje są ze sobą powiązane.

Artykuł "General mapping of multiqudit entanglement conditions to nonseparability indicators for quantum-optical fields" stanowi podstawę cyklu. Praca opisuje ogólną metodę tworzenia pewnej określonej klasy kwantowo-optycznych indykatorów splątania, które wykorzystują korelacje oparte na intensywnościach. Tego typu metody wykrywania splątania są obecnie eksperymentalnie wykonalne. Nasza metoda jest oparta na istnieniu odwzorowania pomiędzy wskaźnikami splątania i nierównościami Bella dla quditów, a analogicznymi indykatorami nieklasyczności dla pól optycznych. W sensie operacyjnym polega to na zamianie prawdopodobieństw koincydencyjnej detekcji cząstki w danym końcowym kanale przez stosunek lokalnie rejestrowanych intensywności pola. Matematycznie rzecz ujmując odwzorowanie polega na zastąpieniu wartości średnich obserwabli Pauliego, lub ich korelacji, średnimi standardowych lub znormalizowanych obserwabli Stoksa, lub ich korelacji. W pracy zaznaczone jest, że w przypadku nierówności Bella nasza metoda nadaje się jedynie dla obserwabli o spektrum pomiędzy $[-1, 1]$. Strategia konstruowania nierówności Bella dla standardowych operatorów Stokesa musi być diametralnie inna i nie jest tu dyskutowana. Tak otrzymane identyfikatory nieklasyczności są testowane dla czteromodowej jasnej ścieśnionej próżni (BSV) oraz jej generalizacji na stany o większej ilości modów optycznych.

Artykuł "Simplified quantum optical Stokes observables and Bell's theorem" również przedstawia nowe narzędzia do wykrywania nieklasycznych korelacji pól optycznych. Zaproponowaliśmy tam nowe obserwable - uproszczone operatory Stokesa - do przeprowadzania eksperymentów Bellowskich. Koncepcja nowych obserwabli jest bardzo prosta i polega na na porównaniu, w którym z lokalnych detektorów zarejestrowano większą intensitywność padającego światła. W zależności od tego takiemu pomiarowi nadawane są wartości ± 1. Gdy oba detektory zarejestrują taką samą częstotliwość przypisywane jest 0. Okazuje się że używając naszych obserwabli można uzyskać lepsze łamanie nierówności Bella niż w przypadku znormalizowanych operatorów Stokesa dla jasnej ścieśnionej próżni oraz stanów otrzymanych w wyniku parametrycznej konwersji trzeciego rzędu tzw "makroskopowego stanu GHZ". Również warto zwrócić uwagę, że zaproponowane obserwable są realizowalne eksperymentalnie, a ich znaczenie fizyczne jest intuicyjne. Niestety nasze obserwable nie nadają się do konstrukcji świadków splątania.

Prace "Can single photon excitation of two spatially separated modes lead to a violation of Bell inequality via weak-field homodyne measurements?" i "Wave–particle complementarity: detecting violation of local realism with photon-number resolving weak-field homodyne measurements" dotyczą analizy i weryfikacji kontrowersyjnych stwierdzeń dotyczących nieklasyczności pojedynczego fotonu nazywaną w literaturze "niekolalnością pojedynczego fotonu" wykrywalną przy użyciu pomiaru homodynowego dla słabych stanów koherentynych lokalnych oscylatorów. Zostały przeanalizowane dwa emblematyczne eksperymenty myślowe odnośnie tego zagadnienia: eksperyment Tana, Wallsa i Colletta (TWC) oraz tzw. paradoks Har-

dy'ego. Obecnie, w czasach gdy jest możliwa eksperymentalna realizacja tych eksperymentów, wyjaśnienie kontrowersji dotyczących łamania nierówności Bella przez pojedynczy foton nabiera znaczenia nie tylko w sensie fundamentalnym, ale też w odniesieniu do rozwoju kwantowych technologii. Eksperyment Hardy'ego jest niepodważalnie poprawny, choć nieoptymalny. Natomiast w przypadku TWC teza okazała się być błędna. W ostatnim z przytoczonych artykułów został zawarty opis modelu ukrytych zmiennych dla doświadczenia TWC, co jednoznacznie zamyka możliwość użycia schematu TWC do bezwarunkowo bezpieczniej kryptografii kwantowej. Ponadto zostały przedstawione eksperymenty, będące zmodyfikowanymi wersjami eksperymentów TWC i Hardy'iego. Okazuje się, że łamanie nierówności Bella przez pojedynczy foton występuje jedynie przy bardzo specyficznych ustawieniach płytek światłodzielących i zmiennych amplitud stanów koherentnych użytych do pomiaru homodynowego.

Wstęp do publikacji jest zorganizowany w następujący sposób. Pierwsze cztery rozdziały wstępu zawierają ogólne uwagi na temat jasnej ścieśnionej próżni i obserwabli używanych do opisu pola optycznego. Rozdziały 5-7 omawiają ogólny zarys prowadzonych badań i wnioski zawarte w wyżej wspomnianych publikacjach. W sekcji 5 została przedstawiona metoda otrzymywania indykatorów nieklasyczności dla pola optycznego. Rozdział 6 omawia uproszczone operatory Stokesa. W rozdziale 7 jest opisana analiza eksperymentów (TWC) oraz Hardy'ego. Również zostały przytoczone zaproponowane przez nas eksperymenty, pozwalające na zaobserwowanie *prawdziwej* nieklasyczności Bella pojedynczego fotonu.

Ostatnia część wstępu jest krótkim opisem możliwej kontynuacji przedstawionych badań.

Abstract

With emerging quantum technologies and the progress in detection schemes it is nowadays of a broad scientific interest (and most probably it will be so in the future) to investigate the phenomena of entanglement of quantum light. This PhD dissertation is a contribution to this endeavour. It comprises of four papers preceded by an introduction. The papers are listed in PhD Series and contain results to which I contributed during my PhD studies. The introduction gives a brief description of new concepts proposed in aforementioned papers. The subject of the research is focused on analyzing nonclassical correlations of quantum optical states using the intensity measurements in context of polarisation and homodyne measurements. The papers are related with each other.

The first one "General mapping of multiqudit entanglement conditions to nonseparability indicators for quantum-optical fields" opens the series. The paper describes a general method that allows to construct a certain class of quantum-optical nonseparability indicators that use intensity-based correlations. The method is based on mappings between entanglement witnesses and Bell inequalities for qudits and analogous nonclassicality indicators for optical fields. The main idea of this concept is to replace the probabilities of the coincidence detection of a particle in a given detection channel by the ratio of intensity of the optical field registered in analogous channel divided by total local intensity. Mathematically speaking, the mapping replaces average values of Pauli observables, or of their correlations, by averages of standard and normalized Stokes observables, or of their correlations. In such a way we obtain methods of quantum-optical entanglement detection that nowadays are experimentally feasible. Also, it is noted in the paper that in the case of Bell's inequality our method is suitable only for normalized observables. The strategy for constructing Bell's inequalities for standard Stokes operators must be radically different, and is not discussed in the dissertation. The nonclassicity identifiers obtained in this way are tested for four-mode bright squeezed vacuum (BSV) and its generalization to states with a greater number of optical modes. Results presented in this paper make a significant contribution in the investigation of problems discussed in the three following papers.

The second paper "Simplified quantum optical Stokes observables and Bell's theorem" also presents new tools for detecting nonclassical correlations of optical fields. We proposed new observables – simplified Stokes operators – for Bell experiments. The idea of new observables is very simple and consists of on a comparison in which local detector related e.g. with the measurement of horizontal and vertical polarisation a higher intensity of light was recorded. Depending on the result, the value of ± 1 is assigned to such a measurement. When both local detectors register the same intensity, 0 is assigned. The new observables turn out to perform better than the normalized Stokes operators in the case of BSV and for the third-order radiation from parametric source i.e. so called "macroscopic GHZ state". It is worth noting that the proposed observables are experimentally realizable and their physical meaning is intuitive. Unfortunately, our observables are not useful for entanglement witnesses,

Papers "Can single photon excitation of two spatially separated modes lead to a violation of Bell inequality via weak-field homodyne measurements?" and "Wave–particle complementarity: detecting violation of local realism with photon-number resolving weak-field homodyne measurements" concern the analysis and verification of statements regarding the nonclassicality of a single photon, aka "single-photon non-locality", using weak field homodyne measurements. We analysed two emblematic thought experiments: one proposed by Tan Walls and Collett (TWC) and the so called Hardy paradox. The general

mapping from the first paper was used to check the validity of TWC and Hardy's claims. Now, when such experiments are not only gedanken anymore and turned real, it is relevant to clarify the controversy concerning the violation of Bell's inequalities by a single photon Solving this problem once for all has, apart from fundamental, also practical consequences. Single photon nonclassical properties could be used in device-independent quantum protocols. Hardy's experiment is indisputably correct, while in the case of TWC the hypothesis turned out to be erroneous. We present a model of local hidden variables for the TWC experiment, which means a no-go statement for unconditionally secure quantum cryptography with the setup and closes the problem of TWC experiment once for all. Still TWC correlations can be used to derive entanglement witnesses, that is done using the general mapping from the first paper. Apart from that, we present schemes enabling witnessing of non-locality of single photon that are modified versions of the TWC and Hardy experiments. It turns out that the violation of the Bell inequality by a single photon occurs only with very specific settings of tunable beamsplitters and also tunable amplitudes of the coherent states of the local oscillators.

The introduction to the papers is organized as follows. First four sections contain general remarks about observables for optical fields and bright squeezed vacuum. Sections 5-7 summarise new results from aforementioned publications. In section 5 is about the general mapping betwwen non-separability indicators for qudits and optical fields. Section 6 discusses simplified Stokes observables. Section 7 analyzes gedankenexperiments of Tan, Wall and Colett (TWC) and Hardy. Last section contains short description of possible continuation of the research line presented in this thesis.

1 Entanglement in physics

Quantum mechanics revolutionized our understanding of the universe and has led to the development of numerous technologies, including transistors, lasers, and superconductors. The term itself was introduced in 1924 by Born, who later in his autobiographic notes wrote "we became to be more and more convinced that a radical change of the foundations of physics was necessary i.e. a new kind of mechanics [...] quantum mechanics". A new approach to fundamental phenomena was proposed by some of the greatest minds of XX-th century. In 1900, Planck proposed the hypothesis of discrete energy emissions of an radiating system. Five years later Einstein introduced "the light quanta" to describe the photoelectric effect. In 1913 Bohr postulated his model of atom. Later, in 1925 Heisenberg formulated basic ideas of matrix quantum mechanics and Schrodinger postulated the famous evolution equation. In 1927 Heisenberg introduced the uncertainty relation. The mathematical formalism of quantum mechanics was coined in terms of matrix mechanics by Heisenberg, Born, and Jordan and wave mechanics by Schrodinger. These two approaches turned out to be equivalent "pictures" of the same theory.

During this cascade of new theories the bold concepts of quantum mechanics and its different interpretations were subjects of controversy e.g. the famous Einstein-Bohr debate. In 1935 Einstein, Podolsky, and Rosen (EPR) presented a thought experiment that questioned the completeness of quantum mechanics [Ref1]. The so called EPR paradox is nowadays mainly known in the scenario proposed by Bohm in which a particle of spin 0 decays into two spin 1/2 particles that are sent faraway in opposite directions [Ref2]. As expected EPR hypothesis inspired comments, among others the famous Bohr's reply [Ref3] and Schrodinger's paper [Ref4] where for the first time the term "entanglement" was introduced to describe a very particular type of EPR (nonclassical) correlations. Unfortunately, at that time EPR experiment was very far from being feasible and the debate about the completeness of quantum mechanics remained inconclusive. Still, most physicists accepted Bohr view.

The nature of quantumness was investigated again by Bell, who in 1964 showed that quantum phenomena cannot fit into a local realistic description [Ref5]. Since then, the study of nonclassical correlations has slowly entered the core of scientific research [Ref6, Ref7, Ref8, Ref9, Ref10, Ref11].

In 1990's the concept of a qubit – i.e. quantum bit – heralded the birth of quantum information theory. A qubit, mathematically associated with a two-dimensional Hilbert space, can be physically implemented e.g. as a spin 1/2 particle, or photon polarisation. Such systems can be characterized using dichotomic observables. Such measurements provide binary results, useful to quantum information, quantum algorithms, and quantum key distribution [Ref12]. Entanglement started to be considered useful for quantum information theory. After all, a system composed of two qubits can exhibit nonclassical correlations.

Nowadays the study of non-separability of physical systems have a significant impact not only on our understanding of Nature but also on the development of modern technology. It underpins quantum information, quantum communication, and quantum computing [Ref13, Ref14, Ref15, Ref16].

Facing these facts it is not surprising that entanglement of qubits and their generalisations to higher dimensional objects, have been widely studied. There is a vast literature about classifying nonclassicality in finite dimensional spaces. Let us concentrate on entanglement witnesses. Already a multitude of entanglement witnesses have been proposed [Ref17, Ref18]. Nevertheless these indicators are only sufficient conditions for entanglement and thus they are specially tailored for only for given classes of states. Also, most of finite dimensional entanglement witnesses are efficient only for states of defined number of

particles.

When the study of entanglement started to be analyzed experimentally within quantum optics [Ref19, Ref20] new types of entanglement indicators needed to be considered see e.g. [Ref21]. Nowadays, quantum optical entanglement finds multiple applications in implementing quantum information processing protocols within the branches of quantum computing [Ref22], quantum metrology [Ref23] and quantum cryptography in the discrete and continuous variables regime [Ref24]. However, it is worth noticing that in quantum optics, as a second quantized theory, one can consider states of undefined number of photons. Thus, the description of entanglement of quantum optical systems compared to entanglement of qudits poses additional challenges. For photons – bosons – the specifics of Bose-Einstein statistics must be taken into account, as well as the fact that many measurements are based on observations of intensities. We will focus on detection of entanglement of photonic states by examining the correlations of intensities with respect to polarization.

The attribute of polarization allows considering quantum optical phenomena in the discrete variable regime. Photon's polarization is an example of a qubit degree of freedom. Also, the conceptual simplicity of polarisation is worth noticing. It is intuitive and can be experimentally realized and analysed using standard polarising analyzers. Nevertheless, as we shall see the detection of such entanglement of optical fields often requires photon number resolving detectors. Fortunately, recent advancements of experimental techniques make it possible, see the pioneering experiments [Ref25, Ref26].

2 Observables for quantum optical fields involivng intensity measurements

2.1 Standard Stokes operators

To describe the polarisation of a quantum optical field one uses Stokes observables. They are quantum-optical analogues of the parameters introduced in XIX-th century by George Stokes for the classical description of a polarisation of light. They are represented by self-adjoint operators denoted here as:

$$\hat{\Theta}_i = \hat{I}_i - \hat{I}_{i_\perp} \tag{1}$$

where $i = 1, 2, 3$. The operator $\hat{I}_{i_{(\perp)}}$ stands for the light intensity related with an i-th polarisation basis $\{i, i_\perp\}$. Indices $i = 1, 2, 3$ denote three complementary, mutually unbiased bases of a given polarisation triad. Here the following identifications will be used:

- $i = 3$ for horizontal/vertical basis $\{H, V\}$,
- $i = 2$ for diagonal/anti-diagonal basis, $\{D, A\}$,
- $i = 1$ for right-handed/left-handed circular polarisation basis, $\{R, L\}$.

Additionally, $\hat{\Theta}_0$ describes the total intensity of the light. We do not make any assumptions about the definition of the intensity of light. If, for simplicity we assume that the intensity of light is proportional to the photon number, we have $\hat{I}_i = \hat{n}_i = \hat{a}_i^\dagger \hat{a}_i$ and Stokes operators take form $\hat{\Theta}_i = \hat{a}_i^\dagger \hat{a}_i - \hat{a}_{i_\perp}^\dagger \hat{a}_{i_\perp}$. The zeroth operator is simply total photon number operator $\hat{I} = \hat{a}_i^\dagger \hat{a}_i + \hat{a}_{i_\perp}^\dagger \hat{a}_{i_\perp} = \hat{N}$ [Ref27].

The degree of polarisation is specified by the parameter $p = \left(\frac{\sum_i \langle \hat{\Theta}_i \rangle^2}{\langle \Theta_0 \rangle^2} \right)^{1/2}$, which takes values $0 \leqslant p \leqslant 1$. Then, it is tempting to introduce the following correlation function: $E(a,b) = \frac{\langle \hat{\Theta}_a^A \hat{\Theta}_b^B \rangle}{\langle \hat{\Theta}_0^A \hat{\Theta}_0^B \rangle}$ where a and b denote local settings chosen by Alice (A) and Bob (B) to test local realism. This approach was used as an attempt to derive Bell inequalities for fields in [Ref28] and then in e.g. [Ref29]. From now on we are going to call these type of inequalities CHSH-like inequalities because they are not "real" Bell-type inequalities. Note that the CHSH-like inequalities hold if one imposes an additional assumption of *non-enhancement of intensity* on the local hidden variable models tested in a Bell experiment. The form of correlation function $E(a,b)$ implies that the total intensity of the light variable within this local-realistic approach does not change with the change of local settings. Thus, the violation of CHSH-like inequality might imply either the violation of local realism or the violation of the *non-enhancement* assumption [Ref30]. This problem will be discussed in further sections.

As below we shall discuss a different approach to quantum optical Stokes parameters, from now on we call the operators defined above "standard" Stokes observables.

2.2 Observables based on intensity rates

In order to provide a correct formulation of Bell inequalities based on Stokes parameters for optical fields one can introduce e.g. new observables based on intensity rates observed in each run of the experiment [Ref30, Ref31].

In case of two mode optical field they can be put as follows:

$$\hat{R}(s) = \hat{\Pi} \frac{\hat{I}(s)}{\hat{I}(s) + \hat{I}(s_\perp)} \hat{\Pi}, \tag{2}$$

where $\hat{I}(s)$ and $\hat{I}(s_\perp)$ are the intensities of a light beam in mode s and respectively in an orthogonal mode $s_\perp$. The operator $\hat{\Pi} = \mathbf{1} - |\Omega\rangle\langle\Omega|$ is a projector that neutralizes the vacuum component $|\Omega\rangle$ in a given beam. The pair $\{s, s_\perp\}$ refers to any two orthogonal modes, e.g. two exclusive detectors in homodyne detection, or a measurement of two orthogonal directions of a polarisations. The normalized Stokes operators of [Ref31] read

$$\hat{S}_i^A = \hat{R}(i) - \hat{R}(i_\perp) = \hat{\Pi} \frac{\hat{n}_i - \hat{n}_{i_\perp}}{\hat{n}_i + \hat{n}_{i_\perp}} \hat{\Pi}. \tag{3}$$

One defines the zeroth normalized Stokes operator $\hat{S}_0 = \hat{\Pi}$. It gives the probability of a non-vacuum event.

Note that the above definition is fully analogous to the one for standard Stokes operators (1) with the only difference that intensities are replaced with intensity rates (2). The spectra of normalized Stokes operators are all rational numbers between $[-1, 1]$ which makes them suitable for Bell inequalities [Ref30]. Several examples show that normalized Stokes operators enable better entanglement detection see e.g. [Ref31], [Other1], although their advantage over the traditional approach depends on the given states. Sometimes standard Stokes observables are better [Other2].

3 Bright squeezed vacuum

An emblematic example of non-classical light of undefined photon number is 2×2 mode bright squeezed vacuum (BSV) discovered as a "by product" in parametric down conversion (PDC) of type II [Ref32]. It is a non-linear process that underpins most of experiments aiming to demonstrate entanglement of quantum optical states [Ref33]. It is a robust source of single photons [Ref34], entangled photon pairs [Ref35], three, four-photon entangled states [Ref36, Ref37, Ref38, Ref39] and so called "bright" entangled states of light [Ref40, Ref41, Ref42].

Bright squeezed vacuum that we consider here is emitted into two distinct optical beams. Each beam carries polarisation optical modes (as our working polarisation basis we choose: horizontal-H and vertical-V). As an expansion in Fock states it reads:

$$\left|\Psi^{-}\right\rangle = \frac{1}{\cosh^2 \Gamma} \sum_{n=0}^{\infty} \mathrm{tgh}^n \Gamma \sum_{r=0}^{n} (-1)^m \left|(n-r)_{A_H}, r_{A_V}, r_{B_H}, (n-r)_{B_V}\right\rangle, \tag{4}$$

where Γ is the amplification gain. Subscripts A and B stand for two beams that reach two observers A and B.

Bright squeezed vacuum is sometimes called " macroscopic singlet" because of its perfect EPR-like anticorrelations of Stokes observables. Also it has perfect correlations in number of photons between the beams [Ref43].[Ref44]. Similarly to EPR singlet state BSV is rotationally invariant with respect to the same rotations of the observers' polarisation analyzers. Its form remains unchanged in any other polarization basis $\{i, i_\perp\}$.

4 The research presented of this thesis

Given the development of quantum technologies and the continuous progress of experimental techniques, exploring nonclassical properties of quantum light becomes nowadays of broad scientific interest. The research undertaken during my PhD studies was focused around nonclassical correlations. It contributed to the following publications [PhD1, PhD2, PhD3, PhD4], see the list PhD Series. In order to distinguish between nonclassical correlations revealed by entanglement witnesses and the ones revealed in tests of Bell inequalities, I will call the correlations revealed with entanglement witnesses – entanglement and the second ones – Bell-nonclassicality. Still, the considered non-classical correlations occur due to the entanglement of quantum optical states. Entanglement and Bell nonclassicality have the same root, e.g. see [Ref45].

In the aforementioned four papers nonclassical aspects of optical fields are described in context of intensity correlation measurements. These papers are strongly related to each other. In [PhD1] we present a general approach enabling to construct a class of entanglement indicators for optical fields. The method is based on the mapping from entanglement conditions and Bell inequalities for qudits to analogous nonseparability indicators for optical fields. Our method is effortless: take an entanglement condition for qubits and replace the averages of Pauli operators or of their correlations with the respective averages of standard and normalized Stokes operators or of their correlations. Also the generalization of the mapping is given in [PhD1]. Such entanglement conditions are experimentally realisable and thus find applications

in quantum technologies. However, in case of Bell inequalities only normalized Stokes operators fit to the mapping. Next, in [PhD2, PhD3, PhD4] it is shown how the mapping form [PhD1] can be useful to detect entanglement of quantum optical states and also to clear up some controversies related to nonclassicality of single photon detected in weak field homodyne regime.

In [PhD2] another approach to detect entanglement of optical fields is proposed: we introduced new simplified sign Stokes observables for better tests of nonclassicality. This observables assign a value of ± 1 accordingly to the fact which of two complementary local detector registered more intensity of light. We assign 0 when the intensity registered by both detectors are the same. The observables are experimentally feasible and have intuitive physical meaning. We showed the cases when they are more efficient compared to normalized Stokes operators. However, sign Stokes operators are not useful for entanglement witnesses.

The papers [PhD3] and [PhD4] investigate the nonclassical behavior of single photons using weak-field homodyne measurements. They analyze the TWC and Hardy thought experiments. We verified that Hardy's experiment is correct although it is optimal. However, TWC's thesis is erroneous. A hidden variables model for TWC correlation is presented, which rules out their possible use in secure quantum cryptography. Still, TWC correlations can be used to derive an entanglement witness. We construct an entanglement condition using the general mapping from [PhD1]. Also, we show that after modifying TWC setup the violation of Bell inequality can occur for single photon when specific settings of beamsplitters and amplitudes of coherent state are used. This kind of research has implications for device-independent quantum protocols.

The further sections of this introduction are organized as follows. Sections 5-7 give the description of new results presented in [PhD1, PhD2, PhD3, PhD4] The secton 5 describes results from [PhD1]. Section 6 is dedicated to simplified Stokes operators introduced [PhD2] for better tests of Bell inequalities. Section 7 is dedicated to concepts given in [PhD3, PhD4]. Moreover in sections 5 and 7 the examples of the straightforward application of the mapping from [PhD1] are given.

5 General mapping from qu*d*it entanglement conditions to non-separability indicators for optical fields

This section introduces the concepts covered in [PhD1] where the new method to construct entanglement witnesses and Bell inequalities for optical fields is given. The method is based on the mapping that implies already derived non-separability indicators for qu*d*its and transform them to respective non-separability indicators for optical fields. The revers mapping exists as well. Such a mapping comes in handy, especially that there is plenty of entanglement indicators for qudits, the mapping is straightforward and precise intensity measurement is nowadays feasible. For quantum-optical entanglement witnesses standard or normalized Stokes operators can be used. This is not the case of Bell inequalities for which standard Stokes operators do not have properties required for the mapping, as their spectra are not between 1 and -1. Still, by using the mapping and normalized Stokes, it is possible to obtain proper Bell inequalities for fields without the *non-enhancement* assumption mentioned in the previous sections and discussed further on (section 6 and 7.1) .

Our mapping applies between the averages of Pauli and Stokes operators. In the following lines the general intuition will be given.

Any separable state of two qubits is a convex combination of product i.e. factorizable states:

$$\rho_{sep}^{AB} = \sum_{\lambda} p_\lambda \rho_\lambda^A \otimes \rho_\lambda^B, \tag{5}$$

where λ is any index (continuous or discrete), ρ_λ^A and ρ_λ^B can be pure, $p_\lambda \geqslant 0$ and $\sum_\lambda p_\lambda = 1$.

An arbitrary entanglement witness for two qubits, as a quantum observable operator, can be expanded in the following way:

$$\hat{w} = \sum_{\mu,\nu=0}^{3} w_{\mu\nu} \hat{\sigma}_\mu^A \hat{\sigma}_\nu^B, \tag{6}$$

where $w_{\mu\nu}$ are real coefficients and witness $\hat{w}$ is defined as an operator, which for every separable state ρ_{sep}^{AB} fulfills the relation: $\langle \hat{w} \rangle_{\rho_{sep}^{AB}} \geqslant 0$ [Ref46].

In the case of quantum four mode optical fields, with two modes propagating to observer A and the other two to B, the general bipartite separable state of an optical field takes the form:

$$\rho_{sep}^{AB} = \sum_{\lambda} p_\lambda f_\lambda^\dagger(\hat{a}, \hat{a}_\perp) g_\lambda^\dagger(\hat{b}, \hat{b}_\perp) \left|\Omega\right\rangle\!\left\langle\Omega\right| f_\lambda(\hat{a}, \hat{a}_\perp) g_\lambda(\hat{b}, \hat{b}_\perp), \tag{7}$$

where $f_\lambda(\hat{a}, \hat{a}_\perp)$ and $g_\lambda(\hat{b}, \hat{b}_\perp)$ are polynomial functions of annihilation operators acting on modes related with parties A and B respectively. The index λ plays the same role as earlier. To put it in a more intuitive way e.g.: $f_\lambda(\hat{a}, \hat{a}_\perp) \left|\Omega\right\rangle$ is any pure state of modes a and $a_\perp$, and we have analogous states for B.

Entanglement indicators (witnesses) for intensity correlations will be denoted by $\hat{\mathcal{W}}_{\hat{\Theta}}$ and $\hat{\mathcal{W}}_{\hat{S}}$ depending on which type of Stokes observables we use. Note that as we assumed here two modes per observer, essentially the situation can be thought of a representing the problem of detecting polarization entanglement of the beams propagating to the two observers. Note further, that all that we show here can be straightforwardly generalized to many parties, and more than two modes per beam, see the generalizations in [PhD1].

The mapping is the following substitution: $\hat{\sigma}_\mu^A \hat{\sigma}_\nu^B \to \hat{\Theta}_\mu^A \hat{\Theta}_\nu^B$ for standard Stokes operators and $\hat{\sigma}_\mu^A \hat{\sigma}_\nu^B \to \hat{S}_\mu^A \hat{S}_\nu^B$ for normalized Stokes operators. We take any entanglement witness for qubits $\hat{w}$, replace Pauli matrices with standard, or normalized Stokes operators and obtain $\hat{\mathcal{W}}_{\hat{\Theta}}$ or $\hat{\mathcal{W}}_{\hat{S}}$ respectively.

For the sake of clarity, before proving of the correctness of the mapping, it is worth to outline the relation between Stokes (standard and normalized) and Pauli observables. Pauli matrices $\vec{\sigma} = (\sigma_x, \sigma_y, \sigma_z)$ span the space of qubit observables represented by Hermitian 2×2 matrices. Stokes operators refer to 2-dimensional polarisation basis and similarly to Pauli matrices, each of the operators is related to one out of three complementary settings of polarisation analyzers. Stokes operator averages can be given as Stokes vectors: $\langle \vec{\hat{\Theta}} \rangle = (\langle \hat{\Theta}_1 \rangle, \langle \hat{\Theta}_2 \rangle, \langle \hat{\Theta}_3 \rangle)$ for standard ones and $\langle \vec{\hat{S}} \rangle = (\langle \hat{S}_1 \rangle, \langle \hat{S}_2 \rangle, \langle \hat{S}_3 \rangle)$ for normalized Stokes operators.

Standard Stokes observable corresponding to an arbitrary polarisation, specified by a unit real vector $\vec{m}$ (if one uses Bloch representation), has the following representation: $\vec{m} \cdot \vec{\hat{\Theta}} = \sum_{k,l=1}^{2} \hat{a}_k^\dagger (\vec{m} \cdot \vec{\sigma})_{kl} \hat{a}_l$, where $k, l \in \{1, 2\}$ represent polarisation directions H and V respectively. The total number of photons is given by $\hat{N} = \sum_{kl} \hat{a}_k^\dagger \delta_{kl} \hat{a}_l$. For normalized Stokes operators we have analogously: $\vec{m} \cdot \vec{S} = \sum_{kl} \hat{\Pi} \frac{\hat{a}_k^\dagger (\vec{m} \cdot \vec{\sigma})_{kl} \hat{a}_l}{\hat{N}} \hat{\Pi}$, and $\hat{S}_0$ reads $\sum_{kl} \frac{\hat{\Pi} \hat{a}_k^\dagger \delta_{kl} \hat{a}_l \hat{\Pi}}{\hat{N}}$.

5.1 Standard Stokes operators and the mapping $\hat{\sigma}_\mu^A \hat{\sigma}_\nu^B \to \hat{\Theta}_\mu^A \hat{\Theta}_\nu^B$

For standard Stokes operators the mapping reads:

$$\hat{w} = \sum_{\mu,\nu=0}^{3} w_{\mu\nu} \hat{\sigma}_\mu^A \hat{\sigma}_\nu^B \quad \to \quad \hat{\mathcal{W}}_{\hat{\Theta}} = \sum_{\mu,\nu=0}^{3} w_{\mu\nu} \hat{\Theta}_\mu^A \hat{\Theta}_\nu^B, \tag{8}$$

where coefficients $w_{\mu\nu}$ stay unchanged. The proof of the correctness of the mapping, which reduces to the proof that $\hat{\mathcal{W}}_{\hat{\Theta}}$ in (8) is indeed an entanglement witness for any bipartite state of the optical field, goes in two steps. First it is enough to show that for any mixed state ρ of the four-mode field one can always find a two-qubit density matrix $\hat{\mathfrak{P}}_\rho^{AB}$ such that:

$$\frac{\langle \hat{\mathcal{W}}_{\hat{\Theta}} \rangle_\rho}{\langle \hat{N}^A \hat{N}^B \rangle_\rho} = \mathrm{Tr}\, \hat{w} \hat{\mathfrak{P}}_\rho^{AB}. \tag{9}$$

As mixed states (7) and (5) are convex combinations of pure states we proceed with the proof for pure states. With any pure state of the optical field $\left|\phi^{AB}\right\rangle$ the following set of states can be associated: $\{\left|\mathbf{\Phi}_{km}^{AB}\right\rangle = \hat{a}_j \hat{b}_k \left|\phi^{AB}\right\rangle\}_{k,m=1,2}$. Using the idea to represent Stokes operators in arbitrary direction using Pauli matrices the expectation value for standard Stokes operators and $\left|\phi^{AB}\right\rangle$ can be expanded as follows:

$$\left\langle \phi^{AB} \right| \hat{\Theta}_\mu^A \hat{\Theta}_\nu^B \left| \phi^{AB} \right\rangle = \sum_{k,l=1}^{2} \sum_{m,n=1}^{2} \sigma_{\mu_A}^{kl} \sigma_{\nu_B}^{mn} \left\langle \mathbf{\Phi}_{km}^{AB} \right| \left. \mathbf{\Phi}_{ln}^{AB} \right\rangle = \mathrm{Tr}\, \hat{\sigma}_\mu^A \hat{\sigma}_\nu^B \hat{P}^{AB}, \tag{10}$$

where $\left\langle \mathbf{\Phi}_{km}^{AB} \right| \left. \mathbf{\Phi}_{ln}^{AB} \right\rangle$ are elements of matrix $\hat{P}^{AB}$. The matrix $\hat{P}^{AB}$ is a Gram matrix so it is Hermitian. Its trace is $\mathrm{Tr}\, \hat{P}^{AB} = \langle \hat{N}_A \hat{N}_B \rangle$. Thus, $\hat{\mathfrak{P}}^{AB} = \hat{P}^{AB} / \langle \hat{N}^A \hat{N}^B \rangle$ is a proper two-qubit density matrix. Therefore $\hat{\mathfrak{P}}^{AB}$ always exists for $\left|\phi^{AB}\right\rangle$ and (10) holds for any pure state. Note that pureness of $\left|\phi^{AB}\right\rangle$ does not guarantee pureness of $\hat{\mathfrak{P}}^{AB}$.

We need now to show that the separability of the state of the field guarantees the separability of $\hat{\mathfrak{P}}_\rho^{AB}$. Let us assume that $\left|\phi^{AB}\right\rangle$ is a product state $\left|\phi^{AB}\right\rangle_{\mathrm{prod}} = \left|\phi^A\right\rangle \left|\phi^B\right\rangle$. Such a structure of $\left|\phi^{AB}\right\rangle$ implies that $\left\langle \mathbf{\Phi}_{km}^{AB} \right| \left. \mathbf{\Phi}_{ln}^{AB} \right\rangle = \left\langle \mathbf{\Phi}_k^A \right| \left. \mathbf{\Phi}_m^A \right\rangle \left\langle \mathbf{\Phi}_l^B \right| \left. \mathbf{\Phi}_n^B \right\rangle$ i.e. $\hat{\mathfrak{P}}^{AB} = \hat{\mathfrak{P}}^A \hat{\mathfrak{P}}^B$ is also factorizable. Thus $\langle \hat{w} \rangle_{\hat{\mathfrak{P}}^{AB}} \geqslant 0$ and $\langle \hat{\mathcal{W}}_{\hat{\Theta}} \rangle_{\phi^{AB}} \geqslant 0$.

For the reverse map the reasoning is trivial. As $\langle \hat{\mathcal{W}}_\Theta \rangle_{\mathrm{prod}} \geqslant 0$, this is also true for two-photon separable state and this is mathematically equivalent with $\hat{\mathcal{W}}_\Theta$ being an entanglement witness for two qubits.

As mixed separable states are convex combinations of pure states, the proof remains valid also for mixed states.

5.2 Normalized Stokes operators and $\hat{\sigma}_\mu^A \hat{\sigma}_\nu^B \to \hat{S}_\mu^A \hat{S}_\nu^B$

The outline of the proof for normalized Stokes operators follows the same lines as the proof for the standard ones so its description will be more concise. The map reads as follows:

$$\hat{w} = \sum_{\mu,\nu=0}^{3} w_{\mu\nu} \hat{\sigma}_\mu^A \hat{\sigma}_\nu^B \quad \to \quad \hat{\mathcal{W}}_{\hat{S}} = \sum_{\mu,\nu=0}^{3} w_{\mu\nu} \hat{S}_\mu^A \hat{S}_\nu^B. \tag{11}$$

The expectation value $\langle\psi^{AB}|\hat{S}^A_\mu\hat{S}^B_\nu|\psi^{AB}\rangle$ can be put as:

$$\begin{aligned}\langle\psi^{AB}|\hat{S}^A_\mu\hat{S}^B_\nu|\psi^{AB}\rangle &= \sum_{k,l=1}^{2}\sum_{m,n=1}^{2}\sigma^{kl}_\mu\sigma^{mn}_\nu\langle\mathbf{\Psi}^{AB}_{km}|\mathbf{\Psi}^{AB}_{ln}\rangle \\ &= \mathrm{Tr}\,\hat{\sigma}^A_\mu\otimes\hat{\sigma}^B_\nu\hat{R}^{AB},\end{aligned} \tag{12}$$

where $\hat{R}^{AB}$ is Gram matrix which after the normalization $\hat{\mathfrak{R}}^{AB}=\hat{R}^{AB}/\langle\hat{\Pi}^A\hat{\Pi}^B\rangle$ becomes a proper density matrix for two qubits. Again, the separability of the state of the field $|\phi\rangle$ warrants the factorisation of Gram matrix $\hat{\mathfrak{R}}^{AB}$.

In [PhD1] we give several generalizations of the mapping. We demonstrate its applicability for observables from unitary operator bases for qu*d*its introduced in [Ref47] for multiport interferometry. Moreover, the mapping remains valid for any general intensity operators. Note, that this allows to reformulate optical coherence theory, see [PhD1] An application of the mapping is shown in [PhD2], [PhD3]. In [Other1] we apply it in multi party case to classify nonclassical correlations of 3 been GHZ-like radiation.

5.3 Robustness with respect to photon losses

Entanglement conditions from the classes of $\hat{\mathcal{W}}_S$ and $\hat{\mathcal{W}}_\Theta$ are highly resistant to losses. The photon losses are usually modelled with a unitary transformation $\hat{\mathcal{U}}(\eta)$ which is operationally equivalent to placing a beamsplitter of transmission coefficient $\sqrt{\eta}$ in front of a perfect detector i.e.

$$\hat{\mathcal{U}}(\eta)\hat{a}^\dagger_j=\hat{a}^\dagger_j(\eta)=\sqrt{\eta}\hat{a}^\dagger_i+\sqrt{1-\eta}\hat{c}^\dagger_j \tag{13}$$

where $\hat{a}^\dagger_j$ stands for the detection channel and $\hat{c}^\dagger_j$ for the loss channel related with j-th mode.

Let us start with standard Stokes operators. Inserting the transformation $\hat{\mathcal{U}}(\eta)$ we get:

$$\langle\psi^{AB}(\eta)|\hat{\mathcal{W}}_\Theta|\psi^{AB}(\eta)\rangle=\langle\psi^{AB}|\hat{\mathcal{W}}_\Theta(\eta)|\psi^{AB}\rangle\,, \tag{14}$$

where $|\psi^{AB}(\eta)\rangle=\hat{\mathcal{U}}(\eta)\,|\psi^{AB}\rangle$ and $\hat{\mathcal{W}}_\Theta(\eta)=\hat{\mathcal{U}}^\dagger(\eta)\hat{\mathcal{W}}_\Theta\hat{\mathcal{U}}(\eta)$. We denote as $\langle\psi^{AB}|\hat{\mathcal{W}}_\Theta|\psi^{AB}\rangle$ the expectation value of given component of $\hat{\mathcal{W}}_\Theta$ not affected by losses.

By analysing the structure of $\langle\psi^{AB}|\hat{\mathcal{W}}_\Theta(\eta)|\psi^{AB}\rangle$ i.e. applying $\hat{\mathcal{U}}(\eta)$ to photon number operators present in the standard Stokes operators, one can show that $\langle\hat{\Theta}^A_\mu(\eta)\hat{\Theta}^B_\nu(\eta)\rangle$ is always proportional to $\eta^A\eta^B$ i.e.

$$\langle\psi^{AB}|\hat{\mathcal{W}}_\Theta(\eta)|\psi^{AB}\rangle=\eta^A\eta^B\langle\psi^{AB}|\hat{\mathcal{W}}_\Theta|\psi^{AB}\rangle\,, \tag{15}$$

where η^X for $X=A,B$ is Alice's and Bob's detector efficiency. Thus, we have entanglement detection with a full resistance with respect to the losses.

For normalized Stokes operators and $\hat{\mathcal{W}}_S$ the dependence on losses does not cancel out as in the case of $\hat{\mathcal{W}}_\Theta$. Having regard to the structure of separable state (7) it is enough to consider pure product state in the Fock basis $|F\rangle=|n^A_i,n^A_{i_\perp},m^B_i,m^B_{i_\perp}\rangle$. Stokes operators (standard and normalized) are diagonal in their eigenbasis and each pure product state $|F^{AB}\rangle$ can be put as a superposition of eigenstates related to a given Stokes operator. That is why, the dependence of efficiency η^X for $X=A,B$ must be related with the behaviour of $|F^{AB}\rangle$ in the eingenbasis of given $\hat{S}^A_\mu\hat{S}^B_\nu$. Following that intuition it is enough

to analyse the average value of a rate observable (2) for its eigenstate $|F_A\rangle = |n_i^A, m_{i_\perp}^A\rangle$ in presence of efficiency η^A. The following dependence of total number of photons in the given beam is obtained

$$\langle F^A(\eta)|R_i|F^A(\eta)\rangle = \frac{n_i^A}{n_i^A + n_{i_\perp}^A}\left(1-(1-\eta)^{n_i^A+n_{i_\perp}^A}\right) = r_i^A\left(1-(1-\eta)^{n_i^A+n_{i_\perp}^A}\right). \tag{16}$$

$|F^{AB}(\eta)\rangle$ is the state $|F^{AB}\rangle$ after introducing the losses in both channels.

Thus, for the expectation value of normalized Stokes operators for Alice and Bob we get

$$\langle F^{AB}(\eta)|\hat{S}_\mu^A\hat{S}_\nu^B|F^{AB}(\eta)\rangle = H_F\langle F|\hat{S}_\mu^A\hat{S}_\nu^B|F\rangle, \tag{17}$$

where

$$H_F = \prod_{X=A,B}[1-(1-\eta^X)^{n_{tot}^X}] = \langle F(\eta)|\hat{S}_0^A\hat{S}_0^B|F(\eta)\rangle$$

is in fact the joint probability of coincident non-vacuum events in presence of losses and n_{tot}^X is the total number of photons in X-th channel without considering the losses.

This simple but widely accepted model of photon losses and the considerations about the efficiency dependence for standard and normalized Stokes operators have an interesting consequence. As the threshold detectors' efficiency becomes irrelevant, an arbitrary number of photons can be lost from the incoming beam and still entanglement conditions of the type of $\hat{\mathcal{W}}_S$ and $\hat{\mathcal{W}}_\Theta$ remain applicable. Then if e.g. the measurement of three mutually complementary Stokes observables is needed, the light beam incoming to the local detection station can be divided into three beams by cascade beamsplitters. Thus, it is enough to prepare the whole setup with three settings at once and perform all needed measurements simultaneously. All statistics can be collected without changing the settings of local analyzers - the idea is depicted in Fig. 1.

5.4 A separability condition for optical fields based on the mapping – example

Consider the following observable $\hat{w} = \hat{\sigma}_0^A\hat{\sigma}_0^B + \sum_{k=1}^3 s_k\hat{\sigma}_k^A\hat{\sigma}_k^B$, where $s_k = \pm 1$. For any separable state ρ^{AB} the expectation value $\langle\hat{w}\rangle_{sep} \geqslant 0$ because $\langle\hat{\sigma}_k^A\hat{\sigma}_k^B\rangle_{prod} = \langle\hat{\sigma}_k^A\rangle\langle\hat{\sigma}_k^B\rangle$ and $\sum_{k=1}^3\langle\hat{\sigma}_k\rangle^2 = 1$. As s_k can be arbitrary, the following entanglement indicator for two qubits emerges

$$\sum_{k=1}^3|\langle\hat{\sigma}_k^A\hat{\sigma}_k^B\rangle_{sep}| \leqslant \langle\hat{\sigma}_0^A\hat{\sigma}_0^B\rangle_{sep}. \tag{18}$$

Condition (18) mapped to normalized and standard Stokes operators reads:

$$\sum_{j=1}^3|\langle\hat{S}_j^A\hat{S}_j^B\rangle_{sep}| \leqslant \langle\hat{\Pi}^A\hat{\Pi}^B\rangle_{sep}. \tag{19}$$

and

$$\sum_{j=1}^3|\langle\hat{\Theta}_j^A\hat{\Theta}_j^B\rangle_{sep}| \leqslant \langle\hat{N}^A\hat{N}^B\rangle_{sep}. \tag{20}$$

For states for which local correlations vanish condition (18) is straightforwardly derivable from the

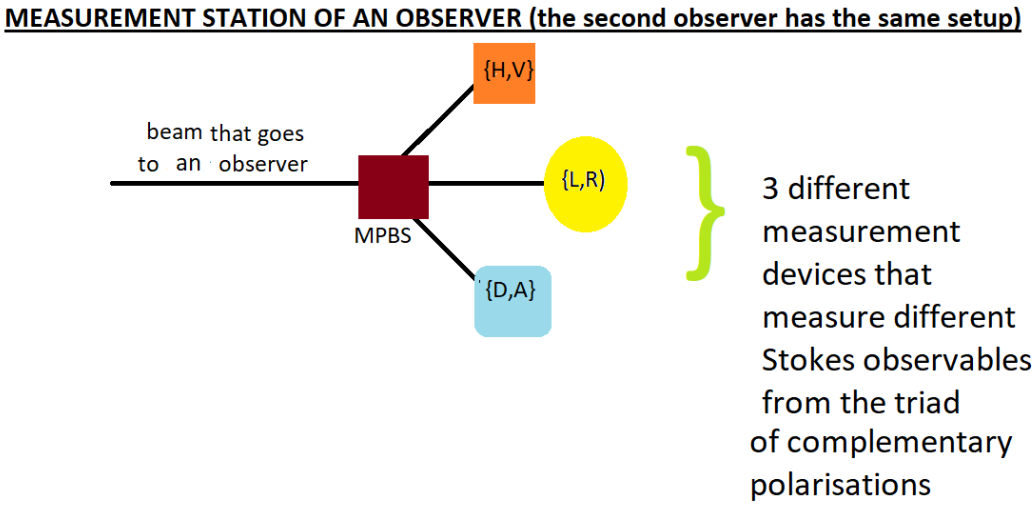

Rysunek 1: Schematic picture of simultaneous measurement of three complementary Stokes observables while testing entanglement of optical fields using entanglement conditions $\hat{\mathcal{W}}_S$ and $\hat{\mathcal{W}}_\Theta$. At each measurement station the beam of incoming light is divided in three by a multi-port beamsplitter (MPBS) of three exists. In each of the exits we measure one of three complementary Stokes observables. There is no need to switch between settings.

family of inequalities which are a consequence of the positive partial transpose conditions of Yu *et.al.* from [Ref48] and therefore it is optimal for such states. Bright squeezed vacuum (4) has this property. It is a consequence of the fact that $\langle\Psi^-|\hat{S}_j^A|\Psi^-\rangle = \langle\Psi^-|\hat{\Theta}_j^A|\Psi^-\rangle = 0$ and the same for the observer B.

5.5 Resistance with respect to a distortion noise

We introduce the following noise model:

$$\rho^{noise} = \frac{1}{4}\left(\left|\Psi^-\right\rangle\!\left\langle\Psi^-\right| + \left|\Psi^+\right\rangle\!\left\langle\Psi^+\right| + \left|\Phi^-\right\rangle\!\left\langle\Phi^-\right| + \left|\Psi^+\right\rangle\!\left\langle\Psi^+\right|\right), \tag{21}$$

where $|\Psi^-\rangle, |\Psi^+\rangle, |\Phi^-\rangle, |\Phi^+\rangle$ are 4 bright squeezed vacuum states. They read respectively:

$$\left|\Phi^\pm\right\rangle = \frac{1}{\cosh^2(\Gamma)} \sum_{n=0}^{\infty} \frac{\mathrm{tgh}^n(\Gamma)}{n!} (a_H^\dagger b_H^\dagger \pm a_V^\dagger b_V^\dagger)^n \left|\Omega\right\rangle, \tag{22}$$

and

$$\left|\Psi^\pm\right\rangle = \frac{1}{\cosh^2(\Gamma)} \sum_{n=0}^{\infty} \frac{\mathrm{tgh}^n(\Gamma)}{n!} (a_H^\dagger b_V^\dagger \pm a_V^\dagger b_H^\dagger)^n \left|\Omega\right\rangle. \tag{23}$$

Our noise shares some similarities with white noise. It is uncorrelated: $\langle\hat{S}_\mu\hat{S}_\nu\rangle = 0$ and $\langle\hat{\Theta}_\mu\hat{\Theta}_\nu\rangle = 0$ for all μ and ν. Also $\mathrm{Tr}\,\hat{\Pi}^A\hat{\Pi}^B\rho^{noise} = \langle\Psi^-|\hat{\Pi}^A\hat{\Pi}^B|\Psi^-\rangle$. One has $\mathrm{Tr}\,\hat{N}^A\hat{N}^B\rho^{noise} = \langle\Psi^-|\hat{N}^A\hat{N}^B|\Psi^-\rangle$, because all noise components have the same amplification gain.

The noisy state reads

$$\varrho^{AB} = v \left|\Psi^-\right\rangle\!\left\langle\Psi^-\right| + (1-v)\varrho^{noise}, \tag{24}$$

where $0 \leqslant v \leqslant 1$ is the visibility.

The robustness with respect to noise can be analyzed by comparing the threshold visibilities above which the separability conditions are violated for the quantum state in question. Thanks to technical lemmas derived for Stokes operators and BSV we have the following identities:

$$\begin{aligned}
&\sum_{i=1}^{3} |\left\langle\Psi^-\right|\hat{S}_i^A \hat{S}_i^B\left|\Psi^-\right\rangle| = \left\langle\Psi^-\right|\hat{\Pi}^A + \hat{\Pi}^A \frac{2}{\hat{N}^A}\hat{\Pi}^A\left|\Psi^-\right\rangle \\
&\left\langle\Psi^-\right|\hat{\Pi}^A\hat{\Pi}^B\left|\Psi^-\right\rangle = \left\langle\Psi^-\right|\hat{\Pi}^A\left|\Psi^-\right\rangle \\
&\sum_{i=1}^{3} |\left\langle\Psi^-\right|\hat{\Theta}_i^A \hat{\Theta}_i^B\left|\Psi^-\right\rangle| = \left\langle\Psi^-\right|\hat{N}^A(\hat{N}^A+2)\left|\Psi^-\right\rangle \\
&\left\langle\Psi^-\right|\hat{N}^A\hat{N}^B\left|\Psi^-\right\rangle = \left\langle\Psi^-\right|(\hat{N}^A)^2\left|\Psi^-\right\rangle .
\end{aligned} \tag{25}$$

Using these, the formulas for the threshold visibility read:

$$v_{crit}^{new} > \frac{\langle\Psi^-|\hat{\Pi}^A\hat{\Pi}^B|\Psi^-\rangle}{\sum_{i=1}^{3}\left|\langle\Psi^-|\hat{S}_i^A\hat{S}_i^B|\Psi^-\rangle\right|} \tag{26}$$

for normalized Stokes operators and

$$v_{crit}^{old} > \frac{\langle\Psi^-|\hat{N}^A\hat{N}^B|\Psi^-\rangle}{\sum_{i=1}^{3}\left|\langle\Psi^-|\hat{\Theta}_i^A\hat{\Theta}_i^B|\Psi^-\rangle\right|} \tag{27}$$

for the standard ones. In Supplemental material of [PhD1] the visibilities v_{crit}^{old} and v_{crit}^{new} were compared as functions of the amplification gain Γ. Normalized Stokes operators turn out to be more efficient. For very weak amplification gain $\Gamma \to 0$ the critical visibility goes to the critical visibility for qubits.

Conditions (19) and (20) and the noise model (21) can be extended to unitary observables [Ref47] for multiport interferometry and $d \times d$ generalized bright squeezed vacuum, see Sup. Mat. in [PhD1].

6 New observables for Bell tests for optical fields

The mapping presented in section 5 can the applied to obtain Bell inequalities for normalized Stokes operators. As mentioned in section 4, the use of standard Stokes operators in Bell inequalities, as it is done in e.g. [Ref28] rests on the *non-enhancement* assumption that the local hidden variable value of total intensity of detected light does not depend on local settings [Ref30]. This assumption, seemingly intuitive from a physical perspective, restricts the range of validity of Bell-like inequalities derived with it to a specific subclass of local realistic models. Measurement stations of Alice and Bob are "black boxes" which have to obey principles of local realism and nothing more. Also note that after introducing the dependence on detector efficiency η, as it was done for entanglement witness $\hat{\mathcal{W}}_{\hat{\Theta}}$ in section 5, the correlation function $E(a,b) = \frac{\langle\hat{\Theta}_a^A\hat{\Theta}_b^B\rangle}{\langle\hat{\Theta}_0^A\hat{\Theta}_0^B\rangle}$, is genuinely free of the dependence on η. This obviously leads to wrong conclusions

even for two photon states as the efficiency loophole is hidden. That is why alternative solutions for the proper formulation of Bell inequalities based on rates, such as normalized Stokes operators [Ref30] or their analogues tailored for weak homodyne detection as in [PhD3] were proposed. Technicalities related with such problems will be discussed in Section 7.1.

In this section new observables for better test of Bell ineqialities for optical fields from [PhD2] are discussed.

Normalized Stokes operators are not the only correct tool to test local realism for polarisation measurement. In [Ref49, Ref50] pseudo-spin operators are proposed e.g. the z component of pseudo-spin is $(-1)^{\hat{n}}$, where $\hat{n}$ is the total photon number operator in the given optical mode. Their spectrum is ± 1 but they are very inefficient with respect to noise or losses. A loss of even one photon flips the value of pseudospin. In [PhD2] we propose another kind of observables: sign Stokes operators. Their concept is very intuitive: use Stokes operators and take the sign function of them, i.e.

$$\hat{G}(s) = \mathrm{sign}(\hat{\Theta}_s) = \mathrm{sign}(U_s(\hat{I}_H - \hat{I}_V)U_s^{\dagger}) = \mathrm{sign}(\hat{I}_s - \hat{I}_{s_\perp}), \tag{28}$$

where $\hat{I}_s$ denotes the intensity measured with the chosen setting s related with the corresponding polarization basis $\{s, s_\perp\}$. Symbol $\hat{U}_s$ denotes a unitary transformation between linear polarisation basis $\{H, V\}$ and an arbitrary polarisation basis $\{s, s_\perp\}$.

As in previous sections we use the model in which intensity is proportional to the expectation value of photon number operator. However, formula (28) remains valid for any model of intensity that can be used for standard Stokes operators. The action of the sign function on Stokes operators is in fact a binning strategy used in homodyne schemes [Ref51, Ref52, Ref53, Ref54] here applied in the context of polarization measurements. The data collected for the measurement of Standard and normalized Stokes operators can be also used for sign Stokes operators.

6.1 Bell inequalities with sign Stokes operators

As the spectrum of sign Stokes operators consist of ± 1 and 0, the derivation of a proper CHSH inequality is straightforward.

For local hidden variables λ and settings a, a' for Alice and b, b' for Bob we define the functions $I^X(x, \lambda)$ and $I^X(x_\perp, \lambda)$ where $x = a, b$ and $X = A, B$ that give the predetermined outcomes of the intensity measurements. The local hidden values for sign operators are given by $G^X(x, \lambda) = \mathrm{sign}(I^X(x, \lambda) - I^X(x_\perp, \lambda))$. These local hidden values are ± 1 and 0, thus one can use standard methods to derive CHSH inequality:

$$\begin{aligned} |\langle G^A(a,\lambda)G^B(b,\lambda) + G^A(a,\lambda)G^B(b',\lambda) + G^A(a',\lambda)G^B(b,\lambda) \\ - G^A(a',\lambda)G^B(b',\lambda)\rangle_{LHV}| \leqslant 2. \end{aligned} \tag{29}$$

As well as in the case of normalized Stokes operators, due to the high probability of the vacuum events inequality (29) cannot be violated for bright squeezed vacuum. In order to reduce the impact of the vacuum term on the CHSH inequality we use the Mermin-Garg trick also used in [Ref30] and modify local hidden values:

$$\hat{G}^X(x) \to \hat{G}^{X-}(x) = \hat{G}^X(x) - \hat{\Pi}_{\Omega^X}, \tag{30}$$

where $\hat{\Pi}_{\Omega^X}$ is the projector on the Fock subspace of states with no photons in the X-th beam. Thus, the new CHSH inequality reads:

$$\begin{aligned}|\langle G^{A-}(a,\lambda)G^{B-}(b,\lambda)+G^{A-}(a,\lambda)G^{B-}(b',\lambda)\\ +G^{A-}(a',\lambda)G^{B-}(b,\lambda)-G^{A-}(a',\lambda)G^{B-}(b',\lambda)\rangle_{LHV}|\leqslant 2.\end{aligned} \tag{31}$$

In [PhD2] we compared the values of CHSH inequalities for sign and normalized Stokes operators in function of the amplification gain Γ for bright squeezed vacuum. The range of Γ in which the violation of the respective CHSH inequality occurs is significantly broader for sign Stokes operators than for normalized ones. Moreover in Suplementary Information in [PhD2] we give a strongly motivated conjecture, based on numerical analysis, that with sign Stokes operators the violation of CHSH inequality occurs in the whole range of Γ. Our conjecture results from the character of the action of sign Stokes operators on the components of bright squeezed vacuum.

Observables (28) need to be modified if one wants to use them in CH inequality. To this end, we introduce non-negative sign Stokes operators, that are simply the projectors onto the subspace in which $m>n$, with m photons in x-th mode and n photons in $x_\perp$-th mode, where again $x=a,b$:

$$\hat{P}(x)=\sum_{n>m}|n_x,m_{x_\perp}\rangle\langle n_x,m_{x_\perp}|\,. \tag{32}$$

From the structure of (32) we see that the eigenvalues are 1 when $m>n$ and 0 if $n\leqslant m$. Note that the expectation value of $\hat{P}^X(x)$ is the probability that the observer X will see more photons in the n_X mode i.e. $n>m$. The quantum joint probability of obtaining the same result, that is $n>m$, by observers A and B for the settings a and b is given by $\langle\hat{P}^A(a)\hat{P}^B(b)\rangle$. Using this notation CH inequality in quantum scenario reads:

$$\begin{aligned}-1\leqslant\langle CH_P\rangle=\left\langle\hat{P}^A(a)\hat{P}^B(b)+\hat{P}^A(a)\hat{P}^B(b')+\hat{P}^A(a')\hat{P}^B(b)\right\rangle\\ -\left\langle\hat{P}^a(a')\hat{P}^B(b')+\hat{P}^A(a)+\hat{P}^B(b)\right\rangle\leqslant 0.\end{aligned} \tag{33}$$

We compare the values of $\langle CH_P\rangle$ and the CH expression for rates in [Ref30] for the optimized settings from [Ref30]. Similarly, as in the case of CHSH inequality better results are obtained with non-negative sign Stokes operators (32).

Sign Stokes operators also are robust for noise and losses. The noise model that we used was introduced in [PhD1] and it is described in the previous sections. The model of losses is an analogue of the one given in [Ref31] and it is based on the binomial distribution.

Also Mermin-like inequality is checked for sign Stokes operators and bright GHZ-like radiation form [Other1]. In this case sign Stokes operatros also are better that normalized ones.

6.2 Sign Stokes observables are not a suitable tool to construct entanglement witnesses

Sign Stokes operators come in handy for Bell inequalities but are not useful for constructing entanglement witnesses. Let us introduce sign Stokes vector $\langle\hat{\vec{G}}\rangle$. We use the notation from previous sections and assign subscripts $1,2,3$ for a triad of mutually unbiased polarisation bases. We have: $\langle\hat{\vec{G}}\rangle=(\langle G_1\rangle,\langle G_2\rangle,\langle G_3\rangle)$.

The norm of standard and normalized Stokes vectors remain invariant with respect to any unitary transformation. This is not the case of $\langle\hat{\vec{G}}\rangle$. For a proof consider the state $|3_H, 0_V\rangle$ and its rotation by $\alpha = \frac{\pi}{4}$ i.e. a rotation of the polarisation of the modes between the bases $\{H, V\}$ and $\{D, A\}$: $a_D^\dagger = \cos\alpha a_H^\dagger + \sin\alpha a_V^\dagger$ and $a_A^\dagger = \cos\alpha a_V^\dagger - \sin\alpha a_H^\dagger$. For such a transformation the norm of $\langle\hat{\vec{G}}\rangle_{|3_H,0_V\rangle}$ is not invariant. Moreover, it exceeds one and according to our calculations it cannot be reasonably bounded.

7 Nonclassicality of single photon

The concepts introduced in previous sections (the mapping and sign Stokes operators) were applied to the bright squeezed vacuum, which is a standard example of "macroscopic" entanglement. In turn, in this section based on [PhD3] and [PhD4] *non-locality of single photon* also called "entanglement with vacuum" will be discussed. A single photon seems to be most microscopical optical object for which Bell inequalities can be tested. However, as we shall see many claims concerning this are incorrect.

In [PhD3] and [PhD4] we reconsider gedanken and real experiments concerning violation of Bell inequalities by a single photon excitation of two spatially separated optical modes. The state in question can be generated by a single photon exciting a balanced beamsplitter. It reads

$$|\psi\rangle = \frac{1}{\sqrt{2}}(|01\rangle_{b_1b_2} + |10\rangle_{b_1b_2}), \tag{34}$$

where $|01\rangle_{b_1b_2}$ stands for "a photon being in the mode b_2 and not in the mode b_1". Formula (34) demonstrates entanglement of optical modes. Revealing nonclassicality of (34) is a complex phenomenon that addresses various research problems such as mode versus particle entanglement [Ref20] or the entangling role of a beamsplitter [Ref55] to name a few. These problems have been widely discussed see e.g. 20 first references from [PhD3]. Various scenarios were proposed. Aharonov and Vaidman, van Enk and Garry, among the others, considered situations in which a single photon exciting a beamsplitter induces entanglement in excitations of atoms placed in spatially separated traps. However, these experiments effectively boil down to Bell tests for two qubits. Thus, we do not have anything new in such schemes.

Nevertheless, it is possible to reveal single photon nonclassicality using only all-optical setups e.g. via strong homodyne measurement [Ref56] or displacement operators [Ref57]. Neither of these examples raise doubts in the scientific community.

We decided to concentrate on the controversial versions of all-optical setups i.e. the experiments in weak local oscillator regime by what we mean that the mean number of photons of the auxiliary field is one or less. We analyzed two emblematic single-photon gedankenexperiments of this type proposed by Tan, Walls, Collett (TWC) [Ref29] and Hardy [Ref58].

Recent progress in the experimental techniques enable the realization of experiments involving schemes of TWC and Hardy, see [Ref25, Ref26]. Thus, the problem of Bell-nonclassicality of single photon gains on interest for applied quantum information and quantum communication.

The schemes of TWC and Hardy are shown Fig. 2. The experimental setup consists of three beamsplitters. A single photon is projected on a balanced beamsplitter BS_0 and a homodyne measurement at spatially separated detection stations $j = 1, 2$ is performed. Each station is equipped with another beamsplitter for homodyne detection denoted by UBS_j for $j = 1, 2$ and two detectors related to the

beamsplitter's outputs. For TWC and Hardy both local beamsplitters UBS_j are balanced. The beamsplitters inputs are denoted by a_j and b_j and outputs by c_j and d_j. The input a_j is fed with the local oscillator $|\alpha_j\rangle$ with amplitude α_1 and tunable phase θ_j. The input b_j is used for the single photon. Behind each beamsplitter UBS_j at the outputs c_j and d_j photon number resolving detectors are placed.

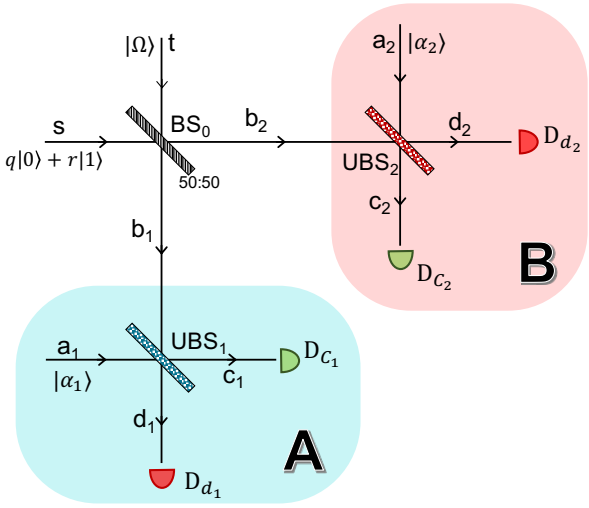

Rysunek 2: Most general schematic representation of the experimental setup for testing single-photon correlational properties, which we consider here. In the Tan-Walls-Collett scenario we have $q = 0$, and $|\alpha_1| = |\alpha_2| = const$ for all settings in Bell-like experiment. In original Hardy's scenario $q \neq 0$ and $|\alpha_j| = 0$, or $\alpha_j = \frac{i^{(1-j)}r}{q\sqrt{2}}$. Here we consider also intermediate cases, including α_j's of varying absolute values and beamsplitters U_{BS_j} with transmissivity varying from setting to setting.

Despite seemingly similar experimental schemes, TWC and Hardy's approaches to test nonclassicality of a single photon differ significantly. First, the preparation of the initial single photon state is different. Hardy's initial state is a non-trivial superposition of single photon and vacuum. After passing through a beamsplitter this state reads: $|\psi\rangle = q\,|00\rangle_{b_1b_2} + \frac{r}{\sqrt{2}}(|01\rangle_{b_1b_2} + |10\rangle_{b_1b_2})$, with $q \neq 0$. For the TWC case we have $q = 0$. Another difference between these two experiments concerns the auxiliary fields. In TWC local oscillators are always turned on and set on the same amplitude α_j during the whole experiment: $\alpha_1 = \alpha_2 = \alpha$. Only the local phase θ_j changes. In contrast, Hardy varies the amplitudes: local oscillators can be turned on or off. With such a setup Hardy defines four complementary situations and proves that their joint local realistic description is not consistent with quantum predictions. Hardy's proof remains impeccable. However TWC experiment raised substantial controversy, see "partial local hidden variable model" for TWC experiment by Santos [Ref59] and the comment by Peres [Ref60]. TWC claim to violate local realism but, as we show in [PhD3] and [PhD4] in their paper they calculate a violation of CHSH-like inequality derived in [Ref28]. Such inequalities do not test local realism for optical fields This was discussed in previous chapters, but for detailed analysis, see the (next) subsection 7.1. The TWC paper had significant impact on the research in quantum optics and quantum information and is widely cited. Despite the controversies, statements about the violation of Bell inequalities with the TWC setup can be found in textbooks [Ref61, Ref62] and research articles e.g. [Ref63] or [Ref64], for the latter see also our comment [Other3]. Thus, this problem needed to be clarified.

7.1 TWC experiment does not reveal Bell nonclassicality

In the TWC scenario the overall input state shared by observers 1 and 2 reads

$$|\Psi(\alpha)\rangle = \frac{1}{\sqrt{2}}\,|\alpha\rangle_{a_1}(|01\rangle_{b_1b_2} + i\,|10\rangle_{b_1b_2})|\alpha\rangle_{a_2}, \tag{35}$$

where we have explicitly added the local oscillators $|\alpha_j\rangle$.

The local hidden variable model of the intensity are denoted here by $I_{x_j}(\theta_j, \lambda)$, where $x = c, d$ stands for the given detector of $j = 1, 2$ detection station, λ is the hidden variable and θ_j is the local setting. The total intensity registered by the detectors c_j and d_j is given by $I_j(\lambda)$. The TWC correlation function in the local realistic description reads:

$$E_T(\theta_1, \theta_2) = \frac{\int d\lambda\rho(\lambda)\prod_{j=1,2}\left(I_{c_j}(\theta_j, \lambda) - I_{d_j}(\theta_j, \lambda)\right)}{\int d\lambda\rho(\lambda)I_1(\lambda)I_2(\lambda)}, \tag{36}$$

where $\rho(\lambda)$ is λ distribution.

In quantum scenario the correlator $E_T(\theta_1,\, \theta_2)$ reads:

$$\begin{aligned} E_T(\theta_1, \theta_2) &= \frac{\langle\Psi(\alpha)|(\hat{n}_{c_1} - \hat{n}_{d_1})(\hat{n}_{c_2} - \hat{n}_{d_2})|\Psi(\alpha)\rangle}{\langle\Psi(\alpha)|(\hat{n}_{c_1} + \hat{n}_{d_1})(\hat{n}_{c_2} + \hat{n}_{d_2})|\Psi(\alpha)\rangle} \\ &= A_T(\alpha)\sin(\theta_1 - \theta_2) \end{aligned} \tag{37}$$

and the amplitude $A_T(\alpha)$ is $A_T(\alpha) = \frac{1}{1+\alpha^2}$.

Then CHSH-like inequality reads:

$$|E_T(\theta_1,\, \theta_2) + E_T(\theta_1',\, \theta_2) + E_T(\theta_1,\, \theta_2') - E_T(\theta_1',\, \theta_2')| \leqslant 2. \tag{38}$$

TWC report a violation of (38) for $\alpha^2 \leqslant \sqrt{2} - 1$.

The form of correlator (36) assumes the *"non-enhancement"* of intensity which can be formulated as follows: $\hat{I}_j(\lambda) = \hat{I}_{c_j}(\lambda, \theta) + \hat{I}_{d_j}(\lambda, \theta)$. Simply a subclass of local hidden variable models is assumed in which the total local realistic intensity does not depend on θ.

A violation of (36) indicates that :

- either the local realism is violated
- or simply for the total intensity one has $\hat{I}_X(\lambda) \neq \hat{I}_{c_X}(\lambda, \theta) + \hat{I}_{d_X}(\lambda, \theta)$.
- or there is no free will i.e. the choice of settings is not random (although this one seems to be very extreme conclusion)

Thus, there is no proof of violation of local realism. Note that weak local oscillator states have in quantum optical description undefined number of photons, which takes specific values only when the detection event happens. Thus, the *non-enhacement* assumption raises strong doubts..

Also, most importantly this model works only for the TWC configuration. The Hardy approach has no local realistic model.

7.2 Rate approach for TWC correlations

We aim to check whether local realism is violated in TWC experiment. As the first step we will formulate CHSH inequality with rate-based observables that for TWC setup read:

$$\hat{\mathrm{R}}_{x_j} = \hat{\Pi}_{c_j d_j} \frac{\hat{n}_{x_j}}{\hat{n}_{c_j} + \hat{n}_{d_j}} \hat{\Pi}_{c_j d_j}, \tag{39}$$

where $x_j = c_j$ or d_j. We define

$$\hat{H}_j(\theta_j) = \hat{R}_{c_j} - \hat{R}_{d_j} = \hat{\Pi}_{c_j d_j} \frac{\hat{n}_{c_j} - \hat{n}_{d_j}}{\hat{n}_{c_j} + \hat{n}_{d_j}} \hat{\Pi}_{c_j d_j}, \tag{40}$$

and analyze the correlation function calculated for TWC experiment:

$$\begin{aligned} E_R(\theta_1, \theta_2) &= \langle \Psi(\alpha) | \, \hat{H}_1(\theta_1) \hat{H}_2(\theta_2) \, | \Psi(\alpha) \rangle \\ &= A_R(\alpha) \sin(\theta_1 - \theta_2), \end{aligned} \tag{41}$$

where most importantly $A_R(\alpha) = \frac{e^{-2\alpha^2}(e^{\alpha^2}-1)^2}{\alpha^2}$. With (41) we shall use the proper CHSH inequality

$$|E_R(\theta_1, \theta_2) + E_R(\theta_1', \theta_2) + E_R(\theta_1, \theta_2') - E_R(\theta_1', \theta_2')| \leqslant 2. \tag{42}$$

A violation of (42) may the observed if the amplitude from (42) $A_R > 1/\sqrt{2}$. However that happens for A_R from (42). This raises doubt whether TWC experiment is indeed a Bell test of local realism. In [PhD4] the definitive answer is given that it is not.

7.3 Local hidden variable model for TWC experiment

The aim of building LHV models is to reconstruct quantum predictions within a theory consistent with local realism. Existence of a LHV model rules out the possibility of violation of Bell inequalities for a given scenario. Thus, a possible application of such a process in device-independent quantum information protocols is impossible. The detailed LHV model for TWC correlations can be found in [PhD4] and the description of the outline how the model was created is demonstrated in [Other4].

The joint probability $p(x, y|a, b)$, of outcomes x and y in presence of settings a and b freely and locally chosen by two observers has a proper LHV model, if it can be reproduced by

$$p(x, y|a, b) = \int d\lambda p(x|a, \lambda) p(y|b, \lambda) \tag{43}$$

where $p(x|a, \lambda)$ is a local probability of getting outcome $x_{(y)}$ in presence of $a_{(b)}$ and λ and $p(y|b, \lambda)$ plays the same role for the second observer.

The quantum probabilities of getting k, l, r or s counts in the x_j-th detector, where $x = c, d$ and $j = 1, 2$ are given by $p(k_{c_1}, l_{d_1}, r_{c_2}, s_{d_2}) = |\langle n_{c_1}, n_{d_1}, n_{c_2}, n_{d_2} | \Psi_{det} \rangle|^2$ where $|\Psi\rangle_{det}$ is (35) after passing through all beamsplitters. We introduce a more concise notation $\mathbf{n} = (k, l, r, s) \in \mathbf{N}^4$ and omit subscripts

of x_j for $x = c, d$ and $j = 1, 2$. We have

$$p(\mathbf{n}) = A(\alpha, \mathbf{n})\Big[(k-l)^2 + (r-s)^2 + 2(k-l)(r-s)\sin(\theta_{12})\Big], \tag{44}$$

where $A(\alpha, \mathbf{n})$ is a coefficient depending on $\mathbf{n}$ and coherent states' amplitude α, whereas θ_{12} denotes $\theta_1 - \theta_2$.

Our LHV model is a convex combination of submodels for specific classes of events. Formula (44) shows that we have two main types of events:

- $\mathcal{N}$ events: (k, l, r, s) such that $k = l$ or $r = s$ that are not dependent on θ_{12}. These events are covered by flat probabilities. Within this set we identify a subclass $\mathcal{O}$ of events such that either $k = l = 0$ or $r = s = 0$.

- $\tilde{\mathcal{N}}$ events: (k, l, r, s) such that $k > l$ and $r > s$ that depend θ_{12}. These events will be called *interferometric events.*

These two classes of events are modelled by two different submodels $\mathcal{M}_{\mathbf{n}}$:

- *Larson-like* submodels denoted by $\mathcal{M}_{\mathbf{n}\in\tilde{\mathcal{N}}\cup\mathcal{O}}$. These models are inspired by LHV models proposed by Larson for 2 qubits [Ref65, Ref66] and cover events $\tilde{\mathcal{N}}$ and events $\mathcal{O}$. There are two hidden variables: uniformly distributed continuous $\lambda \in [0, 2\pi]$ and a coin toss $x \in \{0, 1\}$ that symmetrises the model. The formulas for LHV structured probabilities for interferometric events for Alice $P^A_{\mathbf{n}}(c, d|\theta_1, \lambda, x)$ and Bob $P^B_{\mathbf{n}}(c', d'|\theta_2, \lambda, x)$ are given in the section 3.1 in [PhD4]. The joint probability is given by:

$$P^{AB}_{\mathbf{n}}(c, d, c', d'|\theta_1, \theta_2) = \frac{1 + \mathcal{V}_{\mathbf{n}}\,\mathrm{sgn}\left((c-d)(c'-d')\right)\sin(\theta_{12})}{2\pi}, \tag{45}$$

  where we introduced $\mathcal{V}_{\mathbf{n}}$ that we call is the visibility and is a function of $\mathbf{n}$. Concerning $\mathcal{O}$ events i.e.: $(0, 0, r, s), (0, 0, s, r), (k, l, 0, 0)$ and $(l, k, 0, 0)$, the joint probability is flat and reads $P^{AB}_{\mathbf{n}}(c, d, c', d'|\theta_1, \theta_2) = \frac{1}{4} - \frac{1}{2\pi}$ and results directly from the normalisation condition of local probabilities.

- *Trivial* submodels $\mathcal{M}_{\mathbf{n}\in\mathcal{N}/\mathcal{O}}$ that reproduce probabilities $\mathcal{N}/\mathcal{O}$. They predict fixed outcomes for Alice and Bob, $P^A_{\mathbf{n}}(k, l) = P^B_{\mathbf{n}}(r, s) = 1$, which lead to $P^{AB}_{\mathbf{n}}(k, l, r, s) = 1$.

The overall model is a convex combination of submodels $\mathcal{M}_{\mathbf{n}\in\tilde{\mathcal{N}}\cup\mathcal{O}}$ and $\mathcal{M}_{\mathbf{n}\in\tilde{\mathcal{N}}/\mathcal{O}}$. Each submodel enters the combination with the probability $P(\mathcal{M}_{\mathbf{n}})$, that can be obtained from the comparison of $P^{AB}_{\mathbf{n}}(c, d, c', d'|\theta_1, \theta_2)$ with the corresponding quantum probabilities $p(\mathbf{n}|\theta_{12})$. These values sum up to one $\sum_{n=0}^{\infty} P(\mathcal{M}_{\mathbf{n}}) = 1$, which imposes a certain range of the applicability of the model with respect to the amplitude of local oscillators α. Our model is valid for $\alpha^2 \leqslant \sqrt{2} - 1$ that is the full range of α for which TWC reported the violation of local realism. Thus. despite claims TWC experiment is not a proper test of Bell inequalities.

7.4 Witnessing entanglement of single photon with TWC experiment

In his famous 1964 paper "On the Einstein, Podolski, Rosen Paradox" Bell says that "if [a hidden variable theory] is local it will not agree with quantum mechanics and if it agrees with quantum mechanics it will not be local." Thus, if Bell inequality is violated, the statistics of local measurements of a given quantum

state cannot be reproduced by a local hidden variable model. The considered quantum state in the TWC interferometric configuration may not reveal Bell nonclassicality, but still the TWC setup might reveal entanglement of the two optical modes exiting the initial beamsplitter.

This is so. Below we shall show that the CHSH-like inequality of TWC indeed can be used as an efficient entanglement witness, and it detects the entanglement induced by the single photon state in the TWC configuration. To this end we have to check the relation of the additional "no enhancement" condition with quantum optical separable states. The additional assumption that results from CHSH-like inequalities of TWC and [Ref28] implies simply that $n_{tot_j}(\lambda) = n_{c_j}(\theta_j, \lambda) + n_{d_j}(\theta_j, \lambda)$, where $n_{x_j}(\theta_j, \lambda)$ is the number of detector clicks predicted by an LHV theory in presence of θ_j and λ. This holds for probabilistic combinations of quantum product states i.e. separable states (7), while separable states give per se a possible local hidden variable model. Also, formula (43) could be thought as describing the factorisation of probabilities for a separable state of the field given by (7). This state is a convex combination of factorisable states indexed by λ.

In TWC scenario the local probability of registering n_{x_i} photons for setting θ_i for the local state (the subsystem of the separable state (7)) indexed by λ is

$$\Pr(n_{x_1}|\theta_1)_\lambda = \langle \delta_{(n_{x_1}, \hat{n}_{x_1}(\theta_1))} \rangle_\lambda,$$

where $\delta_{(n,k)}$ is the Kroenecker's delta function. The joint probability goes as follows

$$\begin{aligned} &\Pr(n_{x_1}, n_{x_2}|\theta_1, \theta_2)_{sep} \\ &= \mathrm{Tr}\left[\delta_{(n_{x_1}, \hat{n}_{x_1}(\theta_1))} \delta_{(n_{x_2}, \hat{n}_{x_2}(\theta_2))} \rho^{1,2}_{sep}\right] \\ &= \int d\lambda \rho_\lambda \Pr(n_{x_1}|\theta_1)_\lambda \Pr(n_2|\theta_2)_\lambda, \end{aligned} \tag{46}$$

where $\rho^{1,2}_{sep}$ is given by the formula (7).

Now it is enough to notice that the *no-enhancement* assumption of CHSH-like inequality can be put as:

$$\langle \hat{n}_{tot_i} \rangle(\lambda) = \langle \hat{n}_{c_i}(\theta_i) \rangle(\lambda) + \langle \hat{n}_{d_i}(\theta_i) \rangle(\lambda)$$

that holds for any θ_i and leads to an operator identity

$$\hat{n}_{tot_i} = \hat{n}_{c_i}(\theta_i) + \hat{n}_{d_i}(\theta_i),$$

that is not in contradiction with the structure of separable states. Thus, TWC inequality holds for all separable states.

$$\begin{aligned} &\big\langle 2\hat{n}_{tot_1}\hat{n}_{tot_2} - [\delta\hat{n}_1(\theta_1)\delta\hat{n}_2(\theta_2) + \delta\hat{n}_1(\theta_1)\delta\hat{n}_2(\theta_2') \\ &+\delta\hat{n}_1(\theta_1')\delta\hat{n}_2(\theta_2) - \delta\hat{n}_1(\theta_1')\delta\hat{n}_2(\theta_2')]\big\rangle_{sep} \\ &\geqslant 0, \end{aligned} \tag{47}$$

where $\delta\hat{n}_i(\theta_i) = \hat{n}_{c_i}(\theta_i) - \hat{n}_{d_i}(\theta_i)$.

Thus, CHSH-like inequality of TWC can be used as an entanglement indicator, although it is not

optimal. A tighter separability condition can be proposed. We find it with the help of the general mapping from [PhD1]. The idea is as follows. We map condition (38) to qubits, improve it and remap again to the condition for optical fields. Then, let us start with the qubit case. We will use the intuition that an efficient entanglement witness can be constructed from Bell inequality for qubits when the settings are fully complementary. We reduce Bloch sphere to a circle and introduce pairs of vectors that represent complementary settings of Alice $\{\vec{a}, \vec{a}'\}$ and Bob $\{\vec{b}, \vec{b}'\}$. With these settings the separability condition reads

$$\begin{aligned}&\langle\sqrt{2}\sigma_1^0 \otimes \sigma_2^0 - [\vec{a}\cdot\vec{\sigma}_1 \otimes (\vec{b}+\vec{b}')\cdot\vec{\sigma}_2 \\ &+\vec{a}'\cdot\vec{\sigma}_1 \otimes (\vec{b}-\vec{b}')\cdot\vec{\sigma}_2]\rangle_{sep} \geqslant 0.\end{aligned} \tag{48}$$

Now we use the mapping and assign $\hat{\sigma}_j^{(0)} = \hat{I}_j$, $\hat{\sigma}_j^x = \delta\hat{n}_j(\theta_j)$ and $\hat{\sigma}_j^y = \delta\hat{n}_j(\theta_j + \frac{\pi}{2})$ for $j = 1, 2$ observers. The separability condition goes as follows

$$\begin{aligned}&\big\langle\sqrt{2}\hat{n}_{tot_1}\hat{n}_{tot_2} - [\delta\hat{n}_1(\theta_1)\delta\hat{n}_2(\theta_2) + \delta\hat{n}_1(\theta_1)\delta\hat{n}_2(\theta_2+\tfrac{\pi}{2}) \\ &+\delta\hat{n}_1(\theta_1+\tfrac{\pi}{2})\delta\hat{n}_2(\theta_2) - \delta\hat{n}_1(\theta_1+\tfrac{\pi}{2})\delta\hat{n}_2(\theta_2+\tfrac{\pi}{2})]\big\rangle_{sep} \\ &\geqslant 0.\end{aligned} \tag{49}$$

For rates we get

$$\begin{aligned}&\big\langle\sqrt{2}\hat{\Pi}_1\hat{\Pi}_2 - [\delta\hat{R}_1(\theta_1)\delta\hat{R}_2(\theta_2) + \delta\hat{R}_1(\theta_1+\tfrac{\pi}{2})\delta\hat{R}_2(\theta_2) \\ &+\delta\hat{R}_1(\theta_1)\delta\hat{R}_2(\theta_2+\tfrac{\pi}{2}) - \delta\hat{R}_1(\theta_1+\tfrac{\pi}{2})\delta\hat{R}_2(\theta_2+\tfrac{\pi}{2})]\big\rangle_{sep} \\ &\geqslant 0,\end{aligned} \tag{50}$$

where $\delta\hat{R}_j(\theta_j) = \hat{R}_{c_j}(\theta_j) - \hat{R}_{d_j}(\theta_j)$.

We compared (49) and (50) in function of local oscillators amplitude α. Condition (50) for rates detects entanglement for larger range of α than (49) for intensities.

7.5 Optimal setting for TWC scheme to test Bell nonclassicality

A local hidden variable model exists for the TWC experiment when balanced beamsplitters and weak local oscillators of fixed amplitudes are used constantly during the whole experiment. This demonstrates that local realism cannot be violated in such a setup. Contrarily, the reasoning of Hardy remains correct, so we have an example of all-optical setup demonstrating nonclassicality of single photon. A key difference between TWC and Hardy's experiment is that in Hardy's scheme the strength of the local oscillators vary and the initial state is a superposition of a single photon and vacuum i.e. $c\,|0\rangle + \sqrt{1-|c|^2}\,|1\rangle$ for $c \neq 0$, see Fig. 2. Thus, the analyses of TWC and Hardy arise the following questions:

1. What is the role of vacuum component in the superposition of single photon and vacuum that Hardy uses?

2. What can be modified in TWC scheme so it can reveal nonclassicality of a single photon?

The use of a signal state being the superposition of a single photon and vacuum is an important aspect of the original Hardy's setup because if $c \to 0$ the nonclassicality of the single photon within Hardy's scheme cannot be observed. The CH inequality related with Hardy's paradox is effectively not violated for $c < 0.2$.

Our approach to test nonclassicality of single photon was then the following. We decided to combine TWC and Hardy's schemes, vary all tunable parameters (transmitivities of beamsplitters, local amplitudes and phases) and use only a single photon as a signal state. The tunable beamsplitter's transmitivity (reduction of intensity upon transmission) will be denoted by χ_j for observers $j = 1, 2$.

Yet, even by varying these settings CHSH rate-based inequality is not violated. Thus, perhaps it is worth to consider CH inequality instead. However, CH and CHSH inequalities remain equivalent for qubits but they are not equivalent anymore when we use rates. Despite the fact that rates and probabilities share similar important properties, there is a significant difference. The probabilities sum up to 1 while rates sum up either to 1 or 0, because of the probability for a vacuum event the rate is set to 0. That is why CHSH and CH are no longer equivalent for rates.

For the consistency we denote local tunable settings by $\vec{v}_j$ and $\vec{v}'_j$ for $j = 1, 2$. where $\vec{v}_j = (\chi_j, \alpha_j, \theta_j)$ stands for *on* setting with beamsplitters tuned to transmitivity χ_j and the local oscillator's amplitude is α_j. The primed settings correspond to *off* situation i.e. local oscillators are turned off and beamsplitters are removed i.e. $\vec{v}'_j = (1, 0, 0)$.

In the local realistic scenario CH inequality constructed with rates reads:

$$\begin{aligned} -1 \leqslant \big\langle R_{d_1}(\vec{v}_1)R_{d_2}(\vec{v}_2) + R_{d_1}(\vec{v}_1)R'_{d_2}(\vec{v}'_2) + R'_{d_1}(\vec{v}'_1)R_{d_2}(\vec{v}_2) \\ - R'_{d_1}(\vec{v}'_1)R'_{d_2}(\vec{v}'_2) - R_{d_1}(\vec{v}_1) - R_{d_2}(\vec{v}_2)\big\rangle_{LHV} \leqslant 0. \end{aligned} \tag{51}$$

The violation of inequality (51) obtained in [PhD3] reveals true nonclassicality of single photon.

The optical settings correspond to local beamsplitters with transmitivity $\chi_1 = \chi_2 = 0.79$ and the local oscillator coherent states have mean photon number equal to $1/2$. Moreover, with these settings, the non-classical correlations are detected also in the case of the initial state being one single photon, and not a superposition of it with vacuum i.e. $c = 0$. Thus, the presence of the vacuum component is not necessary to reveal nonclassicality of single photon using inequality (51). Interestingly, for the case of $c = 0$, and nearby, the CH inequality is violated on its left-hand-side, while for Hardy's range of parameters CH is violated on the right hand side.

It is worth noting that the scenario described above has a unique characteristic. The correlation functions and local averages rely on the values of the parameters of the overall initial quantum state (of all four modes involved in the experiment, including the local oscillator ones), denoted as $|\Psi(\alpha)\rangle$ in equation (35). Now coherent states' amplitude α vary depending on the setting. This "dependency on the state" can be eliminated by the description of the measurement in terms of POVMs acting on the single photon input state $|\psi\rangle$ given in equation (34). For the construction of POVMs see Appendix in [PhD3].

Another method proposed in [PhD4] to test the non-classical behavior of a single photon is to construct a CH inequality tailored for specific events (specific photon counts). We denote the events as follows A and A' for the first observer and B and B' for the second observer. By primed event A' we denote a single photon detected in mode d_1 and no-photon in mode c_1 when local oscillator is turned on (*on* setting). By A we denote also a single photon count at d_1 and no count in c_1, however with the local beamsplitter removed

and local oscillator switched off (i.e *off* setting). Events B and B' play the same role for Bob. E.g. the joint probability $P(A', B')$ i.e. for both local settings "*on*" is given by:

$$P(A', B') = |_{c_1,d_1,c_2,d_2} \langle 0, 1, 0, 1|\Psi\rangle|^2,$$

where $|\Psi\rangle$ is given by (35). In such a case CH inequality reads

$$\begin{aligned} -1 \leqslant\ & P(A, B) + P(A, B') + P(A', B) \\ & - P(A', B') - P(A) - P(B) \leqslant 0. \end{aligned} \tag{52}$$

Inequality (52) is violated by quantum prediction. The maximal violation of (52) is obtained for the following parameters $|\alpha|^2 = 0.2$ and beamsplitters' transmitivity $\chi \approx 0.8$ (the values are the same for both observers). Note that $|\alpha|^2 + \chi \approx 1$. This relation is most probably a general rule for optimal detection of violation of realism in such tests with *on/off* settings and for the specific detection events, see a discussion in [Ref67]. Therein, the authors show that this rule survives even imperfect detection. When working on [PhD4] we thought that this interesting relation is accidental. What is the physical meaning of this rule for optimal entanglement detection test is an open question.

The violation of CH only using *on/off* settings can be considered from more fundamental perspective i.e. as the demonstration of the wave-particle complementarity of a quantum state using complementary detection techniques. These techniques consist of a homodyne type (local oscillators *on*) and a direct photon number measurement (local oscillators *off*). That aspect of nonclassicality of single photon can be associated with Dirac's phase vs photon-number uncertainty for quantum optics [Ref68] and points out that violation of Bell inequalities have fundamental role in understanding of quantum physics.

To conclude our analysis, we have also examined the original Hardy paradox using intensity rate-based approach. We found that the original Hardy's setup does not lead to the violation of CH inequality for rates. This remark of course does not make Hardy's reasoning invalid, rather shows the different nature of two approaches.

8 Projects in progress

New technologies allow the experimental realization of the concepts given in [PhD1, PhD2, PhD3, PhD4]. The physical realization of theoretical ideas seems very tempting to me. Such experiments apart from enabling testing fundamental questions have also a very practical meaning. They can be developed in context of possible applications in quantum information theory. Results described in this thesis can lead to the design of secure quantum communication and quantum cryptography.

Still, entanglement conditions based on the mapping from qubits to Stokes operators from [PhD1] can be modyfied. It is well known that adding a non-linear component might improve given entanglement witness. One of the ways on doing so is e.g. to introduce the variance of the Stokes vector for the composed system, see [Other2]. Such a criteria have a straightforward physical interpretation. Specifically, if the range of data points around the average value of a quantum state is less than the minimum range expected for separable states, then that quantum state is entangled. Covariances can be also used to construct Bell inequalities e.g. [Ref69].

Apart from that, in [Other2] we consider bright squeezed vacuum with introduced non-Gaussianity that exhibit strong quantum correlations. Using such states allows testing non classical aspects of optical fields in "event-ready" experiments and finds potential applications in secure communication and other quantum technologies. Also, exploring physics of non-gaussian entanglement in quantum protocols is a problem of growing interest.

Another project in progress related to the mapping from [PhD1] and observables from [PhD2] is about steering in quantum optics. Steering is an interesting phenomena that lies"between" entanglement and Bell nonclassicality. According to my knowledge this problem was studied only for states of defined numbers of particles.

PhD Series **(the alphabetical order of authors indicates their equal involvement)**

[PhD1] Junghee Ryu, Bianka Woloncewicz, Marcin Marciniak, Marcin Wieśniak, and Marek Żukowski. General mapping of multiqudit entanglement conditions to nonseparability indicators for quantum-optical fields. Phys. Rev. Research, 1:032041, Dec 2019.

[PhD2] Konrad Schlichtholz, Bianka Woloncewicz, and Marek Żukowski. Simplified quantum optical stokes observables and bell's theorem. Scientific Reports, 12(1):10101, Jun 2022.

[PhD3] Tamoghna Das, Marcin Karczewski, Antonio Mandarino, Marcin Markiewicz, Bianka Woloncewicz, and Marek Żukowski. Can single photon excitation of two spatially separated modes lead to a violation of bell inequality via weak-field homodyne measurements? New Journal of Physics, 23(7):073042, jul 2021.

[PhD4] Tamoghna Das, Marcin Karczewski, Antonio Mandarino, Marcin Markiewicz, Bianka Woloncewicz, and Marek Żukowski. Wave–particle complementarity: detecting violation of local realism with photon-number resolving weak-field homodyne measurements. New Journal of Physics, 24(3):033017, mar 2022.

Other References related to this thesis that I am a co-author

[Other1] Konrad Schlichtholz, Bianka Woloncewicz, and Marek Żukowski. Nonclassicality of bright greenberger-horne-zeilinger–like radiation of an optical parametric source. Phys. Rev. A, 103:042226, Apr 2021.

[Other2] Bianka Woloncewicz Tamoghna Das and Marek Żukowski. Improved entanglement indicators for quantum optical fields. arXiv:2205.05641, 2022.

[Other3] Tamoghna Das, Marcin Karczewski, Antonio Mandarino, Marcin Markiewicz, Bianka Woloncewicz, and Marek Żukowski. Comment on 'single particle nonlocality with completely independent reference states'. New Journal of Physics, 24(3):038001, mar 2022.

[Other4] Tamoghna Das, Marcin Karczewski, Antonio Mandarino, Marcin Markiewicz, Bianka Woloncewicz, and Marek Żukowski. Remarks about bell-nonclassicality of a single photon. Physics Letters A, 435:128031, 2022.

Other publications that I am a co-author but they are not cited in this thesis

- Ray Ganardi, Ekta Panwar, Mahasweta Pandit, Bianka Woloncewicz and Tomasz Paterek,Quantitative non-classicality of mediated interactions, arXiv:2303.12428, 2023
- Marcin Wieśniak, Palash Pandya, Omer Sakarya, Bianka Woloncewicz, Distance between Bound Entangled States from Unextendible Product Bases and Separable States, Quantum Reports. 2020; 2(1):49-56

Other References

[Ref1] A. Einstein, B. Podolsky, and N. Rosen. Can quantum-mechanical description of physical reality be considered complete? Phys. Rev., 47:777–780, May 1935.

[Ref2] D Bohm. Quantum theory, Prentice Hall Inc., New York,(1951).

[Ref3] N. Bohr. Can quantum-mechanical description of physical reality be considered complete? Phys. Rev., 48:696–702, Oct 1935.

[Ref4] E. Schrödinger. Discussion of probability relations between separated systems. Mathematical Proceedings of the Cambridge Philosophical Society, 31(4):555–563, 1935.

[Ref5] J. S. Bell and Alain Aspect. Speakable and Unspeakable in Quantum Mechanics: Collected Papers on Quantum Philosophy. Cambridge University Press, 2 edition, 2004.

[Ref6] Alain Aspect. Bell's Theorem: The Naive View of an Experimentalist, pages 119–153. Springer Berlin Heidelberg, Berlin, Heidelberg, 2002.

[Ref7] Daniel Erdösi, Marcus Huber, Beatrix C Hiesmayr, and Yuji Hasegawa. Proving the generation of genuine multipartite entanglement in a single-neutron interferometer experiment. New Journal of Physics, 15(2):023033, feb 2013.

[Ref8] Marek Żukowski and Časlav Brukner. Bell's theorem for general n-qubit states. Phys. Rev. Lett., 88:210401, May 2002.

[Ref9] Reinhard F. Werner and Michael M. Wolf. Bell inequalities and entanglement. QIC, 1:1–25, October 2001.

[Ref10] Časlav Brukner and Marek Żukowski. Bell's Inequalities — Foundations and Quantum Communication, pages 1413–1450. Springer Berlin Heidelberg, Berlin, Heidelberg, 2012.

[Ref11] Xiao-song Ma, Stefan Zotter, Johannes Kofler, Rupert Ursin, Thomas Jennewein, Časlav Brukner, and Anton Zeilinger. Experimental delayed-choice entanglement swapping. Nature Physics, 8(6):479–484, 2012.

[Ref12] Charles H. Bennett and Gilles Brassard. Quantum cryptography: Public key distribution and coin tossing. Theoretical Computer Science, 560:7–11, 2014. Theoretical Aspects of Quantum Cryptography – celebrating 30 years of BB84.

[Ref13] Charles H. Bennett and David P. DiVincenzo. Quantum information and computation. Nature, 404(6775):247–255, Mar 2000.

[Ref14] Nicolas Gisin, Grégoire Ribordy, Wolfgang Tittel, and Hugo Zbinden. Quantum cryptography. Rev. Mod. Phys., 74:145–195, Mar 2002.

[Ref15] John Preskill. Quantum information and physics: Some future directions. Journal of Modern Optics, 47(2-3):127–137, 2000.

[Ref16] V. Vedral, M. B. Plenio, M. A. Rippin, and P. L. Knight. Quantifying entanglement. Phys. Rev. Lett., 78:2275–2279, Mar 1997.

[Ref17] Ryszard Horodecki, Paweł Horodecki, Michał Horodecki, and Karol Horodecki. Quantum entanglement. Rev. Mod. Phys., 81:865–942, Jun 2009.

[Ref18] Otfried Gühne and Géza Tóth. Entanglement detection. Physics Reports, 474(1):1–75, 2009.

[Ref19] Jian-Wei Pan, Zeng-Bing Chen, Chao-Yang Lu, Harald Weinfurter, Anton Zeilinger, and Marek Żukowski. Multiphoton entanglement and interferometry. Rev. Mod. Phys., 84:777–838, May 2012.

[Ref20] Rafal Demkowicz-Dobrzański, Marcin Jarzyna, and Jan Kołodyński. Chapter Four - Quantum Limits in Optical Interferometry, volume 60 of Progress in Optics. Elsevier, 2015.

[Ref21] Christoph Simon and Dik Bouwmeester. Theory of an entanglement laser. Phys. Rev. Lett., 91:053601, Aug 2003.

[Ref22] J. Eli Bourassa, Rafael N. Alexander, Michael Vasmer, Ashlesha Patil, Ilan Tzitrin, Takaya Matsuura, Daiqin Su, Ben Q. Baragiola, Saikat Guha, Guillaume Dauphinais, Krishna K. Sabapathy, Nicolas C. Menicucci, and Ish Dhand. Blueprint for a Scalable Photonic Fault-Tolerant Quantum Computer, 2020. arXiv:2010.02905v2.

[Ref23] Marco Barbieri. Optical quantum metrology. PRX Quantum, 3:010202, Jan 2022.

[Ref24] S. Pirandola, U. L. Andersen, L. Banchi, M. Berta, D. Bunandar, R. Colbeck, D. Englund, T. Gehring, C. Lupo, C. Ottaviani, J. L. Pereira, M. Razavi, J. Shamsul Shaari, M. Tomamichel, V. C. Usenko, G. Vallone, P. Villoresi, and P. Wallden. Advances in quantum cryptography. Adv. Opt. Photon., 12(4):1012–1236, Dec 2020.

[Ref25] G. S. Thekkadath, D. S. Phillips, J. F. F. Bulmer, W. R. Clements, A. Eckstein, B. A. Bell, J. Lugani, T. A. W. Wolterink, A. Lita, S. W. Nam, T. Gerrits, C. G. Wade, and I. A. Walmsley. Tuning between photon-number and quadrature measurements with weak-field homodyne detection. Phys. Rev. A, 101:031801, Mar 2020.

[Ref26] G. Donati, T. Bartley, X-M. Jin, M-D. Vidrighin, A. Datta, Barbieri M., and I. A. Walmsley. Observing optical coherence across fock layers with weak-field homodyne detectors. Nat. Commun., 5:5584, 2014.

[Ref27] J. M. Jauch and F. Rohrlich. The Theory of Photons and Electrons: The Relativistic Quantum Field Theory of Charged Particles with Spin One-half. 1976.

[Ref28] M. D. Reid and D. F. Walls. Violations of classical inequalities in quantum optics. Phys. Rev. A, 34:1260–1276, Aug 1986.

[Ref29] S. M. Tan, D. F. Walls, and M. J. Collett. Nonlocality of a single photon. Phys. Rev. Lett., 66:252–255, Jan 1991.

[Ref30] Marek Żukowski, Marcin Wieśniak, and Wiesław Laskowski. Bell inequalities for quantum optical fields. Phys. Rev. A, 94:020102, Aug 2016.

[Ref31] Marek Żukowski, Wiesław Laskowski, and Marcin Wieśniak. Normalized Stokes operators for polarization correlations of entangled optical fields. Phys. Rev. A, 95:042113, Apr 2017.

[Ref32] D.N. Klyshko. Combine epr and two-slit experiments: Interference of advanced waves. Physics Letters A, 132(6):299–304, 1988.

[Ref33] Ulrik L Andersen, Tobias Gehring, Christoph Marquardt, and Gerd Leuchs. 30 years of squeezed light generation. Physica Scripta, 91(5):053001, apr 2016.

[Ref34] A. Christ, A. Eckstein, P. J. Mosley, and C. Silberhorn. Pure single photon generation by type-i pdc with backward-wave amplification. Opt. Express, 17(5):3441–3446, Mar 2009.

[Ref35] Paul G. Kwiat, Klaus Mattle, Harald Weinfurter, Anton Zeilinger, Alexander V. Sergienko, and Yanhua Shih. New high-intensity source of polarization-entangled photon pairs. Phys. Rev. Lett., 75:4337–4341, Dec 1995.

[Ref36] Adán Cabello, David Rodríguez, and Ignacio Villanueva. Necessary and sufficient detection efficiency for the mermin inequalities. Phys. Rev. Lett., 101:120402, Sep 2008.

[Ref37] Jian-Wei Pan, Dik Bouwmeester, Matthew Daniell, Harald Weinfurter, and Anton Zeilinger. Experimental test of quantum nonlocality in three-photon Greenberger–Horne–Zeilinger entanglement. Nature, 403(6769):515–519, February 2000.

[Ref38] Harald Weinfurter and Marek Żukowski. Four-photon entanglement from down-conversion. Phys. Rev. A, 64:010102, Jun 2001.

[Ref39] Dong Ding, Ying-Qiu He, Feng-Li Yan, and Ting Gao. On four-photon entanglement from parametric down-conversion process. Quantum Information Processing, 17:1–10, 2018.

[Ref40] M.V. Chekhova, G. Leuchs, and M. Żukowski. Bright squeezed vacuum: Entanglement of macroscopic light beams. Optics Communications, 337:27–43, 2015.

[Ref41] Magdalena Stobińska, Falk Töppel, Pavel Sekatski, and Maria Chekhova. Entanglement witnesses and measures for bright squeezed vacuum. Physical Review A, 86, 05 2012.

[Ref42] Magdalena Stobińska, Falk Töppel, Pavel Sekatski, and Maria V. Chekhova. Entanglement witnesses and measures for bright squeezed vacuum. Phys. Rev. A, 86:022323, Aug 2012.

[Ref43] Timur Sh. Iskhakov, Ivan N. Agafonov, Maria V. Chekhova, and Gerd Leuchs. Polarization-entangled light pulses of 10^5 photons. Phys. Rev. Lett., 109:150502, Oct 2012.

[Ref44] Krzysztof Rosołek, Magdalena Stobińska, Marcin Wieśniak, and Marek Żukowski. Two copies of the Einstein-Podolsky-Rosen state of light lead to refutation of epr ideas. Phys. Rev. Lett., 114:100402, Mar 2015.

[Ref45] Sixia Yu, Qing Chen, Chengjie Zhang, C. H. Lai, and C. H. Oh. All entangled pure states violate a single Bell's inequality. Phys. Rev. Lett., 109:120402, Sep 2012.

[Ref46] Michał Horodecki, Paweł Horodecki, and Ryszard Horodecki. Separability of mixed states: necessary and sufficient conditions. Physics Letters A, 223(1):1–8, 1996.

[Ref47] Junghee Ryu, Marcin Marciniak, Marcin Wiesniak, and Marek Zukowski. Entanglement conditions for integrated-optics multi-port quantum interferometry experiments. 01 2016.

[Ref48] Sixia Yu, Jian-Wei Pan, Zeng-Bing Chen, and Yong-De Zhang. Comprehensive test of entanglement for two-level systems via the indeterminacy relationship. Phys. Rev. Lett., 91:217903, Nov 2003.

[Ref49] Zeng-Bing Chen, Jian-Wei Pan, Guang Hou, and Yong-De Zhang. Maximal violation of Bell's inequalities for continuous variable systems. Phys. Rev. Lett., 88:040406, Jan 2002.

[Ref50] M M Dorantes and J L Lucio M. Generalizations of the pseudospin operator to test the Bell inequality for the TMSV state. Journal of Physics A: Mathematical and Theoretical, 42(28):285309, jun 2009.

[Ref51] Melvyn Ho, Olivier Morin, Jean-Daniel Bancal, Nicolas Gisin, Nicolas Sangouard, and Julien Laurat. Witnessing single-photon entanglement with local homodyne measurements: analytical bounds and robustness to losses. New Journal of Physics, 16(10):103035, oct 2014.

[Ref52] Su-Yong Lee, Jiyong Park, Jaewan Kim, and Changsuk Noh. Single-photon quantum nonlocality: Violation of the clauser-horne-shimony-holt inequality using feasible measurement setups. Phys. Rev. A, 95:012134, Jan 2017.

[Ref53] Antonio Acín, Nicolas J. Cerf, Alessandro Ferraro, and Julien Niset. Tests of multimode quantum nonlocality with homodyne measurements. Phys. Rev. A, 79:012112, Jan 2009.

[Ref54] W. J. Munro. Optimal states for Bell-inequality violations using quadrature-phase homodyne measurements. Phys. Rev. A, 59:4197–4201, Jun 1999.

[Ref55] M. S. Kim, W. Son, V. Bužek, and P. L. Knight. Entanglement by a beam splitter: Nonclassicality as a prerequisite for entanglement. Phys. Rev. A, 65:032323, Feb 2002.

[Ref56] W. J. Munro. Optimal states for Bell-inequality violations using quadrature-phase homodyne measurements. Phys. Rev. A, 59:4197–4201, Jun 1999.

[Ref57] Konrad Banaszek and Krzysztof Wódkiewicz. Testing quantum nonlocality in phase space. Phys. Rev. Lett., 82:2009–2013, Mar 1999.

[Ref58] Lucien Hardy. Nonlocality of a single photon revisited. Phys. Rev. Lett., 73:2279–2283, Oct 1994.

[Ref59] Emilio Santos. Comment on "nonlocality of a single photon". Phys. Rev. Lett., 68:894–894, Feb 1992.

[Ref60] Asher Peres. Nonlocal effects in fock space. Phys. Rev. Lett., 74:4571–4571, Jun 1995.

[Ref61] Daniel F Walls and Gerard J Milburn. Quantum optics. Springer Science & Business Media, 2007.

[Ref62] Gennaro Auletta, Mauro Fortunato, and Giorgio Parisi. Quantum Mechanics. Cambridge university press, 2012.

[Ref63] Paolo Abiuso, Tamás Kriváchy, Emanuel-Cristian Boghiu, Marc-Olivier Renou, Alejandro Pozas-Kerstjens, and Antonio Acín. Single-photon nonlocality in quantum networks. Phys. Rev. Research, 4:L012041, Mar 2022.

[Ref64] J J Cooper and J A Dunningham. Single particle nonlocality with completely independent reference states. New Journal of Physics, 10(11):113024, nov 2008.

[Ref65] Jan Åke Larsson. Modeling the singlet state with local variables. Physics Letters A, 256(4):245 – 252, 1999.

[Ref66] Sven Aerts, Paul Kwiat, Jan-Åke Larsson, and Marek Żukowski. Two-photon Franson-type experiments and local realism. Phys. Rev. Lett., 83:2872–2875, Oct 1999.

[Ref67] Tamoghna Das, Marcin Karczewski, Antonio Mandarino, Marcin Markiewicz, and Marek Żukowski. Optimal interferometry for Bell nonclassicality induced by a vacuum–one-photon qubit. Phys. Rev. Appl., 18:034074, Sep 2022.

[Ref68] Paul Adrien Maurice Dirac. The quantum theory of the emission and absorption of radiation. Proceedings of the Royal Society of London. Series A, Containing Papers of a Mathematical and Physical Character, 114(767):243–265, 1927.

[Ref69] Victor Pozsgay, Flavien Hirsch, Cyril Branciard, and Nicolas Brunner. Covariance Bell inequalities. Phys. Rev. A, 96:062128, Dec 2017.

Rapid Communications

General mapping of multiqudit entanglement conditions to nonseparability indicators for quantum-optical fields

Junghee Ryu,[1] Bianka Woloncewicz,[2] Marcin Marciniak,[3] Marcin Wieśniak,[3,2] and Marek Żukowski[2]
[1]*Centre for Quantum Technologies, National University of Singapore, 3 Science Drive 2, 117543 Singapore, Singapore*
[2]*International Centre for Theory of Quantum Technologies (ICTQT), University of Gdansk, 80-308 Gdansk, Poland*
[3]*Institute of Theoretical Physics and Astrophysics, Faculty of Mathematics, Physics and Informatics, University of Gdańsk, 80-308 Gdańsk, Poland*

(Received 24 April 2019; published 19 December 2019)

We show that any multiqudit entanglement witness leads to a nonseparability indicator for quantum optical fields, which involves intensity correlations. We get, e.g., *necessary and sufficient* conditions for intensity or intensity-rate correlations to reveal polarization entanglement. We also derive separability conditions for experiments involving multiport interferometers, now feasible with integrated optics. We show advantages of using intensity rates rather than intensities, e.g., a mapping of the Bell inequalities to ones for optical fields. The results have implication for studies of nonclassicality of "macroscopic" systems of undefined or uncontrollable number of "particles."

DOI: 10.1103/PhysRevResearch.1.032041

Nonclassicality due to entanglement initially was studied using quantum optical multiphoton interferometry, see, e.g., Ref. [1]. The experiments were constrained to defined photon number states, e.g., the two-photon polarization singlet [2]. This includes Greenberger-Horne-Zeilinger (GHZ) [3] inspired multiphoton interference, with an interpretation that each detection event signals one photon. Spurious events of higher photon number counts contributed to a lower interferometric contrast. Still, states of undefined photon numbers, e.g., the squeezed vacuum, can be entangled [4–6].

This form of entanglement of quantum optical fields served, e.g., to show that a strongly pumped two-mode (bright) squeezed state allows one to directly refute the ideas of EPR [7], as it approximates their state, and a form of Bell's theorem can be shown for it [4]. The trick was to use displaced parity observables. Recently, it has been shown that this is also possible for four-mode bright squeezed vacuum [8], which can be produced via type II parametric down-conversion, see, e.g., Refs, [5,6]. In this case, the state approximates a tensor product of two EPR states, and interestingly can also be thought of as a polarization "supersinglet" of undefined photon numbers [9]. The approach of Ref. [8] used (effectively) intensity observables, which are less experimentally cumbersome.

With the birth of quantum information science and technology, entanglement became a resource. We have an extended literature on detection of entanglement for systems of finite dimensions, essentially "particles", see e.g., Ref. [10]. It is well known that not all entangled states violate Bell inequalities. Still there is theory of entanglement indicators, called usually witnesses, which allow to detect entanglement, even if a given state for finite-dimensional systems (essentially, qu*d*its) does not violate any known Bell inequalities. The case of two-mode entanglement for optical fields was studied in trailblazing papers [11,12], which discussed "two-party continuous variable systems," and with a direct quantum optical formalism in Ref. [13]. The entanglement conditions reached in the papers did not involve intensity correlations.

An entanglement condition for four-mode fields, which was borrowing ideas from two spin-1/2 (two-qubit) correlations, involved correlations Stokes operators and was first discussed in Ref. [5]. The resulting indicator was used to measure efficiency of an "entanglement laser." The output of the "laser" was bright four-mode vacuum. We shall present here the most extensive generalization of such an approach, i.e., entanglement indicators for optical fields which are derivatives of multiqudit entanglement witnesses involving intensity correlations. In Ref. [14], we give examples of entanglement conditions based on such an approach. Some of them are more tight versions of the entanglement conditions mentioned above.

As a growing part of the experimental effort is now directed at nonclassical features of bright (intensive "macroscopic") beams of light, e.g., Refs. [15–21] so the time is ripe for a comprehensive study of such entanglement conditions. All that may lead to some new schemes in quantum communication and quantum cryptography, perhaps on the lines of Ref. [9]. The emergence of integrated optics allows now to construct stable multiport interferometers [22–29], and is our motivation of going beyond two times mode case.

We present a theory of mapping multiqudit entanglement witnesses [10] into entanglement indicators for quantum optical fields, which employ intensity correlations or correlations

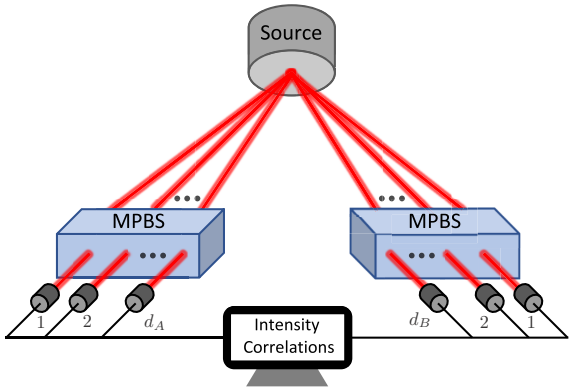

FIG. 1. The experiments (two parties). Two multimode beams propagate to two spatially separated measurement stations. Each station consists of a d input d output tunable multiport beamsplitter-interferometer (MPBS) and detectors at its outputs. For polarization measurements put $d_A = d_B = 2$, and treat the paths as polarization modes.

of intensity rates. By intensity rates we mean the ratio of intensity at a given local detector and the sum of intensities at all local detectors (in some case the second approach leads to better entanglement detection). The method may find applications also in studies of nonclassicality of correlations in "macroscopic" many-body quantum systems of undefined or uncontrollable number of constituents, e.g., Bose-Einstein condensates [30], other specific states of cold atoms [31,32].

The essential ideas are presented for polarization measurements by two observers and the most simple model of intensity observable: photon number in the observed mode. Next, we present further generalization of our approach, and examples employing specific indicators involving intensity correlations for unbiased multiport interferometers. We discuss generalizations to multiparty entanglement indicators. We show that the use of rates leads to a modification of quantum optical Glauber correlation functions, which gives a new tool for studying nonclassicality, and that it also gives a general method of mapping standard Bell inequalities into ones for optical fields.

We discuss spatially separated stations, $X = A, B, \ldots$ with (passive) interferometers of d_X input and output ports, Fig. 1. In each output, there is a detector which measures intensity. One can assume either a pulsed source, sources acting synchronously [33,34] or that the measurement is performed within a short time gate. Each time gate, or pulsed emission, is treated as a repetition of the experiment building up averages of observables.

Stokes parameters. For the description of polarization of light, the standard approach uses Stokes parameters. Using the photon numbers they read $\langle\hat{\Theta}_j\rangle = \langle\hat{a}_j^\dagger\hat{a}_j - \hat{a}_{j_\perp}^\dagger\hat{a}_{j_\perp}\rangle$, where $j, j_\perp$ denote a pair of orthogonal polarizations of one of three mutually unbiased polarization bases $j = 1, 2, 3$, e.g., $\{H, V\}$, $\{45^\circ, -45^\circ\}$, $\{R, L\}$. The zeroth parameter $\langle\hat{\Theta}_0\rangle$ is the total intensity: $\langle\hat{N}\rangle = \langle\hat{a}_j^\dagger\hat{a}_j + \hat{a}_{j_\perp}^\dagger\hat{a}_{j_\perp}\rangle$. Alternative *normalized* Stokes observables were studied by some of us [35–37]. They were first introduced in Ref. [38], however a different technical approach was used. Following Ref. [35], one can put $\langle\hat{S}_j\rangle = \langle\hat{\Pi}\frac{(\hat{a}_j^\dagger\hat{a}_j - \hat{a}_{j_\perp}^\dagger\hat{a}_{j_\perp})}{\hat{N}}\hat{\Pi}\rangle$, and $\langle\hat{S}_0\rangle = \langle\hat{\Pi}\rangle$, where $\hat{\Pi} = \mathbb{1} - |\Omega\rangle\langle\Omega|$ and $|\Omega\rangle$ is the vacuum state for the considered modes, $\hat{a}_j|\Omega\rangle = \hat{a}_{j_\perp}|\Omega\rangle = 0$. Operationally, in the rth run of an experiment, we register photon numbers in the two exits of a polarization analyzer, n_j^r and $n_{j_\perp}^r$, and divide their difference by their sum. If $n_j^r + n_{j_\perp}^r = 0$, the value is put as zero. This does not require any additional measurements, only the data are differently processed than in the standard approach. In Refs. [35–37], examples of the two-party entanglement conditions and Bell inequalities using normalized Stokes operators were given. Here we present a general approach.

Map from two-qubit entanglement witnesses to entanglement indicators for fields involving Stokes parameters. Pauli operators $\vec{\sigma} = (\hat{\sigma}_1, \hat{\sigma}_2, \hat{\sigma}_3)$ and $\hat{\sigma}_0 = \mathbb{1}$ form a basis in the real space of one-qubit observables. Thus any two-qubit entanglement witness $\hat{W}$ has the following expansion: $\hat{W} = \sum_{\mu,\nu} w_{\mu\nu}\hat{\sigma}_\mu^A \otimes \hat{\sigma}_\nu^B$, where $\mu, \nu = 0, 1, 2, 3$ and $w_{\mu\nu}$ are real coefficients. We have $\langle\hat{W}\rangle_{\rm sep} \geqslant 0$, where $\langle\cdot\rangle_{\rm sep}$ denotes an average for a separable state. We will show that with each witness $\hat{W}$ one can associate entanglement indicators for polarization measurements involving correlations of Stokes observables for quantum optical fields. The maps are $\hat{\sigma}_\mu^A \otimes \hat{\sigma}_\nu^B \to \hat{S}_\mu^A\hat{S}_\nu^B$ and $\hat{\sigma}_\mu^A \otimes \hat{\sigma}_\nu^B \to \hat{\Theta}_\mu^A\hat{\Theta}_\nu^B$, and they link $\hat{W}$ with its quantum optical analogues $\hat{\mathcal{W}}_S = \sum_{\mu,\nu} w_{\mu\nu}\hat{S}_\mu^A\hat{S}_\nu^B$, and $\hat{\mathcal{W}}_\Theta = \sum_{\mu,\nu} w_{\mu\nu}\hat{\Theta}_\mu^A\hat{\Theta}_\nu^B$, which fulfill $\langle\hat{\mathcal{W}}_S\rangle_{\rm sep} \geqslant 0$ and $\langle\hat{\mathcal{W}}_\Theta\rangle_{\rm sep} \geqslant 0$. The proof goes as follows.

Normalized Stokes operators case. It is enough to prove that for any mixed state ϱ one can find a 4×4 density matrix $\hat{\mathfrak{R}}_\varrho^{AB}$ for a pair of qubits, such that

$$\frac{\langle\hat{\mathcal{W}}_S\rangle_\varrho}{\langle\hat{\Pi}^A\hat{\Pi}^B\rangle_\varrho} = {\rm Tr}\hat{W}\hat{\mathfrak{R}}_\varrho^{AB}. \tag{1}$$

First, we show that (1) holds for any pure state $|\psi^{AB}\rangle$.

Let us denote the polarization basis H and V as $\hat{x}_H = \hat{x}_1$ and $\hat{x}_V = \hat{x}_2$. Normalized Stokes operators in arbitrary direction can be put as $\vec{m}\cdot\vec{S}^X$, where $\vec{m}$ is an arbitrary unit real vector, or in the matrix form $\sum_{kl}\hat{\Pi}^X\frac{\hat{x}_k^\dagger(\vec{m}\cdot\vec{\sigma})_{kl}\hat{x}_l}{\hat{N}^X}\hat{\Pi}^X$, with $\hat{x} = \hat{a}$ or $\hat{b}$ depending on the beam X, whereas $\hat{S}_0^X$ reads $\sum_{kl}\hat{\Pi}^X\frac{\hat{x}_k^\dagger\delta_{kl}\hat{x}_l}{\hat{N}^X}\hat{\Pi}^X$. We introduce a set of states

$$\left|\Psi_{km}^{AB}\right\rangle = \hat{a}_k\hat{b}_m\frac{1}{\sqrt{\hat{N}^A\hat{N}^B}}\hat{\Pi}^A\hat{\Pi}^B|\psi^{AB}\rangle, \tag{2}$$

where $k, m \in \{1, 2\}$. This allows us to put

$$\begin{aligned}\langle\psi^{AB}|\hat{S}_\mu^A\hat{S}_\nu^B|\psi^{AB}\rangle &= \sum_{k,l=1}^{2}\sum_{m,n=1}^{2}\sigma_\mu^{kl}\sigma_\nu^{mn}\left\langle\Psi_{km}^{AB}\middle|\Psi_{ln}^{AB}\right\rangle \\ &= {\rm Tr}\hat{\sigma}_\mu^A \otimes \hat{\sigma}_\nu^B\hat{R}_\psi^{AB},\end{aligned} \tag{3}$$

where the matrix elements of $\hat{R}_\psi^{AB}$ are $\langle\Psi_{km}^{AB}|\Psi_{ln}^{AB}\rangle$. As a Gramian matrix, $\hat{R}_\psi^{AB}$ is positive. Except for $|\psi^{AB}\rangle$ describing vacuum at one or both sides, we have $0 < {\rm Tr}\hat{R}_\psi^{AB} = \langle\Pi^A\hat{\Pi}^B\rangle \leqslant 1$. Thus, $\hat{\mathfrak{R}}_\psi^{AB} = \hat{R}_\psi^{AB}/\langle\hat{\Pi}^A\hat{\Pi}^B\rangle$ is an admissible density matrix of two qubits.

For mixed states ϱ, i.e., convex combinations of $|\psi_\lambda^{AB}\rangle$'s with weights p_λ, one gets $\hat{R}_\varrho^{AB} = \sum_\lambda p_\lambda\hat{R}_\lambda^{AB}$ which is

positive definite, and its trace is $\sum_\lambda p_\lambda \mathrm{Tr}\hat{R}^{AB}_\lambda \leqslant 1$. Thus after the re-normalization one gets a proper two-qubit density matrix $\hat{\mathfrak{R}}^{AB}_\varrho$. As purity of a field state $|\psi^{AB}_\lambda\rangle$ does not warrant that the corresponding $\hat{R}^{AB}_\lambda$ is a projector, $\hat{\mathfrak{R}}^{AB}_\varrho$ does not have to have the same convex expansion coefficients in terms of pure two-qubit states, as ϱ in terms of $|\psi^{AB}_\lambda\rangle$'s.

For any separable pure state of two optical beams $|\psi^{AB}\rangle_{\mathrm{prod}}$, defined as $F^\dagger_A F^\dagger_B|\Omega\rangle$, where $F^\dagger_X$ is a polynomial function of creation operators for beam (modes) X, and $|\Omega\rangle$ is the vacuum state of both beams, the matrix $\hat{R}^{AB}$ factorizes: $\hat{R}^{AB} = \hat{R}^A \hat{R}^B$. Simply, $_{\mathrm{prod}}\langle \mathbf{\Psi}^{AB}_{km}|\mathbf{\Psi}^{AB}_{ln}\rangle_{\mathrm{prod}}$ factorizes to $\langle \mathbf{\Psi}^A_k|\mathbf{\Psi}^A_l\rangle\langle \mathbf{\Psi}^B_m|\mathbf{\Psi}^B_n\rangle$, where $\langle \mathbf{\Psi}^X_k|\mathbf{\Psi}^X_l\rangle$ are elements of matrix $\hat{R}^X$ and $|\mathbf{\Psi}^X_l\rangle = \hat{x}_l \frac{1}{\sqrt{\hat{N}^X}} \hat{\Pi}^X F^\dagger_X|\Omega\rangle$. As $\langle\Omega|F_X \hat{\Pi}^X F^\dagger_X|\Omega\rangle^{-1}\hat{R}^X$ can be shown to be a qubit density matrix and $\langle\hat{W}\rangle_{\mathrm{sep}} \geqslant 0$, therefore for pure separable states of the optical beams $\langle\hat{\mathcal{W}}_S\rangle_{\mathrm{prod}} \geqslant 0$. Obviously, $\langle\hat{\mathcal{W}}_S\rangle_{\mathrm{sep}} \geqslant 0$ also for all mixed separable states.

Standard Stokes operators case. Any standard Stokes operator can be put as $\vec{m}\cdot\vec{\Theta}^X = \sum_{kl}\hat{x}^\dagger_k(\vec{m}\cdot\vec{\sigma})_{kl}\hat{x}_l$. We introduce state vectors $|\mathbf{\Phi}^{AB}_{jk}\rangle = \hat{a}_j\hat{b}_k|\psi^{AB}\rangle$. One has

$$\langle\psi^{AB}|\hat{\Theta}^A_\mu\hat{\Theta}^B_\nu|\psi^{AB}\rangle = \mathrm{Tr}\hat{\sigma}^A_\mu\hat{\sigma}^B_\nu\hat{P}^{AB}, \tag{4}$$

where the matrix $\hat{P}^{AB}$ has entries $\langle\mathbf{\Phi}^{AB}_{km}|\mathbf{\Phi}^{AB}_{ln}\rangle$, it is positive definite, and its trace is $\langle\hat{N}_A\hat{N}_B\rangle$. Thus $\hat{\mathfrak{P}}^{AB} = \hat{P}^{AB}/\langle\hat{N}^A\hat{N}^B\rangle$ is an admissible two-qubit density matrix, and one has $\langle\hat{\mathcal{W}}_\Theta\rangle_\varrho/\langle\hat{N}^A\hat{N}^B\rangle_\varrho = \mathrm{Tr}\hat{W}\hat{\mathfrak{P}}^{AB}_\varrho$. All that leads to $\langle\hat{\mathcal{W}}_\Theta\rangle_{\mathrm{sep}} \geqslant 0$. Note that, for a general state $\hat{\mathfrak{R}}^{AB}_\varrho$ does not have to be equal to $\hat{\mathfrak{P}}^{AB}_\varrho$. Still $\hat{\mathfrak{R}}^{AB} = \hat{\mathfrak{P}}^{AB}$ for states of defined photon numbers in both beams.

Reverse map. Any linear separability condition expressible in terms of correlation functions of normalized Stokes parameters reads $\sum_{\mu\nu}\omega_{\mu\nu}\langle\hat{S}^A_\mu\hat{S}^B_\nu\rangle_{\mathrm{sep}} \geqslant 0$. As two-photon states, with one at A and the other at B, are possible field states, thus for any separable such state we must have $\sum_{\mu\nu}\omega_{\mu\nu}\langle\hat{S}^A_\mu\hat{S}^B_\nu\rangle_{sep-2-ph} \geqslant 0$. This is algebraically equivalent to $\sum_{\mu\nu}\omega_{\mu\nu}\langle\hat{\sigma}_\mu\otimes\hat{\sigma}_\nu\rangle_{\mathrm{sep}} \geqslant 0$, for any two-qubit state. We get an entanglement witness. Therefore, we have an isomorphism. Similar proof applies to standard Stokes observables.

Examples. In Ref. [14], we show some examples of entanglement indicators which can be derived with the above method. This includes a necessary and sufficient conditions for detection of entanglement of two optical beams with correlations of Stokes parameters of the two considered kinds.

Detection losses. Consider the usual model of losses: a perfect detector in front of which is a beamsplitter of transmission amplitude η, with the reflection channel describing the losses. Then, $\langle\hat{\Theta}^A_\mu\hat{\Theta}^B_\nu\rangle$ scales down as $\eta^A\eta^B$ (see Sec. II in Ref. [14]), where η^X for $X = A, B$ is the local detection efficiency. We have a full resistance of entanglement detection, using any $\hat{\mathcal{W}}_\Theta$, with respect to such losses. A different character of losses may lead to threshold efficiencies.

For the normalized Stokes parameters, it is enough to consider only pure states, because mixed ones, as convex combinations of such, cannot introduce anything new in entanglement conditions linear with respect to the density matrix. Any pure state is a superposition of Fock states $|F\rangle = |n^A_i, n^A_{i_\perp}, n^B_j, n^B_{j_\perp}\rangle$, where n^X_i denotes the number of i polarized photons in beam X, and $\hat{S}^A_\mu\hat{S}^B_\nu$ are diagonal with respect to the Fock basis related with them. Thus, the dependence on efficiencies of the value of an entanglement indicator, in the case of a pure state, depends on the behavior of its Fock components. One can show, see Sec. II in Ref. [14], that $\langle F_\eta|\hat{S}^A_\mu\hat{S}^B_\nu|F_\eta\rangle = H_F\langle F|\hat{S}^A_\mu\hat{S}^B_\nu|F\rangle$, where $|F_\eta\rangle$ is the state $|F\rangle$ after the above described losses in both channels, and $H_F = \langle F_\eta|\hat{S}^A_0\hat{S}^B_0|F_\eta\rangle$, which reads $\prod_{X=A,B}[1-(1-\eta^X)^{m^X}]$, where m^X is the total number of photons in channel X, before the losses. Expanding $|F\rangle$ in terms of Fock states with respect to different polarizations than $i, i_\perp$ and $j, j_\perp$, does not change the values of m^X, and thus the formula stays put for any indices. Again we have a strong resistance of the entanglement indicators with respect to losses. Especially for states with high photon numbers, the entanglement conditions based on normalized Stokes parameters, may be more resistant to losses, because $0 < \eta < 1$, one has $\eta < 1-(1-\eta)^n$.

Multiparty case. Consider three parties, and the case of indicators of genuine three-beam entanglement. Any genuine three-qubit entanglement witness $\hat{W}^{(3)}$ has the property that it is positive for pure product three-qubit states $|\xi\rangle_{AB,C} = |\psi\rangle_{AB}|\phi\rangle_C$, for similar ones with qubits permuted, and for all convex combinations of such states. With any pure partial product state of the optical beams, e.g., $|\Xi\rangle_{AB,C} = F^\dagger_{AB}F^\dagger_C|\Omega\rangle$, where $F^\dagger_{AB}$ is an operator built of creation operators for beams A and B, etc., one can associate, in a similar way as above, a partially factorizable three-qubit density matrix $\hat{\mathfrak{R}}^{AB}_\psi\hat{\mathfrak{R}}^C_\phi$. Thus the homomorphism works. Generalizations are obvious.

General theory. Consider a beam of d_A quantum optical modes propagating toward a measuring station A, and a beam of d_B modes toward station B. We associate with the situation a $d_A\times d_B$-dimensional Hilbert Space, $\mathbb{C}^{d_A}\otimes\mathbb{C}^{d_B}$, which contains pure states of a pair of qudits of dimensions d_A and d_B. For $X = A, B$, let $\hat{V}^X_i$, with $i = 1,\ldots,d^2_X$, be an orthonormal, i.e., $\mathrm{Tr}\hat{V}^X_i\hat{V}^X_j = \delta_{ij}$, Hermitian basis of the space of Hermitian operators acting on $\mathbb{C}^{d_X}$. Therefore products $\hat{V}^A_i\otimes\hat{V}^B_j$ form an orthonormal basis of the space of Hermitian operators acting on $\mathbb{C}^{d_A}\otimes\mathbb{C}^{d_B}$. Thus any entanglement witness for the pair of qudits, $\hat{W}$, can be expanded into

$$\hat{W} = \sum_{j=1}^{d_A^2}\sum_{k=1}^{d_B^2} w_{jk}\hat{V}^A_j\otimes\hat{V}^B_k, \tag{5}$$

with real w_{jk}. The optimal expansion (with the minimal number of terms) is to use a Schmidt basis for $\hat{W}$.

Each $\hat{V}^X_j$ can be decomposed to a linear combination of its spectral projections linked with their respective eigenbases, $|x^{(j)}_l\rangle$, where $x = a$ or b consistently with X and $l = 1,\ldots,d_X$. If one fixes a certain pair of bases in $\mathbb{C}^{d_A}$ and $\mathbb{C}^{d_B}$ as "computational ones," i.e., starting ones, denoted as $|l_x\rangle$, one can always find local unitary matrices $U^X(j)$ such that $U^X(j)|l_x\rangle = |x^{(j)}_l\rangle$. The construction of Reck *et al.* [39] fixes (phases in) a local multiport interferometer, which performs such a transformation. We shall call such interferometers $U^X(j)$ ones. In the case of field modes a passive interferometer performs the following mode transformation: $\sum_k U^X(j)_{lk}\hat{x}^\dagger_k = \hat{x}^\dagger_l(j)$, where $\hat{x}^\dagger_l(j)$ is the photon creation operator in the lth exit mode of interferometer $U^X(j)$.

A two-party entanglement witness $\hat{\mathcal{W}}_R$ for optical fields, which uses correlations of intensity *rates* behind pairs of $U^X(j)$ interferometers can be constructed as follows. For the output l_x of an interferometer, one defines rate observables as $\hat{r}_{l_x} = \hat{\Pi}^X \frac{\hat{n}_{l_x}}{\hat{N}^X} \hat{\Pi}^X$, where $\hat{N}^X = \sum_{l_x=1}^{d_X} \hat{n}_{l_x}$. The witness $\hat{W}$ expanded in terms of the computational basis:

$$\hat{W} = \sum_{k,m}^{d_A} \sum_{l,n}^{d_B} w_{klmn} |k_a, l_b\rangle\langle m_a, n_b|, \tag{6}$$

allows us to form an entanglement witness for fields:

$$\hat{\mathcal{W}}_R = \sum_{k,m} \sum_{l,n} w_{klmn} \hat{\Pi}^A \hat{\Pi}^B \frac{\hat{a}_k^\dagger \hat{b}_l^\dagger \hat{a}_m \hat{b}_n}{\hat{N}^A \hat{N}^B} \hat{\Pi}^A \hat{\Pi}^B. \tag{7}$$

For any pure state of the quantum beams $|\Psi\rangle$

$$\frac{\langle\Psi|\hat{\mathcal{W}}_R|\Psi\rangle}{\langle\Psi|\hat{\Pi}^A\hat{\Pi}^B|\Psi\rangle} = \mathrm{Tr}\hat{W}\hat{\mathcal{R}}, \tag{8}$$

where the matrix $\hat{\mathcal{R}}$ has elements r_{klmn}

$$r_{klmn} = \frac{1}{\langle\Psi|\hat{\Pi}^A\hat{\Pi}^B|\Psi\rangle} \langle\Psi|\hat{\Pi}^A\hat{\Pi}^B \frac{\hat{a}_k^\dagger \hat{b}_l^\dagger \hat{a}_m \hat{b}_n}{\hat{N}^A\hat{N}^B} \hat{\Pi}^A\hat{\Pi}^B|\Psi\rangle. \tag{9}$$

Using a generalization of the earlier derivations, one can show that $\hat{\mathcal{R}}$ is a two-qudit density matrix, and so on.

The actual measurements, to be correlations of local ones, should be performed using the sequence of pairs of $U^X(j)$ interferometers, which enter the expansion of the two-qudit entanglement witness (5). In the entanglement indicator the rates at output $x_l(j)$ of the given local interferometer $U^X(j)$ are multiplied by the respective eigenvalue of $\hat{V}_j^X$ related with the eigenstate $|x_l^{(j)}\rangle$.

To get an entanglement witness for intensities $\hat{\mathcal{W}}_I$ we take $\hat{W}$ and replace the computational basis kets and bras by suitable creation and annihilation operators:

$$\hat{\mathcal{W}}_I = \sum_{k,m}^{d_A} \sum_{l,n}^{d_B} w_{klmn} \hat{a}_k^\dagger \hat{b}_l^\dagger \hat{a}_m \hat{b}_n. \tag{10}$$

For any pure state of the quantum beams $|\Psi\rangle$, one has $\frac{\langle\Psi|\hat{\mathcal{W}}_I|\Psi\rangle}{\langle\Psi|\hat{N}_A\hat{N}_B|\Psi\rangle} = \mathrm{Tr}\hat{W}\hat{\mathcal{P}}$, where the matrix $\hat{\mathcal{P}}$ has elements $\frac{1}{\langle\Psi|\hat{N}_A\hat{N}_B|\Psi\rangle}\langle\Psi|\hat{a}_k^\dagger\hat{b}_l^\dagger\hat{a}_m\hat{b}_n|\Psi\rangle$,and has all properties of a two-qudit density matrix.

Example showing further extension to unitary operator bases. Let d be a power of a prime number. Consider $d_A = d_B = d$ beams experiment (see Fig. 1), with families of $U^X(m)$ interferometers which link the computational basis of a qudit with an unbiased basis m, belonging to the full set of $d+1$ mutually unbiased ones [40,41]. We introduce a set of unitary observables for a qudit: $\hat{q}_k(m) = \sum_{j=1}^d \omega^{jk} |j(m)\rangle\langle j(m)|$,with $|j(m)\rangle = U(m)|j\rangle$ and it is the jth member of mth mutually unbiased basis, and $\omega = \exp(2\pi i/d)$. Operators $\hat{q}_k(m)/\sqrt{d}$ with $k = 1, \ldots, d-1$ and $m = 0, \ldots, d$ and $\hat{q}_0(0)/\sqrt{d}$ form an orthonormal basis in the Hilbert-Schmidt space of all $d \times d$ matrices (see Sec. III in Ref. [14]). Thus we can expand any qudit density matrix as

$$\varrho = \frac{1}{\sqrt{d}} \left[c_{0,0}\hat{q}_0(0) + \sum_{m=0}^{d} \sum_{k=1}^{d-1} c_{m,k}\hat{q}_k(m) \right], \tag{11}$$

where $c_{m,k} = \mathrm{Tr}\hat{q}_k^\dagger(m)\varrho/\sqrt{d}$, and $c_{0,0} = 1/\sqrt{d}$. As the basis observables are unitary the expansion coefficients of an entanglement witness operator in terms of such tensor products of such bases are in general complex. This is no problem for theory, but renders useless a direct application in experiments, as one cannot expect the experimental averages to be real, and thus one has to introduce modifications. Below we present one.

The condition $\mathrm{Tr}\varrho^2 \leqslant 1$ can be put as

$$\frac{1}{d} + \frac{1}{d} \sum_{m=0}^{d} \sum_{k=1}^{d-1} |\mathrm{Tr}\varrho\hat{q}_k(m)|^2 \leqslant 1. \tag{12}$$

Thus, applying Cauchy-Schwartz estimate, we get immediately a separability condition for two qudits:

$$\sum_{m=0}^{d} \sum_{k=1}^{d-1} \left|\mathrm{Tr}\varrho_{\mathrm{sep}}^{AB} \hat{q}_k^A(m) \hat{q}_k^{B\dagger}(m)\right| \leqslant (d-1). \tag{13}$$

Our general method defines a Cauchy-Schwartz-like separability condition homomorphic with (13) as

$$\sum_{m=0}^{d} \sum_{k=1}^{d-1} \left|\left\langle \hat{Q}_k^A(m) \hat{Q}_k^{B\dagger}(m)\right\rangle_{\mathrm{sep}}\right| \leqslant (d-1)\langle\hat{\Pi}^A\hat{\Pi}^B\rangle_{\mathrm{sep}}, \tag{14}$$

where

$$\hat{Q}_k^X(m) = \sum_{j=1}^{d} \hat{\Pi}^X \frac{\omega^{jk}\hat{n}_j^X(m)}{\hat{N}^X} \hat{\Pi}^X. \tag{15}$$

Here, $\hat{n}_j^X(m) = \hat{x}_j^\dagger(m)\hat{x}_j(m)$ is a photon number operator for output mode j of a multiport m, at station X. For generalized observables based on intensity, one can introduce $\hat{\chi}_k(m) = \sum_{j=1}^d \omega^{jk}\hat{n}_j(m)$ to get the following separability condition:

$$\sum_{m=0}^{d} \sum_{k=1}^{d-1} \left|\left\langle \hat{\chi}_k^A(m) \hat{\chi}_k^{B\dagger}(m)\right\rangle_{\mathrm{sep}}\right| \leqslant (d-1)\langle\hat{N}^A\hat{N}^B\rangle_{\mathrm{sep}}. \tag{16}$$

Reference [14] presents other examples.

Implications for optical coherence theory. The approach can be generalized further. Let us take as an example Glauber's correlation functions for optical fields, say $G^{(4)}$ in the form of $\langle\hat{I}_A(\vec{x},t)\hat{I}_B(\vec{x}',t')\rangle$, where the intensity operator has the usual form of $I_X(\vec{x},t) = \hat{F}_X^\dagger(\vec{x},t)\hat{F}_X(\vec{x},t)$, with normal ordering requiring that operator $\hat{F}_X(\vec{x},t)$ is built out of local annihilation operators. The idea of normalized Stokes operators suggests the following alternative correlation function $\Gamma^4(\vec{x},t;\vec{x}',t')$ given by

$$\left\langle \Pi^A\Pi^B \frac{\hat{I}_A(\vec{x},t)\hat{I}_B(\vec{x}',t')}{\int_{a(A)} d\sigma(\vec{x})\hat{I}_A(\vec{x},t)\int_{a(B)} d\sigma(\vec{x}')\hat{I}_B(\vec{x}',t')} \Pi^A\Pi^B \right\rangle, \tag{17}$$

where $a(X)$ denotes the overall aperture of the detectors in location X. Obviously one has $\int_{a(A)} d\sigma(\vec{x}) \int_{a(B)} d\sigma(\vec{x}')\Gamma^4(\vec{x},t;\vec{x}',t') = \langle \Pi^A \Pi^B \rangle$, and for fixed t and t', one can define

$$\varrho(\vec{x},\vec{y},\vec{x}'\vec{y}')_{t,t'} = \langle \Pi^A \Pi^B \rangle^{-1} \left\langle \Pi^A \Pi^B \frac{\hat{F}_A^\dagger(\vec{y},t)\hat{F}_A(\vec{x},t)\hat{F}_B^\dagger(\vec{y}',t')\hat{F}_B(\vec{x}',t')}{\int_{a(A)} d\sigma(\vec{x})\hat{I}_A(\vec{x},t)\int_{a(B)} d\sigma(\vec{x}')\hat{I}_B(\vec{x}',t')} \Pi^A \Pi^B \right\rangle,$$

which behaves like a proper two-particle density matrix, provided one constrains the range of $\vec{x},\vec{y},\vec{x}',\vec{y}'$ to appropriate sets of apertures. As our earlier considerations use simplified forms of (17), it is evident that such correlation functions may help us to unveil nonclassicality in situations in which the standard ones fail, see, e.g., Ref. [8].

Bell inequalities. The above ideas allow one to introduce a general mapping of qudit Bell inequalities to the ones for optical fields. A two-qudit Bell inequality for a final number of local measurement settings α and β has the following form:

$$\sum_{\alpha\beta}\sum_{i=1}^{d_A}\sum_{j=1}^{d_B} K^{ij}_{\alpha\beta} P_{ij}(\alpha,\beta) + \sum_{i=1}^{d_A}\sum_{\alpha} N^i_\alpha P_i(\alpha) + \sum_{j=1}^{d_B}\sum_{\beta} M^j_\beta P_j(\beta) \leqslant L_R, \quad (18)$$

where $P_{ij}(\alpha,\beta)$ denotes the probability of the qudits ending up respectively at detectors i and j, when the local setting are as indicated, and $\sum_j P_{ij}(\alpha,\beta) = P_i(\alpha)$ and $P_j(\beta) = \sum_i P_{ij}(\alpha,\beta)$. The coefficient matrices K, N, M are real, and L_R is the maximum value allowed by local realism. The bound is calculated by putting $P_{ij}(\alpha,\beta) = D^i(\alpha)D^j(\beta)$ and $P_i(\alpha) = D^i(\alpha)$, $P_j(\beta) = D^j(\beta)$, with constraints $0 \leqslant D^i(\alpha/\beta) \leqslant 1$, and $\sum_{i=1}^{d_{A/B}} D^i(\alpha/\beta) = 1$. As for a given run of a quantum optical experiment local measured photon intensity rates $r_i(\alpha)$ and $r_j(\beta)$ satisfy exactly the same constraints. We can replace $P_{ij}(\alpha,\beta) \to \langle r_i(\alpha) r_j(\beta)\rangle_{LR}$, and $P_i(\alpha) \to \langle r_i(\alpha)\rangle_{LR}$, etc., where $\langle . \rangle_{LR}$ is an average in the case of local realism. The bound L_R stays put. To get a Bell operator we further replace the above by rate observables $\hat{r}_i(\alpha)\hat{r}_j(\beta)$, etc. Thus any (multiparty) Bell inequality, see, e.g., Ref. [42], can be useful in quantum optical intensity (rates) correlation experiments. The presented methods for entanglement indicators and the Bell inequalities allow also to get steering inequalities for quantum optics.

Conclusions. We present tools for a construction of entanglement indicators for optical fields, inspired by the vast literature [10] on entanglement witnesses for finite dimensional quantum systems. The indicators would be handy for more intense light beams in states of undefined photon numbers, especially in the emerging field of integrated optics multispatial mode interferometry (see Ref. [14] for examples). One may expect applications in the case of many-body systems, e.g., for an analysis of nonclassicality of correlations in Bose-Einstein condensates, like in the ones reported in Ref. [43].

Acknowledgments. The work is part of the ICTQT IRAP project of FNP, financed by structural funds of EU. MZ acknowledges COPERNICUS grant-award and discussions with Maria Chekhova and Harald Weinfurter. JR acknowledges the National Research Foundation, Prime Minister's Office, Singapore, and the Ministry of Education, Singapore, under the Research Centres of Excellence programme, and discussions with Dagomir Kaszlikowski. MW acknowledges NCN Grants No. 2015/19/B/ST2/01999 and No. 2017/26/E/ST2/01008.

[1] J.-W. Pan, Z. B. Chen, C. Y. Lu, H. Weinfurter, A. Zeilinger, and M. Żukowski, Rev. Mod. Phys. **84**, 777 (2012).
[2] A. Aspect, P. Grangier, and G. Roger, Phys. Rev. Lett. **49**, 91 (1982).
[3] D. M. Greenberger, M. A. Horne, and A. Zeilinger, *Bell's Theorem, Quantum Theory, and Conceptions of the Universe*, edited by M. Kafatos (Kluwer, Dordrecht, 1989), pp. 69–72.
[4] K. Banaszek and K. Wódkiewicz, Phys. Rev. A **58**, 4345 (1998); Acta. Phys. Slov. **49**, 491 (1999).
[5] C. Simon and D. Bouwmeester, Phys. Rev. Lett. **91**, 053601 (2003).
[6] M. V. Chekhova, G. Leuchs, and M. Żukowski, Opt. Commun. **337**, 27 (2015).
[7] A. Einstein, B. Podolsky, and N. Rosen, Phys. Rev. **47**, 777 (1935).
[8] K. Rosołek, K. Kostrzewa, A. Dutta, W. Laskowski, M. Wieśniak, and M. Żukowski, Phys. Rev. A **95**, 042119 (2017).
[9] G. A. Durkin, C. Simon, and D. Bouwmeester, Phys. Rev. Lett. **88**, 187902 (2002).
[10] R. Horodecki, P. Horodecki, M. Horodecki, and K. Horodecki, Rev. Mod. Phys. **81**, 865 (2009).
[11] R. Simon, Phys. Rev. Lett. **84**, 2726 (2000).
[12] L. M. Duan, G. Giedke, J. I. Cirac, and P. Zoller, Phys. Rev. Lett. **84**, 2722 (2000).
[13] M. Hillery and M. S. Zubairy, Phys. Rev. Lett. **96**, 050503 (2006).
[14] See Supplemental Material at http://link.aps.org/supplemental/10.1103/PhysRevResearch.1.032041 for more details.
[15] T. Sh. Iskhakov, I. N. Agafonov, M. V. Chekhova, and G. Leuchs, Phys. Rev. Lett. **109**, 150502 (2012).
[16] B. Kanseri, T. Iskhakov, G. Rytikov, M. Chekhova, and G. Leuchs, Phys. Rev. A **87**, 032110 (2013).
[17] H. S. Eisenberg, G. Khoury, G. A. Durkin, C. Simon, and D. Bouwmeester, Phys. Rev. Lett. **93**, 193901 (2004).
[18] T. Sh. Iskhakov, K. Y. Spasibko, M. V. Chekhova, and G. Leuchs, New J. Phys. **15**, 093036 (2013).
[19] A. Lamas-Linares, J. C. Howell, and D. Bouwmeester, Nature (London) **412**, 887 (2001).

[20] A. Eckstein, A. Christ, P. J. Mosley, and C. Silberhorn, Phys. Rev. Lett. **106**, 013603 (2011).
[21] K. Yu. Spasibko, D. A. Kopylov, V. L. Krutyanskiy, T. V. Murzina, G. Leuchs, and M. V. Chekhova, Phys. Rev. Lett. **119**, 223603 (2017).
[22] K. Mattle, M. Michler, H. Weinfurter, A. Zeilinger, and M. Żukowski, Appl. Phys. B **60**, S111 (1995).
[23] G. Weihs, M. Reck, H. Weinfurter, and A. Zeilinger, Phys. Rev. A **54**, 893 (1996).
[24] A. Peruzzo, A. Laing, A. Politi, T. Rudolph and J. L. O'Brien, Nat. Commun. **2**, 224 (2011).
[25] T. Meany, M. Delanty, S. Gross, G. D. Marshall, M. J. Steel, and M. J. Withford, Opt. Express **20**, 26895 (2012).
[26] B. J. Metcalf *et al.*, Nat. Commun. **4**, 1356 (2013).
[27] N. Spagnolo, C. Vitelli, L. Aparo, P. Mataloni, F. Sciarrino, A. Crespi, R. Ramponi, and R. Osellame, Nat. Commun. **4**, 1606 (2013).
[28] J. Carolan *et al.*, Science **349**, 711 (2015).
[29] C. Schaeff, R. Polster, M. Huber, S. Ramelow, and A. Zeilinger, Optica **2**, 523 (2015).
[30] A. Sørensen, L.-M. Duan, J. I. Cirac, and P. Zoller, Nature (London) **409**, 63 (2001).
[31] J. Hald, J. L. Sørensen, C. Schori, and E. S. Polzik, Phys. Rev. Lett. **83**, 1319 (1999).
[32] A. S. Sørensen and K. Mølmer, Phys. Rev. Lett. **86**, 4431 (2001).
[33] M. Żukowski, A. Zeilinger and H. Weinfurter, Ann. NY Acad. Sci. **755**, 91 (1995).
[34] R. Kaltenbaek, B. Blauensteiner, M. Żukowski, M. Aspelmeyer, and A. Zeilinger, Phys. Rev. Lett. **96**, 240502 (2006).
[35] M. Żukowski, W. Laskowski, and M. Wieśniak, Phys. Rev. A **95**, 042113 (2017).
[36] M. Żukowski, W. Laskowski, and M. Wieśniak, Phys. Scr. **91**, 084001 (2016).
[37] M. Żukowski, M. Wieśniak, and W. Laskowski, Phys. Rev. A **94**, 020102(R) (2016).
[38] Q. Y. He, M. D. Reid, T. G. Vaughan, C. Gross, M. Oberthaler, and P. D. Drummond, Phys. Rev. Lett. **106**, 120405 (2011); Q. Y. He, T. G. Vaughan, P. D. Drummond, and M. D. Reid, New J. Phys. **14**, 093012 (2012).
[39] M. Reck, A. Zeilinger, H. J. Bernstein, and P. Bertani, Phys. Rev. Lett. **73**, 58 (1994).
[40] W. K. Wootters and B. D. Fields, Ann. Phys. **191**, 363 (1989).
[41] I. D. Ivanovic, J. Phys. A: Math. Gen. **14**, 3241 (1981).
[42] N. Brunner, D. Cavalcanti, S. Pironio, V. Scarani, and S. Wehner, Rev. Mod. Phys. **86**, 419 (2014).
[43] R. Schmied, J.-D. Bancal, B. Allard, M. Fadel, V. Scarani, P. Treutlein, and N. Sangouard, Science **352**, 441 (2016).

scientific reports

Check for updates

OPEN

Simplified quantum optical Stokes observables and Bell's theorem

Konrad Schlichtholz✉, Bianka Woloncewicz✉ & Marek Żukowski

We discuss a simplified form of Stokes operators for quantum optical fields that involve the known concept of binning. Behind polarization analyzer photon numbers (more generally intensities) are measured. We have two outputs, say, for horizontal and vertical polarization. If the value obtained in horizontal output is greater than in vertical one we put 1. Otherwise, we put – 1. For equal photon numbers, we put 0. Such observables do not have all properties of the Stokes operators, but can be employed in Bell type measurements, involving polarization analyzers. They are especially handy for states of undefined number of photons, e.g. squeezed vacuum and their realisation is intuitive. We show that our observables can lead to quite robust violations of associated Bell inequalities. We formulate a strongly supported numerically conjecture that one can observe with this approach violations of local realism for the four mode squeezed vacuum for all pumping powers (i.e. gain values).

The discussion about what is the essence of quantumness started with the first attempts of formulating quantum mechanics. With the emblematic paper of Einstein et al.[1] the problem of completeness of quantum mechanics became a point of discussion among the scientific community. This started with the response by Bohr[2]. Many years later, after the paper of Bell[3] the challenge of revealing non-classicality, in terms of violation of local realism, has entered the core of contemporary research. All that in the meantime gained in importance with the emergence of quantum information and communication.

The ultimate test of non-classicality is the violation of Bell inequalities. This is now also the essence of testing of device-independent quantum communication protocols. Formulations of Bell's theorem for situations of fixed numbers of particles have already a vast literature, and well established methods, see e.g. reviews[4–7]. However, if one moves to situations with undefined numbers of particles, still the situation is quite open. This is of course e.g. the case of general quantum optical fields. A lot of approaches are tested.

Polarization entanglement experiments are classic examples of experimental tests of Bell's inequalities. The two photon experiments are a realization of two qubit-entanglement[8,9]. A deceptively obvious step in the direction towards optical fields of undefined photon numbers is to use quantum Stokes observables. The usual definition of these runs as follows. If one assumes that the intensity of light is proportional to the photon number, then (standard) quantum Stokes observables are given by $\hat{\Theta}_i = \hat{a^\dagger}_i \hat{a}_i - \hat{a^\dagger}_{i_\perp} \hat{a}_{i_\perp}$, where $\hat{a}$ is an annihilation operator. Indices $i = 1, 2, 3$ mark three mutually unbiased (fully complementary) polarization analyzers settings. The indexes, i and $i_\perp$ stand for two orthogonal polarizations. E.g., one might choose the i's to represent horizontal-vertical, $\{H, V\}$, diagonal-antidiagonal, $\{45°, -45°\}$, or right-left handed circular, $\{R, L\}$, polarization analyzer settings. The zeroth Stokes operator is given by the total photon number operator $\hat{\Theta}_0 = \hat{N} = \hat{a^\dagger}_i \hat{a}_i + \hat{a^\dagger}_{i_\perp} \hat{a}_{i_\perp}$[10].

If we are interested in the degree of polarisation of light we use $\left(\frac{\sum_i \langle \Theta_i \rangle^2}{\langle \Theta_0 \rangle^2}\right)^{1/2}$. Obviously, this parameter is not a formal quantum observable (a self-adjoint linear operator). Neither is $\frac{\langle \Theta_i \rangle}{\langle \Theta_0 \rangle}$. This is one of the reasons why attempts to build Bell inequalities using such parameters and their correlators for observation stations A and B in the form of $\frac{\langle \Theta_i^A \Theta_j^B \rangle}{\langle \Theta_0^A \Theta_0^B \rangle}$ fail and lead to misleading conclusions[11]. This is because such attempts involve additional assumptions, beyond the usual ones for Bell inequalities, which limit the range of local hidden variable theories for with such Bell inequalities must hold.

Bell inequalities for Stokes parameters can be formulated if one introduces normalized Stokes observables[12–14]:

$$\hat{S}_j = \hat{\Pi} \frac{\hat{n}_j - \hat{n}_{j_\perp}}{\hat{n}_j + \hat{n}_{j_\perp}} \hat{\Pi}, \tag{1}$$

where $\hat{\Pi} = \mathbb{I} - |\Omega\rangle\langle\Omega|$, and $|\Omega\rangle$ is the vacuum state (of the optical beam in question).

University of Gdansk, International Centre for Theory of Quantum Technologies (ICTQT), 80-308 Gdańsk, Poland. ✉email: konrad.schlichtholz@phdstud.ug.edu.pl; bianka.woloncewicz@phdstud.ug.edu.pl

It has been shown that such operators allow for the construction of stronger entanglement criteria, and they are a handy tool for formulation of Bell inequalities. One of their properties, crucial in this case, is the fact that these operators have a spectrum bounded by -1 and 1. That is, they have the basic property of observables which allows one to derive the CHSH-Bell inequalities. Thus, a derivation of a version of CHSH inequality applicable for such Stokes operators is essentially a replacement procedure. With the recent development of measurement techniques allowing photon number resolving detection[15,16] the discussion about normalized Stokes parameters stops to be only theoretical and its use in experiments is becoming feasible.

Note that what makes Pauli operators so straightforwardly applicable to Bell inequalities is their dichotomic nature. One of the attempts to construct field operators of a similar property was the formulation of pseudo-spin operators. For example, the z component of pseudo-spin is $(-1)^{\hat{n}}$, where $\hat{n}$ is the total photon number operator in the given optical mode[17,18]. The spectrum of pseudo-spin operators is the same as the spectrum of Pauli matrices, but their use introduces great difficulties from the experimental point of view. Even a loss of one photon (due to e.g. detector inefficiency) or a single dark count reverses the result of a measurement.

Here we analyze a simpler approach, which leads to proper Bell inequalities for polarization measurements of quantum optical fields. Our aim is to construct a family of operators that would have the usual spectrum for Bell experiments and would be robust with respect to experimental noise. We present polarization quantum field observables that have spectrum limited to ± 1 and 0. Our initial ideas on such binning can be found in[19]. The approach to binning presented here is concurrent with the method used in[20] in the context of correlation in Bose-Einstein condensates. With the observables, we construct Bell inequalities. We test their resilience under losses and noise for 2×2 mode bright squeezed vacuum and bright GHZ radiation. The observables are realizable in the laboratory with standard measurement devices. They are described in the next section.

New operators: sign Stokes operators

It was shown that Bell inequalities constructed with normalized Stokes operators can be violated by macroscopic states of light such as 2×2 (bright) squeezed vacuum (BSV)[14] and its GHZ-like generalization (BGHZ)[21]. However, for a higher mean number of photons, the violation of Bell inequalities by these states is quickly damped. This results in lowering of the threshold values for pumping strength after which violation cannot be observed.

We address those problems by another normalization scheme, based on the so-called binning, which we call Sign approach normalization. To obtain new operators, we use the sign function and apply it to Stokes operators:

$$\hat{G}(s) = \mathrm{sign}(\hat{n}_s - \hat{n}_{s_\perp}) = \mathrm{sign}(\hat{\Theta}_s) = \mathrm{sign}(\hat{U}_s(\hat{n}_H - \hat{n}_V)U_s^\dagger), \tag{2}$$

where s denotes the chosen setting related with the corresponding polarization basis with the eingenstates given by s and $s_\perp$. Subscripts H and V refer to horizontal and vertical polarizations, and the operator $\hat{U}_s$ is a unitary transformation that transforms the polarization modes H, V into another orthogonal pair of, in general, elliptic polarization modes $\{s, s_\perp\}$. From (2) we see that the eigenstates of $G(s)$ are $|j_s k_{s_\perp}\rangle = \frac{1}{\sqrt{j!k!}} \hat{a}_s^{\dagger j} \hat{a}_{s_\perp}^{\dagger k} |\Omega\rangle$, where $\hat{a}_s^\dagger$ and $\hat{a}_{s_\perp}^\dagger$ are creation operators related to the respective polarization modes of the given beam. The spectral form of (2) is given by:

$$\hat{G}(s) = \sum_{k>j} \Big(|k_s, j_{s_\perp}\rangle\langle k_s, j_{s_\perp}| - |j_s, k_{s_\perp}\rangle\langle j_s, k_{s_\perp}| \Big). \tag{3}$$

Formula (3) clearly shows that the new operators are well-defined Hermitian operators and that each $\hat{G}(i)$ has three eigenvalues ± 1 and 0. Although formula (2) implies photon number operators, the basic idea of sign as well as standard and normalized Stokes operators is based on differences and sums of intensities. These in turn do not need to be modeled with photon counts. Note that formula (3) does not imply any particular model of intensity as long as the intensity increases with number of counts (even nonlinearly).

The action of the sign function on Stokes operators can be regarded as some form of the binning strategy used in the context of polarization measurements. Binning strategies are e.g. used in homodyne schemes for observing non-classicality[22–25].

We shall call the new operators sign Stokes operators. Following the usual approach, we shall define a triad of sign Stokes operators, related to the three maximally complementary settings of a polarization analyzer. For the usual triad of such settings, we denote by $\hat{G}_1$ the sign operator the eigenstates of which refer to $\{s = D, s_\perp = A\}$ polarization basis, and by $\hat{G}_2$ and $\hat{G}_3$ for respectively $\{R, L\}$ and $\{H, V\}$ bases. However, this notation is also extended to other triads of maximally complementary settings.

The sign operators share some properties of Stokes and normalized Stokes operators. Importantly, once one has a photon-number-resolving detection setup, the data collected in each run allows one to compute the obtained values of each of Stokes operators for the given basis i: standard, normalized, and sign ones, as they depend solely on the measured photon numbers n_i and $n_{i\perp}$. As we see, the new approach is in fact just a new form of data analysis that turns out to be simple and efficient. Further, in order to measure different sign operators $\hat{G}_{s'}$, that is, to move from s to s', it is enough to change the polarization analysis basis. Being useful from experimental point of view, unfortunately sign Stokes operators do not share all properties of quantum Stokes operators, what puts some limitations on their use in entanglement detection.

Stokes-like vector cannot be formed out of sign Stokes operators. Standard Stokes operators form a Stokes vector. We will discuss this property for pure states. However, it works also for mixed ones. We have $\langle \vec{\hat{\Theta}} \rangle_\psi = (\langle \hat{\Theta}_1 \rangle_\psi, \langle \hat{\Theta}_2 \rangle_\psi, \langle \hat{\Theta}_3 \rangle_\psi)$ where $|\psi\rangle$ is an arbitrary state of the optical field. The Euclidean norm of this vector fulfills : $|| \langle \vec{\hat{\Theta}} \rangle_\psi || \leq \langle \hat{\Theta}_0 \rangle_\psi$. We can construct an analogue vector for normalized Stokes opera-

tors and $||\langle\hat{\mathbf{S}}\rangle_\psi|| \leq \langle\hat{S}_0\rangle_\psi \leq 1$[13]. These norms remain invariant under any unitary transformation between two triads of mutually maximally complementary polarization analysers. This transformation can be put as $a_{3'} = U_{11}a_3 + U_{12}a_{3_\perp}$ and $a_{3'_\perp} = U_{21}a_3 + U_{22}a_{3_\perp}$, where U_{ij} are elements of a certain two-dimensional unitary matrix. Properly defined Stokes vector has its Euclidean norm invariant with respect to such mode transformations. As a transformation of this kind can also be expressed as a transformation of the state, one can introduce $|\psi'\rangle$, which is in the following relation with $|\psi\rangle$. If $|\psi\rangle = f(a_3^\dagger, a_{3_\perp}^\dagger)|\Omega\rangle$, then $f(a_{3'}^\dagger, a_{3'_\perp}^\dagger)|\Omega\rangle = |\psi'\rangle$, where $f(x, y)$ is a polynomial of both variables. We put this relation as $|\psi'\rangle = \hat{U}_{mode}^\dagger|\psi\rangle$, as it is obviously a specific unitary transformation of the state.

For such mode transformations we have $||\langle\hat{\vec{\Theta}}\rangle_\psi|| = ||\langle\hat{\vec{\Theta}}\rangle_{\psi'}||$ and $||\langle\hat{\vec{S}}\rangle_\psi|| = ||\langle\hat{\vec{S}}\rangle_{\psi'}||$. The norm of Stokes vectors, standard and normalized, is constant under any unitary transformation of the triads polarization analysis bases. These features of Stokes observables play a key role in the construction of entanglement indicators involving Stokes operators.

Such properties are not shared by sign operators. Let us construct $\langle\hat{\vec{G}}\rangle_\psi = (\langle\hat{G}_1\rangle_\psi, \langle\hat{G}_2\rangle_\psi, \langle\hat{G}_3\rangle_\psi)$. It can be shown that $||\langle\vec{G}\rangle_\psi|| \neq ||\langle\vec{G}\rangle_{\psi'}||$. It is enough to find one counterexample. Consider the state $|\psi\rangle = |3_H, 0_V\rangle$ i.e. the Fock state with 3 photons polarized horizontally. It can be easily checked that for this state $||\langle\vec{G}\rangle_\psi|| = 1$. Now let us apply a unitary transformation on optical modes of $|\psi\rangle$ such that the creation operators transform as follows: $\hat{a}_H^\dagger \to \hat{a}^\dagger(\alpha) = \cos\alpha\hat{a}_H^\dagger + \sin\alpha\hat{a}_V^\dagger$ and $\hat{a}_V^\dagger \to \hat{a}_\perp^\dagger(\alpha) = -\sin\alpha\hat{a}_H^\dagger + \cos\alpha\hat{a}_V^\dagger$. Let $\alpha = \pi/8$. One gets: $||\langle\vec{G}\rangle_{\psi'}|| \approx 1,5$. Thus, the norm is not an invariant of the unitary transformations, and additionally it is not bounded by 1. This fact prohibits one to use methods of construction of entanglement indicators presented in[13], which work via a simple replacement of Pauli operators in entanglement conditions for qubits, by Stokes operators, standard or normalized. Still, as we shall see, there is no obstacle to using this method in the case of construction of Bell inequalities.

Rotational *covariance* of polarization variables is not a necessary feature required to derive Bell inequalities (however, see[26] for the consequences of demanding exactly that). This allows one to construct CHSH and CH inequalities for fields with sign Stokes observables.

CHSH inequality. To derive Bell inequalities satisfied by any local realistic description, we start by defining local hidden values that predetermine the output of the measurement of sign Stokes operators (2). We denote the local hidden variables by λ. The functions $I^X(s,\lambda)$ and $I^X(s_\perp,\lambda)$ give the predetermined outcomes of the intensity measurements of polarizations s, $s_\perp$ in the local beam for the observer X. We define the local hidden values for sign operators as $G^X(s,\lambda) = \text{sign}(I^X(s,\lambda) - I^X(s_\perp,\lambda))$. These local hidden values are ±1 and 0, thus one can use standard methods to derive CHSH inequality. The alternative settings will be denoted here by s, s' for the first observer and r, r' for the second observer. The resulting CHSH inequality reads:

$$|\langle G^1(s,\lambda)G^2(r,\lambda) + G^1(s,\lambda)G^2(r',\lambda) + G^1(s',\lambda)G^2(r,\lambda) - G^1(s',\lambda)G^2(r',\lambda)\rangle_{LHV}| \leq 2. \tag{4}$$

For further reference, we put it as $|CHSH_G| \leq 2$.

However, this inequality cannot be violated by states with a significant vacuum component, e.g. the (polarization) four-mode squeezed vacuum state, which will be our working example, see next sections. This situation is analogous to the case of normalized Stokes operators, see[14]. Following ideas of[14] we modify sign Stokes operators as follows:

$$\hat{G}^X(s) \to \hat{G}^{X-}(s) = \hat{G}^X(s) - \hat{\Pi}_{\Omega^X}, \tag{5}$$

where $\hat{\Pi}_{\Omega^X}$ is the projector on the subspace of the Fock space of states with no photons in the local beam. Such a projection allows for reduction of the impact of vacuum term, which often appears with the highest probability. Also local hidden values need to be modified:

- $G^{X-}(s,\lambda) = \text{sign}(I^X(s,\lambda) - I^X(s_\perp,\lambda))$ if $I^X(s,\lambda) + I^X(s_\perp,\lambda) \neq 0$
- $G^{X-}(s,\lambda) = -1$ if $I^X(s,\lambda) + I^X(s_\perp,\lambda) = 0$

As this modification does not change local hidden values $G^{X-}(s,\lambda) \in \{0,\pm1\}$ we use the following CHSH inequality:

$$\begin{aligned} |CHSH_{G-}| = |\langle & G^{1-}(s,\lambda)G^{2-}(r,\lambda) + G^{1-}(s,\lambda)G^{2-}(r',\lambda) \\ & + G^{1-}(s',\lambda)G^{2-}(r,\lambda) - G^{1-}(s',\lambda)G^{2-}(r',\lambda)\rangle_{LHV}| \leq 2. \end{aligned} \tag{6}$$

Violation of Bell inequality for four mode squeezed vacuum—asymptotic behaviour. We are going to analyze how the use of sign Stokes operators in CHSH inequality helps to reveal the non-classicality of quantum states. Our working example is 2×2 mode squeezed vacuum state (BSV) which is the generalization of EPR singlet. It reads:

$$|\psi_-\rangle = \frac{1}{\cosh^2(\Gamma)}\sum_{n=0}^{\infty}\frac{\tanh^n(\Gamma)}{n!}(a_H^\dagger b_V^\dagger - a_V^\dagger b_H^\dagger)^n|\Omega\rangle = \frac{1}{\cosh^2(\Gamma)}\sum_{n=0}^{\infty}\sqrt{n+1}\tanh^n(\Gamma)|\psi^n\rangle, \tag{7}$$

where Γ is the amplification gain and

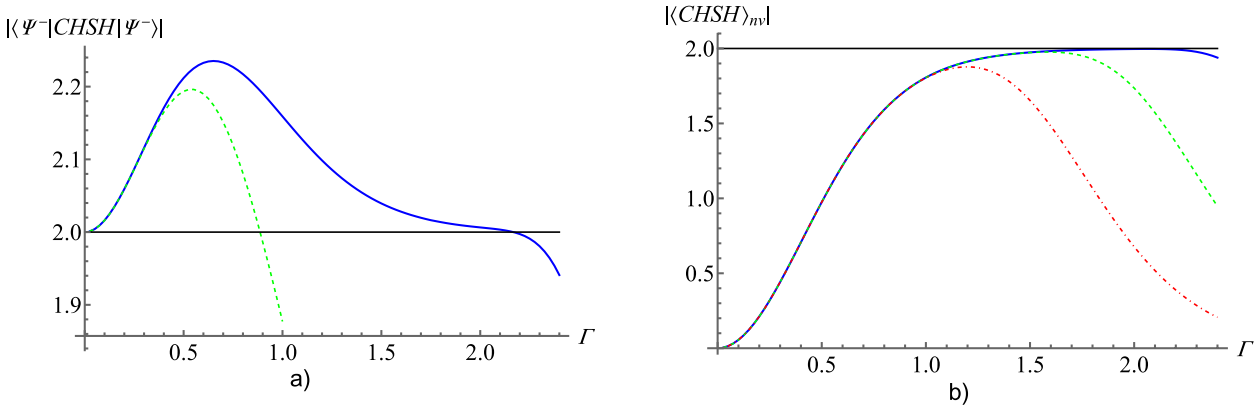

Figure 1. (**a**) The blue curve: the value of the $CHSH_{G-}$ expression based on sign operators, see (6), and the green dashed curve: $CHSH_{S-}$ based on normalized Stokes operators[14] in a function of amplification gain Γ of the *BSV* state. The numerical results were obtained with a cut-off of the expansion of the BSV state at the term $|\psi^{n=150}\rangle$. The maximal values of amplification gain (Γ_{tr}), such that for all $\Gamma < \Gamma_{tr}$ CHSH inequalities are violated, are $\Gamma_{tr} \approx 0.88$ for normalized Stokes operators[14] and $\Gamma_{tr} \approx 2.16$ for sign Stokes operators. Thus, with sign Stokes operators, the range of violation with respect to amplification gain is much larger than in the case of normalized Stokes operators. (**b**) The graphs show the non-vacuum term of $CHSH_{G-}$ as a function of amplification gain Γ for the BSV state, which was computed for cutoffs of 15, 47, 150 photons. This is done to illustrate that the descent of the curves for high Γ's is an artefact of the applied cutoff. The blue curve represents calculations with the cutoff at 150 photons,for the green dashed curve it is at 47 photons and for the red dot-dashed curve at 15 photons. The cutoff seems to be responsible for the decrease of the value in (**a**) for high Γ's.

$$|\psi^n\rangle = \frac{1}{\sqrt{n+1}} \sum_{m=0}^{n} (-1)^m |(n-m)_{H_1}, m_{V_1}, m_{H_2}, (n-m)_{V_2}\rangle. \tag{8}$$

Subscripts $H_{1(2)}$ and $V_{1(2)}$ specify the polarization of each mode and to which of the two optical beams it corresponds. We use the convention that $a_s^\dagger$ denotes the creation operator for the photon heading observer A, and $b_s^\dagger$ is the creation operator related to the observer B. The amplification gain determines the intensity of the pumping field and thus Γ sets the expectation value of the intensity of the BSV state.

Assume that both observers choose to measure only linear polarizations. thus, the angles by which the measurement polarization basis is rotated with respect to $\{H, V\}$ basis define the settings. With the notation used in "Stokes-like vector cannot be formed out of sign Stokes operators" section for unitary transformation between linear polarization modes we chose for the first observer $\alpha_s = 0$, $\alpha_{s'} = \pi/4$, and for the second one $\alpha_r = \pi/8$ and $\alpha_{r'} = -\pi/8$. It was shown that these settings are optimal in case of violation of CHSH inequality with normalized Stokes operators for BSV[14].

Figure 1 shows quantum predictions for $CHSH_{G-}$ (6) and the values of CHSH expression for normalized Stokes parameters for BSV taken from[14] as a function of the amplification gain Γ. Sign Stokes operators give $|\langle\psi_-|CHSH_{G-}|\psi_-\rangle| > 2$ for a wider range of an amplification gain that is up to $\Gamma_{tr} \approx 2.16$. For normalized Stokes operators, this maximal value of amplification gain is significantly lower, i.e. $\Gamma_{tr} \approx 0.8866$. Thus, with sign Stokes operators it is possible to reveal the non-classicality of BSV for a much higher value of amplification gain.

In Fig. 1 we can see that for $\Gamma \approx 2.1$ for sign Stokes operators $|CHSH_{G-}|$ drops down suspiciously suddenly. We presume that such behaviour might be a consequence of a cut-off. The expansion of $|\psi_-\rangle$ was cut off in the numerical calculations at $|\psi^{n=150}\rangle$. This still requires further investigation.

Because of the rotational invariance of $|\psi_-\rangle$, it is a "super-singlet", the expectation values of the correlators entering the Bell inequalities depend, if we measure linear polarizations on both sides, only on *relative angle* of the orientation of the polarization analyzers at the two spatially separated observation stations.

Note that standard, normalized, and sign Stokes operators are composed of functions of photon number operators, which do not change the number of photons. Thus, the expression $\langle\psi_-|CHSH_{G-}|\psi_-\rangle$ consists of two terms: *vacuum term*, that is CHSH inequality averaged over the vacuum component of BSV and *non-vacuum term*. The vacuum and non-vacuum terms in (6) for our settings are both negative. That is why we can consider the CHSH inequality in question as the sum of absolute values of these both terms. The vacuum term can be easily calculated:

$$|\langle\Omega|CHSH_{G-}|\Omega\rangle| = \frac{2}{\cosh^4\Gamma}. \tag{9}$$

The non-vacuum term $\langle CHSH_{G-}\rangle_{nv} = \langle\psi_-|CHSH_{G-}|\psi_-\rangle - \langle\Omega|CHSH_{G-}|\Omega\rangle$ results from the expectation values of $|\psi^n\rangle$. Note that as Γ increases, the role of non-vacuum terms in $\langle\psi_-|CHSH_{G-}|\psi_-\rangle$ increases too. For small Γ the contribution of vacuum term is dominant.

In Fig. 1 the value of the non-vacuum $|\langle CHSH_{G-}\rangle_{nv}|$ is presented. The calculation is performed for BSV state truncated to $n = 150$, blue curve, $n = 47$, green curve, and $n = 15$, red curve. These numbers increase approximately as a geometrical sequence by $\sqrt{10}$ what allows as to analyze the behaviour of $\langle CHSH_{G-}\rangle_{nv}$ within

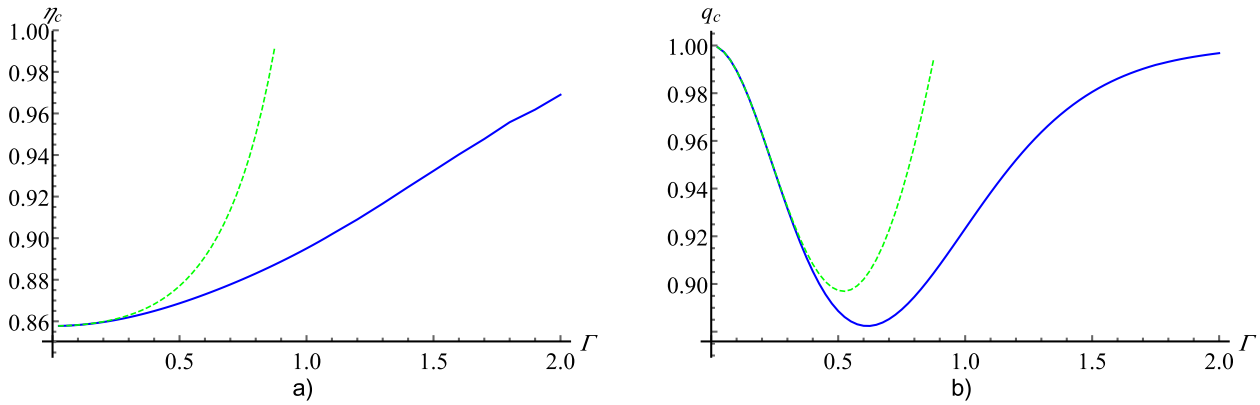

Figure 2. (**a**) Critical efficiency η_c versus Γ for the CHSH inequalities for the BSV state. A blue curve represents η_c for sign approach and a green dashed curve for normalized Stokes operators. (**b**) Critical value of q versus Γ for the BSV state. A blue curve represents q_c for sign approach and a green dashed curve for normalized stokes operators. Assuming that asymptotic behaviour of violation of CHSH inequality for sing parameters discussed in "Violation of Bell inequality for four mode squeezed vacuum—asymptotic behaviour" section is correct the q_c for the sign Stokes operators goes to 1 in the limit $\Gamma \to \infty$.

the whole order of magnitude. All curves asymptotically go to 2 (classical bound) up to some point for which they both start to decrease. Note that the curves for $n = 15$ and $n = 47$ start to decrease for smaller Γ than the curve for $n = 150$. It is highly probable that the decrease is conditioned by not including components with a high enough number of photons and the non-vacuum term $|\langle CHSH_{G-}\rangle_{nv}|$ goes asymptotically to 2 from the left. The vacuum term goes asymptotically to 0 from the right, see (9). Thus, our hypothesis is that CHSH inequality with sign Stokes operators is violated for BSV for any Γ. In Supplementary Discussion A we present a reasoning, based on a numerical calculation, supporting this conjecture.

CHSH inequality with losses. One of the crucial aspects of experimental realization of Bell experiments is detectors with high efficiency η. Here, we will analyze the critical value of efficiency η_c such that for $\eta < \eta_c$ one cannot observe a violation of (6). We model inefficient detectors in the standard way: a perfect detector ($\eta = 1$) with a beamspliter with transmissivity $\sqrt{\eta}$ in front of it. We denote by k the number of photons that reach the beamsplitter. Of these, only $\kappa \leq k$ counts are registered due to losses on the beamspliter. The probability of registration of κ photons is given by the binomial distribution:

$$p(\kappa|k) = \binom{k}{\kappa}\eta^{\kappa}(1-\eta)^{k-\kappa}. \tag{10}$$

In Fig. 2 we can see the minimal value of efficiency η_c for which the violation of CHSH inequality can be observed for normalized and sign Stokes operators in function of Γ. Note that for small Γ (up to $\Gamma \approx 0.3$) the curves for sign and normalized Stokes operators behave almost identically. However, as Γ increases, the value of η_c for sign Stokes operators grows slower than that for normalized ones. Such a change in rate of growth for a higher Γ should be expected because, for a high number of photons, loss of one photon matters less in the case of sign Stokes operators.

CHSH inequality with noise. In a realistic scenario of a Bell experiment apart from photon losses one shall consider also noise. Our noise is modeled in the similar way as "white noise" for qubits. Let us introduce four squeezed vacuum states which are related with the Bell state basis for two qubits[27]:

$$|\Phi^{\pm}\rangle = \frac{1}{\cosh^2(\Gamma)}\sum_{n=0}^{\infty}\frac{\tanh^n(\Gamma)}{n!}(a_H^{\dagger}b_H^{\dagger} \pm a_V^{\dagger}b_V^{\dagger})^n|\Omega\rangle, \tag{11}$$

and

$$|\Psi^{\pm}\rangle = \frac{1}{\cosh^2(\Gamma)}\sum_{n=0}^{\infty}\frac{\tanh^n(\Gamma)}{n!}(a_H^{\dagger}b_V^{\dagger} \pm a_V^{\dagger}b_H^{\dagger})^n|\Omega\rangle. \tag{12}$$

Our noise model can be defined as follows:

$$\rho_{noise} = \frac{1}{4}(|\phi^+\rangle\langle\phi^+| + |\phi^-\rangle\langle\phi^-| + |\psi^+\rangle\langle\psi^+| + |\psi^-\rangle\langle\psi^-|). \tag{13}$$

Note that ρ_{noise} is uncorrelated. Let q be the visibility. The noisy state reads:

$$\rho' = q|BSV\rangle\langle BSV| + (1-q)\rho_{noise}, \tag{14}$$

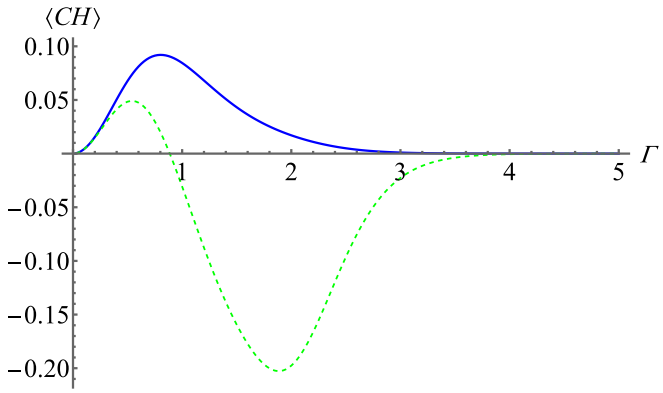

Figure 3. Quantum predictions for expectation value of CH expression for the 'sign' approach (blue curve) and rate approach[14] (green dashed curve) as a function of the amplification gain Γ for BSV state. The numerical results were obtained with a cut-off of the expansion of the BSV state at the term $|\psi^{n=50}\rangle$. The upper bound of CH inequality for the 'sign' approach is violated in the whole range of Γ covered in the figure, while the violation of the inequality in the case of the normalized Stokes operators is quickly damped and after that CH expression goes asymptotically from bellow to the classical bound.

The value $1-q$ determines the probability of registering noise. Figure 2 shows the minimal value of visibility q_c that ensures the violation of CHSH inequality for normalized and Stokes operators. We see that sign Stokes operators have a similar advantage over normalized Stokes operators as in the case of losses, i.e. for small Γ normalized and sign Stokes operators are similarly resistant to noise. As Γ increases sign Stokes operators result to be significantly more efficient, Moreover from the results shown on Fig. 2 and the reasoning presented in "Violation of Bell inequality for four mode squeezed vacuum—asymptotic behaviour" section we can conclude that $q_c \to 1$ when $\Gamma \to \infty$.

CH inequality. Going along with the idea of sign operators and rate approach to CH inequality[14] we can construct a new CH inequality for quantum optical fields. Let us move directly to the quantum scenario and start with the CH operator (CH_R) for intensity rates. In[14] the rates are defined by $\hat{R}_+(s) = \hat{\Pi}\hat{n}_s/(\hat{n}_s + n_{s_\perp})\hat{\Pi}$. Note that such an operator is simply the first term of normalized Stokes operator (1). Its eigenvalues are rational numbers in (1/2, 1] for photon number states $|n_s, m_{s_\perp}\rangle$ where $n > m$ and in [0, 1/2) for states where $n < m$. If $m = n$ the eigenvalue of the rates is 1/2. Combining the idea CH inequality for rates and the concept sign Stokes operators we construct operators for CH inequality based binning. We seek for operators of eigenvalues with the following properties: we have 1 when $m > n$ and 0 if $n \leq m$. Such a dichotomic observable is simply a projector onto subspace $n > m$:

$$\hat{P}(s) = \sum_{n>m} |n_s, m_{s_\perp}\rangle\langle n_s, m_{s_\perp}|. \tag{15}$$

The expectation value of $\hat{P}^X(s)$ is equal to the probability that the observer X will see $n > m$. We shall denote by $\langle \hat{P}^X(j)\hat{P}^Y(k)\rangle$ the quantum joint probability of obtaining the same result $n > m$ by observers X and Y for their respective polarization basis j and k. Had these probabilities in the experiment been classical, and if the assumptions of local realism hold Clauser–Horne inequality tailored for the quantum scenario is given by:

$$-1 \leq \langle CH_P\rangle = \left\langle \hat{P}^1_+(\theta)\hat{P}^2_+(\phi) + \hat{P}^1_+(\theta)\hat{P}^2_+(\phi') + \hat{P}^1_+(\theta')\hat{P}^2_+(\phi) - \hat{P}^1_+(\theta')\hat{P}^2_+(\phi') - \hat{P}^1_+(\theta) - \hat{P}^1_+(\phi)\right\rangle \leq 0. \tag{16}$$

Figure 3 shows the expectation value of the CH expression (16) and its rate counterpart for the same settings as in the case of CHSH inequality. The 'sign' approach gives violation of upper bound of CH expression for all Γ while the rate approach gives a violation only for $\Gamma < 0.8866$ which is the same case as for CHSH. Note that this CH inequality is not equivalent to CHSH inequality (6) (see Supplementary Discussion A)

Violation of Bell inequalities with sign approach for Bright GHZ state

As another example, let us consider a Bright GHZ state which is a generalization of the two beam squeezed vacuum considered above, to three beam emissions.

Such a process for years was thought to be infeasible, but current experimental progress allows one to think of such a possibility. The usual parametric approximation of the theoretical description of generation process of such states, which describes the pumping field as classical, does not work because of the divergence of perturbation series. Still, with an employment of a version of Padè approximation one can find an approximate parametric description, with convergent perturbation series, see[21]. The approximation gives a state of the following form:

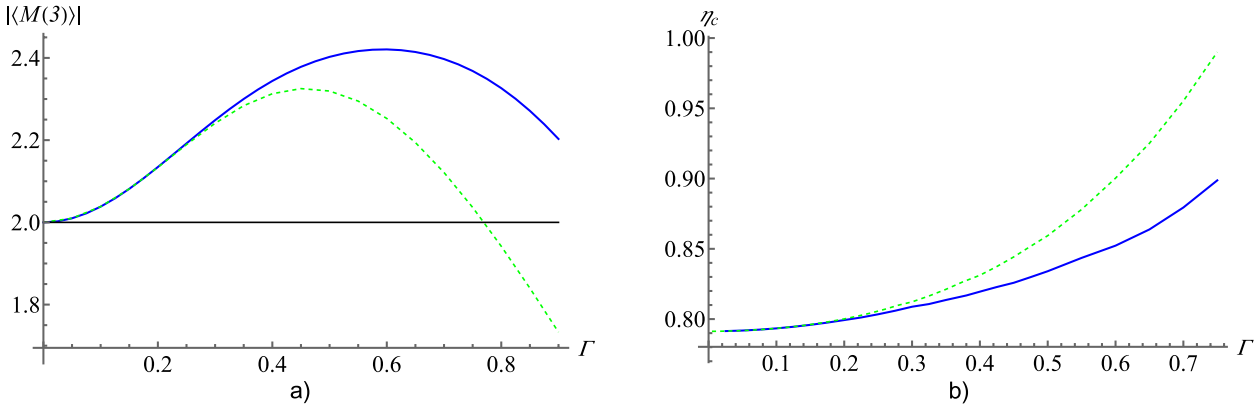

Figure 4. (**a**) Quantum values of $|M(3)_{G-}|$ expression (blue curve) and $|M(3)_{S-}|$ (green dashed curve) as a function of the amplification gain Γ for BGHZ state. (**b**) Critical efficiency η_c versus Γ for Mermin inequalities for the BGHZ state. The blue curve represents η_c for the sign approach and a green dashed curve for normalized Stokes operators.

$$|BGHZ\rangle = \sum_{k=0}^{\infty}\sum_{m=0}^{k} C_{k-m}(\Gamma)C_m(\Gamma)(\hat{a}_i^\dagger \hat{b}_i^\dagger \hat{c}_i^\dagger)^{k-m}(\hat{a}_{i_\perp}^\dagger \hat{b}_{i_\perp}^\dagger \hat{c}_{i_\perp}^\dagger)^m|\Omega\rangle. \tag{17}$$

The method of obtaining the coefficients $C_m(\Gamma)$ can be found in[21], and we base our numerical computations on the results established in this reference. The symbols $\hat{a}_p^\dagger$, $\hat{b}_p^\dagger$ and $\hat{c}_p^\dagger$ stand for creation operators in two orthogonal polarization modes $p = i, i_\perp$, of a beam which goes to respectively observers A, B and C. For simplicity, we assumed the polarization modes to be H, V, that is, $i = 3$.

Mermin-like inequality. Let us consider Mermin-like inequality for quantum optical fields[21]:

$$|M(3)_S| = |\langle S_1^1(\lambda)S_1^2(\lambda)S_1^3(\lambda) - S_1^1(\lambda)S_2^2(\lambda)S_2^3(\lambda) - S_2^1(\lambda)S_1^2(\lambda)S_2^3(\lambda) - S_2^1(\lambda)S_2^2(\lambda)S_1^3(\lambda)\rangle_{LHV}| \leq 2, \tag{18}$$

where $S_i^X(\lambda)$ are local hidden values corresponding to normalized Stokes operators with polarization bases: $\{45°, -45°\}$, $\{R, L\}$, for $i = 1, 2$ respectively. The observers are now marked by $X = 1, 2, 3$. The inequality (18) generalizes Mermin inequality for three qubits[28] for three photon beams with two polarisation modes each from a parametric source, for details see:[21]. Of course, in general the settings 1, 2 could be different.

The derivation of this inequality requires only that local hidden values are bounded by ±1. Because local hidden values for sign Stokes operators fulfil this requirement, we can replace $S_i^X(\lambda)$ by $G_i^X(\lambda)$ and obtain a new inequality

$$|M(3)_G| = |\langle G_1^1(\lambda)G_1^2(\lambda)G_1^3(\lambda) - G_1^1(\lambda)G_2^2(\lambda)G_2^3(\lambda) - G_2^1(\lambda)G_1^2(\lambda)G_2^3(\lambda) - G_2^1(\lambda)G_2^2(\lambda)G_1^3(\lambda)\rangle_{LHV}| \leq 2. \tag{19}$$

However, this inequality is not violated by the BGHZ state. We have to again modify sign Stokes operators (as well as normalized Stokes operators):

$$\hat{G}_i^X \to \hat{G}_i^{X-} = \hat{G}_i^X - \hat{\Pi}_{\Omega^X}. \tag{20}$$

One can easily write modified local hidden values for such operators as in "CHSH inequality" section and obtain inequality:

$$\begin{aligned} |M(3)_{G-}| = |\langle & G_1^{1-}(\lambda)G_1^{2-}(\lambda)G_1^{3-}(\lambda) - G_1^{1-}(\lambda)G_2^{2-}(\lambda)G_2^{3-}(\lambda) \\ & - G_2^{1-}(\lambda)G_1^{2-}(\lambda)G_2^{3-}(\lambda) - G_2^{1-}(\lambda)G_2^{2-}(\lambda)G_1^{3-}(\lambda)\rangle_{LHV}| \leq 2. \end{aligned} \tag{21}$$

Figure 4 presents quantum values of $|\langle BGHZ|\hat{M}(3)_{G-}|BGHZ\rangle|$ and of analogous expression, $|\langle BGHZ|\hat{M}(3)_{S-}|BGHZ\rangle|$, for a Mermin inequality for modified normalized Stokes operators, $\hat{S}_i^{X-} = \hat{S}_i^X - \hat{\Pi}_{\Omega^X}$, which is of the form (18) with $\hat{S}_i^{X-}$ replacing $\hat{S}_i^X$. All that is with respect to the amplification gain Γ. The range of Γ for which the inequality is violated by BGHZ state in the case of sign Stokes operators exceeds the range of applicability of the method used to approximate the probability amplitudes for BGHZ state. We also stress that this result is more robust than in the case of normalized Stokes operators. The graphs in Fig. 4 are discontinued at $\Gamma = 0.9$ because for higher values the approximation of ref.[21] breaks down.

Mermin-like inequality with losses. We use the model of losses due to inefficient detectors as in "CHSH inequality with losses" section for the inequality (21). In Fig. 4 critical values of efficiency of detectors η_c, for sign and normalized Stokes operators, are compared. We can see that for small Γ inequalities exhibit similar resistance to losses. However, with increasing Γ difference between the performance of sign and normalized Stokes observables increases in favour of the former ones.

Conclusions and some open questions

We have proposed, based on a version of the binning approach[19,20], new Stokes-like polarization observables for quantum optical fields which have a clear operational meaning. In presented examples, the sign Stokes observables allow observation of Bell non-classicality of squeezed-vacuum-type states for pumping powers, for which normalized Stokes observables fail to do so. Sign Stokes operators are easier in experimental realization than normalized ones. Also, they are more resistant to imperfect detection and presence of a noise. One could be tempted to use sign Stokes observables to derive entanglement indicators not based on Bell inequalities. However, such Stokes observables do not possess properties which are commonly used in derivations of bounds for separable states. Simply a triad of them does not form a Stokes vector with proper covariance properties. Thus, this requires a different approach. Similar questions arise when one thinks of a steering condition involving sign Stokes observables.

Another question would be if there is a type of state for which normalized Stokes operators allow for violating of some Bell inequality and for which this is impossible using sign Stokes operators.

The presented results give a possible way to search for violations of local realism in situations with undefined particle numbers, which are so common in especially quantum optics. The associated Bell inequalities are correctly defined. That is, the sole assumption is local realism (and tacitly freedom of the choice of the random settings for all observers involved). No additional "reasonable" assumptions are used. As, according to our numerical estimates, one can conjecture that the associated inequalities are violated for an arbitrary Γ, they may serve as tool to reveal Bell non-classicality of bright quantum optical states, see[29]. This indicates that such states may find an application in, e.g. quantum communication, provided one finds new suitable Bell inequalities which would lead to more robust violations of local realism.

Received: 17 December 2021; Accepted: 11 May 2022
Published online: 16 June 2022

References

1. Einstein, A., Podolsky, B. & Rosen, N. Can quantum-mechanical description of physical reality be considered complete?. *Phys. Rev.* **47**, 777–780. https://doi.org/10.1103/PhysRev.47.777 (1935).
2. Bohr, N. Can quantum-mechanical description of physical reality be considered complete?. *Phys. Rev.* **48**, 696–702. https://doi.org/10.1103/PhysRev.48.696 (1935).
3. Bell, J. S. On the Einstein Podolsky Rosen paradox. *Phys. Phys. Fiz.* **1**, 195–200. https://doi.org/10.1103/PhysicsPhysiqueFizika.1.195 (1964).
4. Aspect, A. *Bell's Theorem: The Naive View of an Experimentalist* 119–153 (Springer, Berlin, 2002).
5. Brukner, Č & Żukowski, M. *Bell's Inequalities—Foundations and Quantum Communication* 1413–1450 (Springer, Berlin, 2012).
6. Pan, J.-W. *et al.* Multiphoton entanglement and interferometry. *Rev. Mod. Phys.* **84**, 777–838. https://doi.org/10.1103/RevModPhys.84.777 (2012).
7. Werner, R. F. & Wolf, M. M. Bell inequalities and entanglement. *QIC* **1**, 1–25. https://doi.org/10.26421/QIC1.3-1 (2001).
8. Aspect, A., Grangier, P. & Roger, G. Experimental realization of Einstein–Podolsky–Rosen–Bohm gedankenexperiment: a new violation of Bell's inequalities. *Phys. Rev. Lett.* **49**, 91–94. https://doi.org/10.1103/PhysRevLett.49.91 (1982).
9. Giustina, M. *et al.* Significant-loophole-free test of Bell's theorem with entangled photons. *Phys. Rev. Lett.* **115**, 250401. https://doi.org/10.1103/PhysRevLett.115.250401 (2015).
10. Jauch, J. M. & Rohrlich, F. *The Theory of Photons and Electrons: The Relativistic Quantum Field Theory of Charged Particles with Spin One-half. Texts and Monographs in Physics* 2nd edn. (Springer, Berlin, 1976).
11. Das, T. *et al.* Can single photon excitation of two spatially separated modes lead to a violation of Bell inequality via weak-field homodyne measurements?. *New J. Phys.* **23**, 073042. https://doi.org/10.1088/1367-2630/ac0ffe (2021).
12. He, Q. Y. *et al.* Einstein–Podolsky–Rosen entanglement strategies in two-well Bose–Einstein condensates. *Phys. Rev. Lett.* **106**, 120405. https://doi.org/10.1103/PhysRevLett.106.120405 (2011).
13. Żukowski, M., Laskowski, W. & Wieśniak, M. Normalized Stokes operators for polarization correlations of entangled optical fields. *Phys. Rev. A* **95**, 042113. https://doi.org/10.1103/PhysRevA.95.042113 (2017).
14. Żukowski, M., Wieśniak, M. & Laskowski, W. Bell inequalities for quantum optical fields. *Phys. Rev. A* **94**, 020102. https://doi.org/10.1103/PhysRevA.94.020102 (2016).
15. Thekkadath, G. S. *et al.* Tuning between photon-number and quadrature measurements with weak-field homodyne detection. *Phys. Rev. A* **101**, 031801. https://doi.org/10.1103/PhysRevA.101.031801 (2020).
16. Donati, G. *et al.* Observing optical coherence across fock layers with weak-field homodyne detectors. *Nat. Commun.* **5**, 5584. https://doi.org/10.1038/ncomms6584 (2014).
17. Chen, Z.-B., Pan, J.-W., Hou, G. & Zhang, Y.-D. Maximal violation of Bell's inequalities for continuous variable systems. *Phys. Rev. Lett.* **88**, 040406. https://doi.org/10.1103/PhysRevLett.88.040406 (2002).
18. Dorantes, M. M. & M, J. L. L. Generalizations of the pseudospin operator to test the bell inequality for the TMSV state. *J. Phys. A: Math. Theor.* **42**, 285309. https://doi.org/10.1088/1751-8113/42/28/285309 (2009).
19. Schlichtholz, K.*Nieklasyczne korelacje w optyce kwantowej i ich zastosowania (Non-classical correlations in quantum optics and their applications)*. Unpublished Master's thesis, University of Gdańsk, Gdańsk, Poland (2020).
20. Kitzinger, J. *et al.* Bell correlations in a split two-mode-squeezed Bose–Einstein condensate. *Phys. Rev. A* **104**, 043323. https://doi.org/10.1103/PhysRevA.104.043323 (2021).
21. Schlichtholz, K., Woloncewicz, B. & Żukowski, M. Nonclassicality of bright Greenberger–Horne–Zeilinger-like radiation of an optical parametric source. *Phys. Rev. A* **103**, 042226. https://doi.org/10.1103/PhysRevA.103.042226 (2021).
22. Ho, M. *et al.* Witnessing single-photon entanglement with local homodyne measurements: analytical bounds and robustness to losses. *New J. Phys.* **16**, 103035. https://doi.org/10.1088/1367-2630/16/10/103035 (2014).
23. Lee, S.-Y., Park, J., Kim, J. & Noh, C. Single-photon quantum nonlocality: Violation of the Clauser–Horne–Shimony–Holt inequality using feasible measurement setups. *Phys. Rev. A* **95**, 012134. https://doi.org/10.1103/PhysRevA.95.012134 (2017).
24. Acín, A., Cerf, N. J., Ferraro, A. & Niset, J. Tests of multimode quantum nonlocality with homodyne measurements. *Phys. Rev. A* **79**, 012112. https://doi.org/10.1103/PhysRevA.79.012112 (2009).
25. Munro, W. J. Optimal states for bell-inequality violations using quadrature-phase homodyne measurements. *Phys. Rev. A* **59**, 4197–4201. https://doi.org/10.1103/PhysRevA.59.4197 (1999).

26. Nagata, K., Laskowski, W., Wieśniak, M. & Żukowski, M. Rotationalinvariance as an additional constraint on local realism. *Phys. Rev. Lett.* **93**, 230403. https://doi.org/10.1103/PhysRevLett.93.230403 (2004).
27. Ryu, J., Woloncewicz, B., Marciniak, M., Wieśniak, M. & Żukowski, M. General mapping of multiqudit entanglement conditions to nonseparability indicators for quantum-optical fields. *Phys. Rev. Res.* **1**, 032041. https://doi.org/10.1103/PhysRevResearch.1.032041 (2019).
28. Mermin, N. D. Extreme quantum entanglement in a superposition of macroscopically distinct states. *Phys. Rev. Lett.* **65**, 1838–1840. https://doi.org/10.1103/PhysRevLett.65.1838 (1990).
29. Chekhova, M., Leuchs, G. & Żukowski, M. Bright squeezed vacuum: entanglement of macroscopic light beams. *Opt. Commun.* **337**, 27–43. https://doi.org/10.1016/j.optcom.2014.07.050 (2015).

Acknowledgements

The work is a part of 'International Centre for Theory of Quantum Technologies' project (contract no. 2018/MAB/5), which is carried out within the International Research Agendas Programme (IRAP) of the Foundation for Polish Science (FNP) co-financed by the European Union from the funds of the Smart Growth Operational Programme, axis IV: Increasing the research potential (Measure 4.3).

Author contributions

All authors contributed equally to this work.

Competing interests

The authors declare no competing interests.

Additional information

Supplementary Information The online version contains supplementary material available at https://doi.org/10.1038/s41598-022-14232-8.

Correspondence and requests for materials should be addressed to K.S. or B.W.

Reprints and permissions information is available at www.nature.com/reprints.

Publisher's note Springer Nature remains neutral with regard to jurisdictional claims in published maps and institutional affiliations.

New Journal of Physics
The open access journal at the forefront of physics

Deutsche Physikalische Gesellschaft DPG IOP Institute of Physics

PAPER · OPEN ACCESS

Can single photon excitation of two spatially separated modes lead to a violation of Bell inequality via weak-field homodyne measurements?

To cite this article: Tamoghna Das *et al* 2021 *New J. Phys.* **23** 073042

New Journal of Physics
The open access journal at the forefront of physics

Deutsche Physikalische Gesellschaft DPG
IOP Institute of Physics

Published in partnership with: Deutsche Physikalische Gesellschaft and the Institute of Physics

OPEN ACCESS

RECEIVED
26 February 2021

REVISED
12 May 2021

ACCEPTED FOR PUBLICATION
30 June 2021

PUBLISHED
27 July 2021

PAPER

Can single photon excitation of two spatially separated modes lead to a violation of Bell inequality via weak-field homodyne measurements?

Tamoghna Das, Marcin Karczewski, Antonio Mandarino, Marcin Markiewicz*, Bianka Woloncewicz and Marek Żukowski

International Centre for Theory of Quantum Technologies, University of Gdańsk, 80-308 Gdańsk, Poland
* Author to whom any correspondence should be addressed.

E-mail: marcin.markiewicz@ug.edu.pl

Keywords: nonclassicality of single photon excitation, Bell inequalities, homodyne measurement, mode entanglement, entanglement witness, operators based on rates

Abstract

We reconsider the all-optical weak homodyne-measurement based experimental schemes aimed at revealing Bell nonclassicality ('nonlocality') of a single photon. We focus on the schemes put forward by Tan *et al* (TWC, 1991) and Hardy (1994). In our previous work we show that the TWC experiment can be described by a local hidden variable model, hence the claimed nonclassicality is apparent. The nonclassicality proof proposed by Hardy remains impeccable. We investigate which feature of the Hardy's approach is crucial to disclose the nonclassicality. There are consequential differences between TWC and Hardy setups: (i) the initial state of Hardy is a superposition of a single photon excitation with vacuum in one of the input modes of a 50–50 beamsplitter. In the TWC case there is no vacuum component. (ii) In the final measurements of Hardy's proposal the local settings are specified by the presence or absence of a local oscillator field (on/off). In the TWC case the auxiliary fields are constant, only phases are varied. We show that in Hardy's setup the violation of local realism occurs due to the varying strength of the local oscillators. Still, one does not need to operate in the fully on/off detection scheme. Thus, the nonclassicality in a Hardy-like setup cannot be attributed to the single-photon state alone. It is a consequence of its interference with the photons from auxiliary local fields. Neither can it be attributed to the joint state of the single photon excitation and the local oscillator modes, as this state is measurement setting dependent. Despite giving spurious violations of local realism, the TWC scheme can serve as an entanglement indicator, for the TWC state. Nevertheless an analogue indicator based on intensity rates rather than just intensities overperforms it.

1. Introduction

The 'nonlocality of a single photon', also known as 'entanglement with vacuum', has long been a subject of controversy [1–12]. In its basic form, the problem concerns the nature of the state $\frac{1}{\sqrt{2}}(|01\rangle_{b_1b_2}+|10\rangle_{b_1b_2})$, obtained by casting a photon on a balanced beamsplitter. Here, the notation $|10\rangle_{b_1b_2}$ indicates the presence of a photon in mode b_1 and its absence in b_2. Although the resulting state can be considered as mode entangled [13], it can also be interpreted as a mere superposition of mode excitations—the photon being either here or there. This point of view is supported by writing down the state as $\widehat{a}^\dagger|00\rangle_{b_1b_2}$, where $\widehat{a}^\dagger=\frac{1}{\sqrt{2}}(\widehat{b}_1^\dagger+\widehat{b}_2^\dagger)$, and $\widehat{b}_j^\dagger$ are photon creation operators for modes b_j.

Thus, one could question whether it can be used to demonstrate Bell nonclassicality—both on its own, or with some additional resources like local auxiliary optical fields.

Aharonov and Vaidman [3, 14] observed that the single-photon superposition can induce an entangled state of two atoms in spatially separated traps. In such a case violation of local realism by the pair of entangled atoms is easy to prove, and the entanglement is (in theory) easily detectable (see e.g. the

discussion in [15, 16]). However, this puts us effectively back to the two-qubit entanglement. Moreover, note that the atoms used in such schemes should be treated as auxiliary systems. Therefore, such an approach will not be discussed here. We want to discuss situations which involve only quantum optical fields, passive optics and photon number resolving (macroscopic) detectors, as there are many open questions related to observability of violations of local realism in all-optical scenarios.

Many experiments, some feasible, some gedanken, have been proposed to address this fundamental problem. Let us briefly present their three major types.

The first one originates from a paper by Tan, Walls and Collett (TWC) [1], in which homodyne-based coincidence intensity measurements with weak coherent light as local auxiliary fields were used to violate the Bell-like inequality of [17]. However, the Bell-like inequality in [17] does not rest entirely on Bell's assumptions. Because of that, one can question whether the TWC scheme can be used to violate local realism. For instance, Santos [18] provided an ad hoc and incomplete local realistic model for the correlation functions considered by TWC. Recently, this line of critique has been reinforced in [19] by presenting a model that reproduces all detection events in the TWC experimental proposal for the range of local oscillator strengths for which the paper [1] reported 'nonlocality' of the single-photon state. In the section 4.2 of this work we show that optical Bell inequalities [20], which must hold for any local realistic description, are not violated for the TWC setup. Thus this case is closed. Still, TWC correlations are interesting in themselves, and variants of this scheme have been realized experimentally in [4, 11]. Recently one can observe an experimental breakthrough: papers [21, 22] test techniques of weak homodyne measurements involving photon number resolution—also for the TWC configuration—making a re-analysis timely.

Another idea was put forward by Hardy [2]. He considered states $q|00\rangle_{b_1b_2} + \frac{r}{\sqrt{2}}(|01\rangle_{b_1b_2} + |10\rangle_{b_1b_2})$, with $q \neq 0$ which can be produced by sending a superposition of a vacuum state and a single photon one on a 50–50 beamsplitter. Hardy investigated four mutually complementary experimental situations and proved that their joint local realistic description would contradict the quantum predictions. His setup relied on tunable amplitudes of the auxiliary coherent fields (local oscillators). Its modification with mixed-state auxiliary states was proposed in [6], and a generalization to multimode initial states in [7]. The question is whether the vacuum component, $q \neq 0$, or variable local oscillator strengths are crucial for Hardy configuration. Answering this question may also shed light on other experimental configurations which use homodyne detection with weak local oscillators to get violation of local realism.

Yet another direction is suggested by Banaszek and Wódkiewicz: a measurement setup implementing the displacement of the input field in the optical phase space for the single photon superposition ($q = 0$) [23]. The settings of the Bell experiment they considered were defined by turning the displacements on or off. A combination of this approach with homodyne measurements was investigated in [12], while an adaptation to multimode input states was given in [9]. Optical displacement was also used in a scheme for a heralded distribution of a single-particle entanglement [24]. We shall not analyze the approach of [23] as, first, their proof of violation of local realism is impeccable, and second, despite the fact that their scheme involves only all-optical measurements, the employed technique is essentially different from the ones of TWC and Hardy.

In this work we shall concentrate on homodyne measurements which involve in general arbitrary beamsplitters, and essentially weak local oscillator fields. By weak local field we mean here the situation in which the average photon number in the local oscillator is of the same order of magnitude as the mean photon number in the signal state, that is around one or less. In this regime the local auxiliary fields have to have a full quantum description, and the performed measurements can be interpreted as revealing particle-like properties of the quantum fields. This has to be contrasted with the strong-field homodyne correlation measurements (see e.g. [25]). These can be interpreted to reveal the wave-like properties, as they lead to quadrature phase measurements. Concerning the transition between weak and strong homodyne measurement see the current discussion in [22], and their experimental results. Most importantly, reference [22] clearly shows that current state-of-the-art techniques allow one to experimentally observe the full range of phenomena which we discuss here.

This includes not only the setups of TWC and Hardy, but also the intermediate cases which have not been discussed yet. We start by analyzing the mechanism behind the occurrence of the spurious nonclassicality, manifested by the violation of the inequality of [17] in the TWC setup. Further we shall test the ability of inequalities [20] to detect violations of local realism in situations which are a kind of a hybrid of the TWC configuration and the Hardy one. That is, we shall show that the inequalities detect violation of local realism if one admits varying strengths of the local oscillators for different settings in the Bell experiment. It turns out that the approach allows to find genuine violations of local realism for the initial state of the form of TWC (i.e. for $q = 0$). In the last section we show that the original TWC approach, although it fails as a test of local realism, still is a realization of an entanglement witness.

2. Detailed aims and analysis

In order to test the potentially nonclassical character of the correlations appearing in the schemes of TWC and Hardy, we use the intensity rates of optical fields as local observables. They were first introduced as a proposal of normalized Stokes observables in [26, 27] and rediscovered in the context of Bell's theorem in [20], further developed in references [28, 29]. Essentially, by an intensity rate we mean the ratio of measured intensity in the given local detector to the total intensity measured in all local detectors, in a given run of the experiment. In contrast to the CHSH Bell-like inequalities of [17] used by TWC, this approach to analyzing optical correlations does not lead to spurious violations.

The inequalities for intensities of reference [17] involve additional constraints on local hidden variable description of intensities passing beamsplitters. The additional constraints are a version of no-enhancement assumption for CH-like inequalities (discussed in [30]), or a fair-sampling one in the case of CHSH-like inequalities. Therefore the inequalities of reference [17] cannot be used to test Bell nonclassicality, however, as we show further, they have an interpretation of entanglement indicators. The problematic status of the additional assumption in the inequalities of [17] in the context of TWC setup has been pointed out by Hardy [31] and Santos [18]. Nevertheless, because of the seemingly 'innocent' naturality of this assumption, the inequalities of [17] can be found in discussions of Bell's theorem in some textbooks on quantum optics e.g. [32]. In this work, we show that Bell inequalities based on rates of intensities [20], which do not invoke any additional constraints, are not violated. This result is in perfect agreement with the fact that a recently proposed local hidden variable model [19] reproduces all the probabilities of events considered 'nonlocal' by TWC in [1]. It shows that the rate-based inequalities are more reliable than the ones of [17], as they do not lead to spurious violations of Bell classicality. Interestingly, this is the first found example supporting that claim. It complements the previous investigations in which the rate-based inequalities were always more strongly violated in case of genuine nonclassicality [20].

In contrast with the above, our analysis of the Hardy-like proposal using the intensity rates approach indicates the presence of nonclassical correlations. We have confirmed them in case of the initial state being just a single photon ($q = 0$). Thus, the crucial change in the TWC setup introduced by Hardy consists in the ability to vary the intensities of the coherent local oscillators by turning them on or off.

We have also investigated a transition between the Hardy-like and TWC setups. Our numerical calculations show that nonclassical correlations can still be obtained when the amplitudes of auxiliary coherent fields are non-zero for both local measurement settings. This means that turning the auxiliary oscillators off, as proposed by Hardy, is not necessary. However, their amplitudes must still be different for the alternative local settings of the Bell-type experiment.

The local oscillators of the homodynes used to detect the violations of local realism induced by the state $\frac{1}{\sqrt{2}}(|01\rangle_{b_1b_2} + |10\rangle_{b_1b_2})$ must be treated as a part of the local measuring devices. In fact, in such all optical scenario the local oscillators can be incorporated in the operational definition of the measurements which are of the positive-operator-value measurement (POVM) class.

3. Experimental setup

Here, we discuss the basic setup of the TWC and Hardy *gedankenexperiments* and its variations which were studied in the literature, in greater detail. As depicted in figure 1, the experimental configuration consists of three spatially separated beamsplitters BS_j with $j = 0, 1, 2$, whose action is in general described by the unitary transformation:

$$U_{\mathrm{BS}}(\chi,\theta) = \begin{pmatrix} \cos\chi & \mathrm{e}^{-\mathrm{i}\theta}\sin\chi \\ -\mathrm{e}^{\mathrm{i}\theta}\sin\chi & \cos\chi \end{pmatrix}, \tag{1}$$

where $\cos^2\chi$ is the transmission coefficient of the beamsplitter and θ is the phase acquired by the reflected beam. As a beamsplitter is a passive optical device this transformation links the photon annihilation operators of the incoming beams with annihilation operators of the output beams. We assume that all photons in the experiment have the same polarization.

An initial state, $q|0\rangle_s + r|1\rangle_s$, a superposition of vacuum and single-photon excitation in mode s, impinges on a symmetric beamsplitter BS_0 (defined by $\chi = \frac{\pi}{4}$ and $\theta = -\frac{\pi}{2}$). Such will be our notation, $|n\rangle_m$ is a Fock state of n photons in (spatial) mode m. If the initial state is a single photon, i.e. $q = 0$, then it transforms to:

$$|\psi\rangle_{b_1,b_2} = \frac{1}{\sqrt{2}}\left[|01\rangle_{b_1,b_2} + i|10\rangle_{b_1,b_2}\right], \tag{2}$$

where b_1, b_2, are the output modes of beamsplitter BS_0.

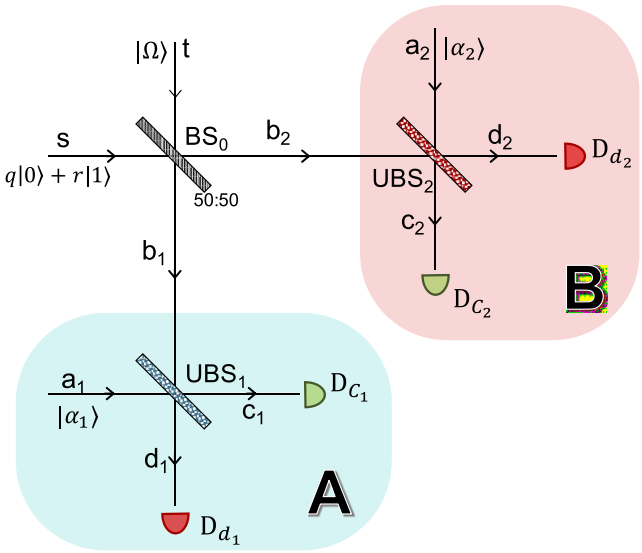

Figure 1. Most general schematic representation of the experimental setup for testing single-photon correlational properties, which we consider here. In the Tan–Walls–Collett scenario we have $q = 0$, and $|\alpha_1| = |\alpha_2| = \text{const.}$ for all settings in Bell-like experiment. In original Hardy's scenario $q \neq 0$ and $|\alpha_j| = 0$, or $\alpha_j = \frac{i^{(1-j)}}{q\sqrt{2}}r$. Here we consider also intermediate cases, including α_j's of varying absolute values and beamsplitters U_{BS_j} with transmissivity varying from setting to setting.

In the TWC scheme the quantum state, given in equation (2) is then shared between two parties Alice and Bob, who perform a homodyne detection. We assume that the homodyne measurement stations operated by local observers consist of a θ_j-dependent balanced beamsplitter BS_j, realizing the transformation $U_{\text{BS}}(\frac{\pi}{4}, \theta_j)$, an auxiliary coherent beam impinging on the remaining input mode of BS_j, and two photo-detectors D_{c_j} and D_{d_j}, placed in front of the output modes of BS_j, for $j = 1, 2$, as shown in figure 1. The amplitudes of the coherent beams $|\alpha\rangle_{a_1}$ and $|\alpha\rangle_{a_2}$ are equal in the case of TWC scheme. For simplicity we assume that α is real. After all that, the total state at the inputs of the two beamsplitters BS_1 and BS_2, is:

$$|\Psi(\alpha)\rangle = \frac{1}{\sqrt{2}}\,|\alpha\rangle_{a_1}(|01\rangle_{b_1b_2} + i\,|10\rangle_{b_1b_2})|\alpha\rangle_{a_2}. \tag{3}$$

The necessity of introducing auxiliary systems in such measurement schemes is related to the fact that it is impossible to perform a projection onto a superposition between vacuum and a single photon using only passive optical devices. This was already pointed out by Peres [33] in a comment to the Hardy's work.

The photo-detectors D_{c_j} and D_{d_j} monitor output modes $\widehat{c}_j$ and $\widehat{d}_j$ of BS_j, for $j = 1, 2$. These modes are linked with modes $\widehat{a}_j$ and $\widehat{b}_j$ via symmetric beamsplitter transformation $U_{\text{BS}}(\frac{\pi}{4}, \theta_j)$, that is we have:

$$\begin{aligned} \widehat{c}_j &= \frac{1}{\sqrt{2}}(\widehat{a}_j + \mathrm{e}^{-\mathrm{i}\theta_j}\,\widehat{b}_j), \\ \widehat{d}_j &= \frac{1}{\sqrt{2}}(-\mathrm{e}^{\mathrm{i}\theta_j}\,\widehat{a}_j + \widehat{b}_j). \end{aligned} \tag{4}$$

It is assumed that the detectors measure photon numbers. The phases θ_1 and θ_2 in the TWC case are tunable, and define the local settings in the purported Bell experiment.

3.1. Generalizations

In further discussions we will consider also a generalized scheme with arbitrary tunable beamsplitters BS_1 and BS_2, for which the mode transformation reads:

$$\begin{pmatrix} \widehat{c}_j \\ \widehat{d}_j \end{pmatrix} = U_{\text{BS}_j}(\chi_j, \theta_j) \begin{pmatrix} \widehat{a}_j \\ \widehat{b}_j \end{pmatrix}, \tag{5}$$

where the unitary matrix is given in equation (1). Such devices have a realization in the form of Mach–Zehnder interferometers. One can further generalize the scheme, and assume that the local auxiliary fields may have different amplitudes for both observers, therefore the overall state at the entry ports of the

final beamsplitters takes a more general form:

$$|\Phi(\alpha_1,\alpha_2)\rangle = \frac{1}{\sqrt{2}}\,|\alpha_1\rangle_{a_1}(|01\rangle_{b_1b_2} + i\,|10\rangle_{b_1b_2})|\alpha_2\rangle_{a_2}. \tag{6}$$

In this generalized case the dependence on the real parameters α_1 and α_2 is local with respect to subsystems defined by modes $\{\widehat{a}_1, \widehat{b}_1\}$ and $\{\widehat{a}_2, \widehat{b}_2\}$, so they can be also used as local settings together with local phases θ_1 and θ_2.

One can further generalize this to initial states of mode s being superpositions of vacuum and single photon states (i.e. $q \neq 0$). In such case the state behind the first beamsplitter is given by:

$$|\psi'\rangle_{b_1,b_2} = q|00\rangle_{b_1,b_2} + \frac{r}{\sqrt{2}}\left[|01\rangle_{b_1,b_2} + i|10\rangle_{b_1,b_2}\right]. \tag{7}$$

4. Intensities vs intensity rates in analysis of TWC correlations

4.1. Bell inequalities for intensity rate measurements

For the analysis of nonclassicality the authors of [1] used Bell-like inequalities derived in [17]. The inequalities involved correlation functions of intensities at pairs of spatially separated detectors, one in Alice's station one in Bob's. They are applicable for the following models:

$$E_T(\theta_1,\theta_2) = \frac{\int \mathrm{d}\lambda\rho(\lambda)\prod_{j=1,2}\left(I_{c_j}(\theta_j,\lambda) - I_{d_j}(\theta_j,\lambda)\right)}{\int \mathrm{d}\lambda\rho(\lambda)I_1(\lambda)I_2(\lambda)}. \tag{8}$$

In the above formula λ symbolizes a hidden variable, $\rho(\lambda)$ is its distribution, $I_{x_j}(\theta_j,\lambda)$ is the hidden variable model of the local intensity (registered in a detector placed in front of mode $x = c, d,$) at station $j = 1, 2$, i.e. respectively A and B of figure 1, for the local (phase) setting θ_j. Finally $I_j(\lambda)$ is the total intensity at station $j = 1, 2$. However, the inequalities of [17] cannot be used to refute altogether the possibility of local realistic description of an experiment, as in addition to local realism and 'free will', they rely on an additional assumption (which holds in classical optics, but not in e.g. stochastic electrodynamics [34]). This assumption states that the total local intensity of light $I_j(\lambda)$, for a given values of a hidden variable λ does not depend on the local setting of the measuring device. Namely, the authors of [17] assumed that:

$$I_j(\lambda) = I_{c_j}(\theta_j,\lambda) + I_{d_j}(\theta_j,\lambda), \tag{9}$$

is independent of the local value of θ_j. A possible violation of inequalities of [17] indicated a failure of either local realism, or 'free will', or of the assumption (9). However, in an earlier paper [19] we showed an explicit hidden variable model which reproduces exactly the quantum predictions for the TWC experiment for the whole range of α for which inequalities of [17] are shown to be violated in [1]. Therefore, the violation reported in [1] cannot be attributed to Bell's nonclassicality of the state under consideration.

As mentioned above, the inequalities of [1] lead to drastically wrong conclusions about the non-existence of local hidden variable description of TWC experiment. To study this type of questions one must therefore use an alternative approach, which uses Bell's inequalities for field intensities, since they rest only on the assumptions of local realism and 'free will'. The approach given in [20], allows to construct a class of Bell's inequalities having this trait. The Bell's inequalities of [20] involve correlations of functions of the intensities that we will refer to as intensity rates. They are defined as the ratios of the measured intensities in a given local mode to the total intensity measured across all local modes:

$$R_{x_j}(\theta_j,\lambda) = \frac{I_{x_j}(\theta_j,\lambda)}{I_{c_j}(\theta_j,\lambda) + I_{d_j}(\theta_j,\lambda)}, \tag{10}$$

where we assume that $R_{x_j}(\theta_j,\lambda)$ is assigned the value of 0 whenever the total intensity in the denominator is equal to 0.

The differences of intensity rates (10), when averaged over the probability distribution of the LHV, can be used to construct the following correlation functions:

$$E_R(\theta_1,\theta_2) = \left\langle \prod_{j=1}^{2}\left(R_{c_j}(\theta_j,\lambda) - R_{d_j}(\theta_j,\lambda)\right)\right\rangle_{\mathrm{HV}}, \tag{11}$$

depending on the value of the local settings defined by the variable θ_j for $j = 1, 2$. This correlation function satisfies the CHSH inequality for rates:

$$|E_R(\theta_1, \theta_2) + E_R(\theta_1', \theta_2) + E_R(\theta_1, \theta_2') - E_R(\theta_1', \theta_2')| \leqslant 2. \tag{12}$$

Note that the above inequality holds regardless of whether the condition (9) is satisfied or not.

4.2. Homodyne detection with intensity rates vs Bell CHSH inequality for rates

Quantum optical observables that describe the rates can be defined as follows [20]. If one assumes, like in [1], that the intensity observables of beams are modeled by photon number operators for the given mode, the rate operator is defined by:

$$\widehat{R}_{x_j} = \widehat{\Pi}_{c_j d_j} \frac{\widehat{n}_{x_j}}{\widehat{n}_{c_j} + \widehat{n}_{d_j}} \widehat{\Pi}_{c_j d_j}, \tag{13}$$

where $\widehat{n}_{x_j} = \widehat{x}_j^{\dagger} \widehat{x}_j$, represents the photon number operator in the x_jth mode of the optical field registered in the detector D_{x_j}. Here, $\widehat{x}_j^{\dagger}, \widehat{x}_j$ are the photon creation and annihilation operators of the local output mode $\widehat{x}_j$, $x = c, d$, of the beamsplitter for observer j. The operators $\widehat{\Pi}_{c_j d_j} = \mathbb{I}_{c_j d_j} - \left|\Omega_{c_j d_j}\right\rangle\left\langle\Omega_{c_j d_j}\right|$, $j = 1, 2$, are projectors onto the subspace spanned by the Fock basis of modes $\widehat{c}_j, \widehat{d}_j$, devoid of the vacuum state. It is worth mentioning that the two mode vacuum $\left|\Omega_{c_j d_j}\right\rangle$ and the operators $\widehat{\Pi}_{c_j d_j}$ are invariant under the action of the local mode transformations given in equations (1) and (5). Since the operators $\widehat{R}_{x_j}$ and $\widehat{\Pi}_{c_j d_j} \frac{1}{\widehat{n}_{c_j} + \widehat{n}_{d_j}} \widehat{\Pi}_{c_j d_j}$ commute with each other, depending on needs one can put the rate operator also as follows:

$$\widehat{R}_{x_j} = \widehat{n}_{x_j} \frac{1}{\widehat{n}_{\mathrm{tot}_j}} \widehat{\Pi}_{c_j d_j} = \widehat{\Pi}_{c_j d_j} \frac{1}{\widehat{n}_{\mathrm{tot}_j}} \widehat{n}_{x_j} = \widehat{\Pi}_{c_j d_j} \frac{1}{\sqrt{\widehat{n}_{\mathrm{tot}_j}}} \widehat{n}_{x_j} \frac{1}{\sqrt{\widehat{n}_{\mathrm{tot}_j}}} \widehat{\Pi}_{c_j d_j}, \tag{14}$$

where $\widehat{n}_{\mathrm{tot}_j} = \widehat{n}_{c_j} + \widehat{n}_{d_j}$.

We also define

$$\widehat{H}_j(\theta_j) = \widehat{R}_{c_j} - \widehat{R}_{d_j} = \widehat{\Pi}_{c_j d_j} \frac{\widehat{n}_{c_j} - \widehat{n}_{d_j}}{\widehat{n}_{c_j} + \widehat{n}_{d_j}} \widehat{\Pi}_{c_j d_j}, \tag{15}$$

with $j = 1, 2$, and the implicit θ_j-dependence is specified via mode transformations (4). With an abuse of notation, we also call $E_R(\theta_1, \theta_2)$, the correlation coefficient of the joint homodyne measurement on the initial state $|\Psi(\alpha)\rangle$ (3), performed by both Alice and Bob:

$$E_R(\theta_1, \theta_2) = \langle \Psi(\alpha)| \widehat{H}_1(\theta_1) \widehat{H}_2(\theta_2) |\Psi(\alpha)\rangle = A_R(\alpha) \sin(\theta_1 - \theta_2), \tag{16}$$

where θ_1 and θ_2 are the tunable phases of the local beamsplitters. The amplitude $A_R(\alpha)$ of the correlation function reads explicitly:

$$A_R(\alpha) = \frac{\mathrm{e}^{-2\alpha^2} (\mathrm{e}^{\alpha^2} - 1)^2}{\alpha^2}. \tag{17}$$

The correlation function (16) depends on the fixed initial state parameter α denoting the amplitude of the auxiliary local field. We can express the correlation function (16) as arising from a POVM measurement performed solely on the initial single-photon superposition (2) in modes b_1 and b_2:

$$E_R(\theta_1, \theta_2) = \langle \psi| \widehat{\mathcal{M}}_{b_1}(\alpha, \theta_1) \widehat{\mathcal{M}}_{b_2}(\alpha, \theta_2) |\psi\rangle . \tag{18}$$

The POVM operators $\widehat{\mathcal{M}}_{b_j}(\alpha, \theta_j)$ are explicitly constructed in appendix A. We note that a similar analysis of the homodyne detection in terms of POVM operators has been already performed [35], here we extend such an approach to homodyne detection with intensity rate operators (15).

Our aim is to check whether the following CHSH inequality for rates, constructed by substituting (16) into (12), is violated by the quantum state given in (3):

$$A_R(\alpha) |\sin(\theta_1 - \theta_2) + \sin(\theta_1' - \theta_2) + \sin(\theta_1 - \theta_2') - \sin(\theta_1' - \theta_2')| \leqslant 2. \tag{19}$$

The term depending on the phases of the auxiliary coherent states can reach the maximal value of $2\sqrt{2}$, hence (19) will be violated if $A_R(\alpha) > \frac{\sqrt{2}}{2}$. The amplitude $A_R(\alpha)$ has been plotted in the figure 2, as the solid red line. The blue dotted straight line depicts the value of $\frac{\sqrt{2}}{2}$. The position of the solid red line below the dotted blue straight line, for all values of α shows that the correlation function (16) does not lead to any violation of the CHSH inequality for rates (19).

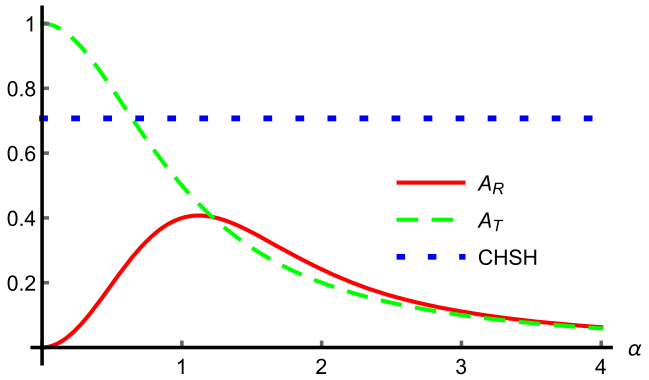

Figure 2. Comparison of the amplitudes of correlation functions $E_R(\theta_1, \theta_2)$ and $E_T(\theta_1, \theta_2)$ for different amplitudes α of the auxiliary coherent field. The solid red line corresponds to the amplitude $A_R(\alpha)$ of $E_R(\theta_1, \theta_2)$, and the dashed green line is for $A_T(\alpha)$. For weak coherent light the amplitude $A_T(\alpha)$ exceeds the threshold needed to violate the CHSH inequality.

We compare our results with the ones given in [1], where the following CHSH-like inequality has been considered:

$$|E_T(\theta_1, \theta_2) + E_T(\theta_1', \theta_2) + E_T(\theta_1, \theta_2') - E_T(\theta_1', \theta_2')| \leqslant 2. \tag{20}$$

The correlation functions $E_T(\theta_1, \theta_2)$ have been already defined in equation (8). The quantum implementation of the correlators $E_T(\theta_1, \theta_2)$ used in [1] reads as follows:

$$E_T(\theta_1, \theta_2) = \frac{\langle\Psi(\alpha)|(\widehat{n}_{c_1} - \widehat{n}_{d_1})(\widehat{n}_{c_2} - \widehat{n}_{d_2})|\Psi(\alpha)\rangle}{\langle\Psi(\alpha)|(\widehat{n}_{c_1} + \widehat{n}_{d_1})(\widehat{n}_{c_2} + \widehat{n}_{d_2})|\Psi(\alpha)\rangle} = A_T(\alpha)\sin(\theta_1 - \theta_2), \tag{21}$$

and the amplitude $A_T(\alpha)$ reads explicitly:

$$A_T(\alpha) = \frac{1}{1+\alpha^2}. \tag{22}$$

The coefficient $A_T(\alpha)$ as a function of the amplitude α of the auxiliary coherent field has been plotted in figure 2, as the dashed green line. We observe a violation of the inequality (20) for the range $0 < \alpha^2 < 0.414$. This indication of Bell's nonclassicality is apparent, since in a recent work [19] we have shown an LHV model simulating the discussed correlations. The apparent nonclassicality occurs due to the additional assumption (9). Therefore the inequality (20) is not suitable for Bell-type considerations concerning the setup. Nevertheless it can be utilised as an entanglement witness, which is discussed in more details in section 6.

5. Violation of Clauser–Horne inequality based on intensity rates

In the previous section we have shown directly that the Bell-CHSH inequality (12) based on intensity rates (10) is not violated in the TWC setup. This result is concurrent with the existence of an LHV model for the TWC scenario proposed by us in a recent work [19]. The crucial feature of the TWC experiment is the fact that the local oscillators have constant amplitudes. Hence, in order to search for a Bell violation within the general single-photon setup (figure 1) we need to relax this assumption, as it was done by Hardy [2] in his version of the *single-photon nonlocality* test. Contrary to the original Hardy case we do not use the single-photon-with-vacuum superposition as the initial state and keep just the single photon one. On the other hand we introduce one more modification with respect to both TWC and Hardy versions, namely the local beamsplitters BS_1 and BS_2 in figure 1 have now tunable transmissivities, and are specified by formula (5). In his work [2] Hardy used Clauser–Horne (CH) inequality [30], as it was better suited to describe his *possibilistic* paradox (meaning that the contradiction occurs with a non-zero probability).

5.1. Non-equivalence of CH and CHSH inequalities for optical fields

The CH inequality in its most general form reads as follows [30]:

$$-1 \leqslant P(A, B) + P(A, B') + P(A', B) - P(A', B') - P(A) - P(B) \leqslant 0, \tag{23}$$

where A, A' denote fixed outcomes of arbitrary Alice's measurements, and B, B' refer to Bob's ones. In the case of dichotomic outcomes, namely $A, A', B, B' = \pm 1$, the CH inequality (23) can be written in four

versions, each corresponding to a definite choice of ± 1 values for all the four outcomes A, A', B, B'. Interestingly each of these versions is equivalent to the CHSH inequality. This equivalence rests on the following property of dichotomic measurements: $P(-1|\theta, \lambda) + P(+1|\theta, \lambda) = 1$.

The equivalence persists even in the case of imperfect detection if one uses the Garg–Mermin trick [36]. The trick simply leaves them with dichotomic outcomes, despite possible three results, detection in channel $+1$, in channel -1, or no detection at all. Simply the idea in reference [36] is to ascribe value -1 also for the non-detection event.

Note that for qubits the upper bound is often thought to be the CH inequality, as it can be elegantly derived using geometric concepts [37]. This can be done by noticing that $S(A, B) = P(A) + P(B) - P(A, B)$ is non-negative, $S(A, A) = 0$, and it satisfies the triangle inequality. The CH inequality is then the quadrangle inequality.

Any Bell inequality for two, or more qubits can be rewritten into an inequality for intensity rates of fields, via a replacement:

$$P(n_{x_i} = 1|\theta_i, \lambda) \to R_{x_i}(\theta_i|\lambda), \tag{24}$$

where $P(n_{x_i} = 1|\theta, \lambda)$ is an LHV probability for the qubit to be registered at x_i, while the rates R_{x_i} are defined in equation (10). This holds due to the fact that rates, just like probabilities, have values between zero and one. For a detailed presentation and justification of this method see [20, 29]. In the case of the experimental setup discussed throughout this paper the CH inequality for rates can be written in four different versions, depending which pair of output modes we choose from the set $\{(c_1, c_2), (c_1, d_2), (d_1, c_2), (d_1, d_2)\}$. Choosing the pair (d_1, d_2), which coincides with the choice done in Hardy's work [2], we obtain the following form:

$$-1 \leqslant \left\langle R_{d_1} R_{d_2} + R_{d_1} R'_{d_2} + R'_{d_1} R_{d_2} - R'_{d_1} R'_{d_2} - R_{d_1} - R_{d_2} \right\rangle_{\mathrm{HV}} \leqslant 0, \tag{25}$$

in which the unprimed rates correspond to first setting, and the primed ones to the second.

It turns out that the CH and CHSH inequalities for rates obtained by application of the procedure (24) are no longer equivalent. In the classic two qubit scenario of Bell a qubit-particle can hit only one detector: we have $\sum_{x_i} P(n_{x_i} = 1|\theta, \lambda) = 1$. However, in the case of states which have non-zero probability of vacuum events, rates of mutually exclusive detection events, do not have to add up to 1. We have $\sum_{x_i} R_{x_i}(\theta, \lambda) = 1$ or 0. This *prohibits* one to show that the CHSH inequality (12) for rates is equivalent to the CH one for rates (25). Clearly the same conclusion holds for other choices of pairs of output modes for the CH inequality for rates.

5.1.1. The surprising case of CH inequalities for rates

In the case of dichotomic outcomes the lower and the upper bound of the CH inequality (23) are equivalent. Namely by a replacement of $P(A)$ by $1 - P(\tilde{A})$, where $\tilde{A}$ is an event opposite to A, i.e. $P(A) = 1 - P(\tilde{A})$, and subsequent replacements of the form $P(A, B^{(\prime)}) = P(B^{(\prime)}) - P(\tilde{A}, B^{(\prime)})$, one can transform the upper bound of the inequality (23) into an inequality of the form of the lower bound, for events $\{\tilde{A}, A'\}$ for Alice and $\{B, B'\}$ for Bob.

However by performing an analogous replacement of R_{d_1} by $R_{\mathrm{tot}_1} - R_{c_1}$, where $R_{\mathrm{tot}_1} = R_{c_1} + R_{d_1}$, which follows the rule (24), utilising the upper bound and transforming it to the lower bound by change of sign of both sides we obtain the following form of the CH inequality for rates (25):

$$\left\langle (R_{\mathrm{tot}_1} - 1)(R_{d_2} + R'_{d_2}) - R_{\mathrm{tot}_1} \right\rangle_{\mathrm{HV}} \leqslant \left\langle R_{c_1} R_{d_2} + R_{c_1} R'_{d_2} + R'_{d_1} R'_{d_2} - R'_{d_1} R_{d_2} - R_{c_1} - R'_{d_2} \right\rangle_{\mathrm{HV}}. \tag{26}$$

The above inequality is also a CH inequality for rates, where in contrast to the original inequality in (25) the measurement of Alice for the first setting is now performed in mode c_1 and the role of primed and unprimed settings for Bob's measurement are swapped. A glance at the lower bound shows that for $R_{\mathrm{tot}_1} = 0$ the algebraic expression which is averaged there, reads $(R_{\mathrm{tot}_1} - 1)(R_{d_2} + R'_{d_2}) - R_{\mathrm{tot}_1} = -R_{d_2} - R'_{d_2}$ and this can reach even the value of -2.

Thus the two sides of the CH inequality lead, via the procedure (24), to two different CH inequalities for rates. This explains the phenomenon which we shall see further down. In our analysis we get a violation of only the lower bound of the CH inequality for rates (25). Surprisingly this inequality is a stronger bound on local realism in the case of rates, than the upper bound.

5.2. CH violation in the extended setup

As already mentioned, in this section we consider measurement settings that generalize the proposed measurement setup in [1]. Now a single photon ($q = 0$ in our initial state), impinges on a balanced beamsplitter, BS_0 and then the output modes interact with auxiliary coherent beams $|\alpha_1\rangle$ and $|\alpha_2\rangle$ through additional two $SU(2)$ beamsplitters $U_{\mathrm{BS}_1}(\chi_1, \theta_1)$ and $U_{\mathrm{BS}_2}(\chi_2, \theta_2)$, given by the unitary (1). We assume that

the amplitudes of the local auxiliary fields α_1 and α_2 are real. Following the idea of Hardy setup we treat amplitudes of local fields as a part of measurement settings as well, therefore local settings are specified by vectors:

$$\begin{aligned}\vec{v}_1 &= (\chi_1, \alpha_1, \theta_1),\\ \vec{v}_2 &= (\chi_2, \alpha_2, \theta_2).\end{aligned} \tag{27}$$

The CH inequality for rates specified in the previous section (25) can be expressed in the following convenient form:

$$-1 \leqslant K(\vec{v}_1, \vec{v}_2) + K(\vec{v}_1', \vec{v}_2) + K(\vec{v}_1, \vec{v}_2') - K(\vec{v}_1', \vec{v}_2') - S_1(\vec{v}_1) - S_2(\vec{v}_2) \leqslant 0. \tag{28}$$

The correlators $K(\vec{v}_1, \vec{v}_2)$ and the local averages $S_j(\vec{v}_j)$ are defined as follows:

$$\begin{aligned}&K(\vec{v}_1, \vec{v}_2)\langle R_{d_1}(\vec{v}_1) R_{d_2}(\vec{v}_2)\rangle_{\mathrm{HV}},\\ &S_j(\vec{v}_j)\left\langle R_{d_j}(\vec{v}_j)\right\rangle_{\mathrm{HV}},\end{aligned} \tag{29}$$

where the rates $R_{d_j}(\vec{v}_j)$ are defined as in (10), with the only difference that now the hidden local intensities $I_{d_j}(\vec{v}_j, \lambda)$ explicitly depend on the new local settings $\vec{v}_j$.

To study the Bell nonclassicality in this extended setup, we replace in (28) the quantum-mechanical expressions for the two-mode correlators and the local terms:

$$\begin{aligned}K(\vec{v}_1, \vec{v}_2) &= \langle \Phi(\alpha_1, \alpha_2)|\, \widehat{R}_{d_1}(\chi_1, \theta_1)\widehat{R}_{d_2}(\chi_2, \theta_2)\, |\Phi(\alpha_1, \alpha_2)\rangle\,,\\ S_j(\vec{v}_j) &= \langle \Phi(\alpha_1, \alpha_2)|\, \widehat{R}_{d_j}(\chi_j, \theta_j)\, |\Phi(\alpha_1, \alpha_2)\rangle\,,\end{aligned} \tag{30}$$

where $|\Phi(\alpha_1, \alpha_2)\rangle$ is a generalized initial state specified in (6). Note that we encounter here a peculiar feature, namely that the correlation functions and local averages depend on the settings via parameters of the initial state Φ. If we would like to remove this feature of the setup we have to use POVM operators, and calculate the expressions (30) as follows:

$$\begin{aligned}K(\vec{v}_1, \vec{v}_2) &= \langle \psi|\, \widehat{\mathcal{M}}_{b_1}(\vec{v}_1)\widehat{\mathcal{M}}_{b_2}(\vec{v}_2)\, |\psi\rangle\,,\\ S_j(\vec{v}_j) &= \langle \psi|\, \widehat{\mathcal{M}}_{b_j}(\vec{v}_j)\, |\psi\rangle\,,\end{aligned} \tag{31}$$

in which $|\psi\rangle$ denotes the initial single photon superposition (2), and the POVM operators $\widehat{\mathcal{M}}_{b_j}(\vec{v}_j)$ are explicitly constructed in appendix B.

We choose to detect the transmitted beam D_{d_j}, $j = 1, 2$, however we stress that any other choice of the detectors is possible and equivalent conclusions can be addressed. The terms read as follows:

$$\begin{aligned}K(\vec{v}_1, \vec{v}_2) = \frac{\mathrm{e}^{-\alpha_1^2}\,\mathrm{e}^{-\alpha_2^2}}{2}\Bigg[&\left(\frac{(\mathrm{e}^{\alpha_2^2}-1)(1+\mathrm{e}^{\alpha_1^2}(\alpha_1^2-1))}{\alpha_1^2} + \frac{(\mathrm{e}^{\alpha_1^2}-1)(1+\mathrm{e}^{\alpha_2^2}(\alpha_2^2-1))}{\alpha_2^2}\right)\sin^2\chi_1\sin^2\chi_2\\ &+\frac{(\mathrm{e}^{\alpha_1^2}-1)(\mathrm{e}^{\alpha_2^2}-1)}{\alpha_2^2}\sin^2\chi_1\cos^2\chi_2 + \frac{(\mathrm{e}^{\alpha_1^2}-1)(\mathrm{e}^{\alpha_2^2}-1)}{|\alpha_1|^2}\cos^2\chi_1\sin^2\chi_2\\ &+\frac{(\mathrm{e}^{\alpha_1^2}-1)(\mathrm{e}^{\alpha_2^2}-1)}{2\alpha_1\alpha_2}\sin 2\chi_1\sin 2\chi_2\sin(\theta_1-\theta_2)\Bigg],\end{aligned} \tag{32}$$

$$S_j(\vec{v}_j) = \frac{\mathrm{e}^{-\alpha_j^2}}{2}\left[\sin^2\chi_j\left((\mathrm{e}^{\alpha_j^2}-1) + \frac{1+\mathrm{e}^{\alpha_j^2}(\alpha_j^2-1)}{\alpha_j^2}\right) + \cos^2\chi_j\,\frac{\mathrm{e}^{\alpha_j^2}-1}{\alpha_j^2}\right]. \tag{33}$$

As mentioned we follow the Hardy-like pattern of settings, for which the first setting of each observer corresponds to zero auxiliary field and local beamsplitter acting as identity:

$$\begin{aligned}\vec{v}_1 &= (0,0,0)\\ \vec{v}_1' &= (\chi_1', \alpha_1', \theta_1')\\ \vec{v}_2 &= (0,0,0)\\ \vec{v}_2' &= (\chi_2', \alpha_2', \theta_2').\end{aligned} \tag{34}$$

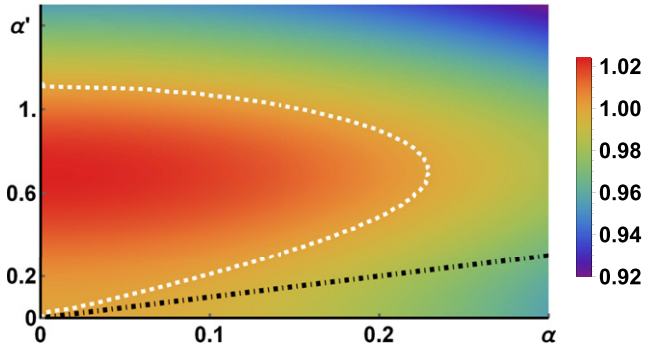

Figure 3. Violation of the left-hand-side of the CH inequality (28) as a function of amplitudes α, α' of the auxiliary fields corresponding to two local settings. The CH-value is sign-flipped for the sake of clarity of the plot. The amplitudes of auxiliary fields for a given setting (α or α') are the same for both observers (36), while they are different for the first (α) and second setting (α'). The black dashed line represents points for which $\alpha = \alpha'$, whereas the white dashed line is an envelope of the violation region with the sign-flipped CH value strictly greater than 1. Notice that the black-line points lie strictly outside the violation region. This means that it is impossible to obtain the CH violation if we just tune the phases of the local oscillators. The amplitude tuning is necessary for the violation.

We checked by numerical optimization that the double inequality (28) is violated only on the left-hand side and the minimal achievable quantum value reads -1.0239. The almost optimal settings for the violation read:

$$\begin{aligned}\vec{v}_1' &= \left(\chi_1' = \frac{3\pi}{20}, \alpha_1' = \frac{\sqrt{2}}{2}, \theta_1' = 0\right),\\ \vec{v}_2' &= \left(\chi_2' = \frac{3\pi}{20}, \alpha_2' = \frac{\sqrt{2}}{2}, \theta_2' = -\frac{\pi}{2}\right),\end{aligned} \tag{35}$$

which corresponds to local beamsplitters with transmissivity about 79% and local coherent fields with average photon number equal to $\frac{1}{2}$.

We have also investigated numerically the possibility of violating the CH inequality for rates (28) for the case when for both local settings the auxiliary field has non-zero amplitude, as opposed to (34). We assumed arbitrary parameters for both settings, with the constraint that the amplitudes of auxiliary fields corresponding to a given setting are the same for both observers, which allows for easy graphical representation:

$$\begin{aligned}\vec{v}_1 &= (\chi_1, \alpha, \theta_1),\\ \vec{v}_1' &= (\chi_1', \alpha', \theta_1'),\\ \vec{v}_2 &= (\chi_2, \alpha, \theta_2),\\ \vec{v}_2' &= (\chi_2', \alpha', \theta_2').\end{aligned} \tag{36}$$

The results of our findings are shown in the figure 3, in which we present a plot of a CH-value as a function of the amplitudes α, α' of auxiliary fields corresponding to two settings. The CH-values for each pair of α and α' are optimized over all the remaining parameters in (36). It turns out that a CH violation still exists for sufficiently small but non-zero values of α. On the other hand there is no violation for any value $\alpha = \alpha'$, which is consistent with our previous findings that nonclassical correlations cannot be found for fixed-amplitude auxiliary fields. The situation depicted in the figure 3 shows an intermediate case between the Hardy setup, in which we have on-off tuning of the auxiliary field's amplitudes and the TWC case in which the amplitudes are constant.

To complete our investigation, we have also examined the original Hardy paradox from the point of view of the intensity rate-based approach. We found that the Hardy setup with intensity rate operators does not lead to a violation of the CH inequality for rates. Our result does not invalidate the Hardy's one, however it indicates a very different nature of the nonclassicality tests based on aggregation of outcomes (like in rate approach) and the ones based on very specific outcomes (like in Hardy case). All the detailed considerations on this topic are presented in a forthcoming publication [38].

6. Bell operators as entanglement witnesses: intensities vs rates

It is well known that Bell operators can be turned into entanglement witnesses. Thus, the question arises if the inequality in [17], used in the TWC paper, could also serve this purpose. As they are not proper Bell inequalities the answer requires a careful analysis. Below we show how to understand the additional condition (9) in this context. Next, we build an optimized entanglement indicator based on the CHSH-like inequality of [17]. As the method which we employ to build entanglement indicators for fields is also immediately applicable for Bell operators based on intensity rates, we build an analogous entanglement indicator for this case.

Since the CHSH-like inequality (20) seems to be more sensitive to the correlations present in the TWC setup than the CHSH inequality for rates (12), it suggests that the inequality (20) might be a stronger entanglement indicator than (12). Surprisingly, it turns out the latter inequality leads to an entanglement witness which is more efficient in the case of TWC correlations. That is, it detects entanglement for a broader range of values of α.

6.1. The additional assumption (9) in the case of separable states

The original TWC correlations (with $|\alpha_j| = \alpha = \text{const.}$ for all settings in the experiment) [1], do not violate local realism, as shown by the local model presented in [19]. The model covers the whole range of values of α for which TWC obtained violations of the inequality of [17]. As said earlier, the inequality of [17] cannot be obtained without the additional assumption (9), which states that for the given value of the hidden variable λ the total local intensity predicted by the local hidden variable model does not vary with the measurement settings. Let us assume the model of intensity, which was used above and leads to the predictions of [1]. It is in the form of number of registered photons (in the given run of the experiment). In such a case the additional assumption transforms into:

- Either

$$n_{\text{tot}_i}(\lambda) = n_{c_i}(\theta_i, \lambda) + n_{d_i}(\theta_i, \lambda), \tag{37}$$

  where $n_{x_i}(\theta_i, \lambda)$ is the number of photons predicted by an LHV theory, for the given λ, to be detected at detector x_i, under local setting θ_i. The total number to be detected, in this case, at both outputs $n_{\text{tot}_i}(\lambda)$ is assumed to be independent of the local setting. Such must be the form of the condition (9), if we assume the numbers of photons to be detected are predetermined by the model for each value of λ.

- Or, for stochastic local hidden variable models, the condition (9) has to be put as

$$\langle n_{\text{tot}_i}\rangle(\lambda) = \langle n_{c_i}(\theta_i)\rangle(\lambda) + \langle n_{d_i}(\theta_i)\rangle(\lambda), \tag{38}$$

  where $\langle n_{x_i}(\theta_i)\rangle(\lambda) = \sum_{n_{x_i}=1}^{\infty} n_{x_i} P(n_{x_i}|\theta_i, \lambda)$ for $x = c, d$.

Note that condition (38) does not imply (37).

We shall show below that in the case of hidden quantum product state model (i.e. for separable states), which is a subclass of LHV models, the condition of [17] should be understood as (38).

6.1.1. *Condition (38) for separable states*

As already discussed, assumption (37) imposes an additional constraint on the structure of local hidden variable model. Still, a local hidden product (quantum) state model is a form of local hidden variable model, which we get when we consider a separable quantum state as the one that causes the correlations. In such a case condition (38) definitely holds.

This suggests that the inequality of [17] can be an entanglement witness.

Consider a density matrix describing separable states for optical fields, for the operational scenario which we consider here. They are always a convex combination of pure 'product' states (inverted commas are for field theories, see below). We shall use now λ as an index related with any such element of the convex combination, and the weights of the convex combination we shall denote, as earlier, by ρ_λ. An arbitrary separable state for the optical fields of the considered experiments reads

$$\rho_{\text{sep}}^{1,2} = \int \mathrm{d}\lambda \rho_\lambda f_\lambda^\dagger(\widehat{a}_1, \widehat{b}_1) g_\lambda^\dagger(\widehat{a}_2, \widehat{b}_2) \, |\Omega\rangle\langle\Omega| f_\lambda(\widehat{a}_1, \widehat{b}_1) g_\lambda(\widehat{a}_2, \widehat{b}_2), \tag{39}$$

where $f_\lambda^\dagger(\widehat{a}_1, \widehat{b}_1)$ and $g_\lambda^\dagger(\widehat{a}_2, \widehat{b}_2)$ are polynomial functions of annihilation operators acting on modes $\widehat{a}_i$ and $\widehat{b}_i$ of ith party. Note that for arbitrary local observables $\widehat{O}_i(\widehat{a}_i, \widehat{a}_i^\dagger, \widehat{b}_i, \widehat{b}_i^\dagger)$, and for any of the pure states $f_\lambda^\dagger(\widehat{a}_1, \widehat{b}_1) g_\lambda^\dagger(\widehat{a}_2, \widehat{b}_2) \, |\Omega\rangle$ one has $\langle \widehat{O}_1 \widehat{O}_2\rangle_\lambda = \langle \widehat{O}_1\rangle_\lambda \langle \widehat{O}_2\rangle_\lambda$. Thus, this is a proper description of separability for optical fields.

The probability of getting result n_{x_1} for 1st party, with setting θ_1 for state indexed by λ is given by:

$$\Pr(n_{x_1}|\theta_1)_\lambda = \mathrm{Tr}\left[\delta_{(n_{x_1},\widehat{n}_{x_1}(\theta_1))} f_\lambda^\dagger(\widehat{a}_1,\widehat{b}_1)\,|\Omega\rangle\langle\Omega|\, f_\lambda(\widehat{a}_1,\widehat{b}_1)\right] = \langle\delta_{(n_{x_1},\widehat{n}_{x_1}(\theta_1))}\rangle_\lambda, \tag{40}$$

where $\delta_{(n,k)}$ is the Kroenecker's delta function.

A similar formula holds for 2nd party for results n_{x_2} under setting θ_2. Following formula (40) the joint probability for two parties goes as follows:

$$\Pr(n_{x_1}, n_{x_2}|\theta_1,\theta_2)_{\mathrm{sep}} = \mathrm{Tr}\left[\delta_{(n_{x_1},\widehat{n}_{x_1}(\theta_1))}\delta_{(n_{x_2},\widehat{n}_{x_2}(\theta_2))}\rho_{\mathrm{sep}}^{1,2}\right] = \int \mathrm{d}\lambda\rho_\lambda \Pr(n_{x_1}|\theta_1)_\lambda \Pr(n_2|\theta_2)_\lambda. \tag{41}$$

Thus we have a typical structure of a local hidden variable model. Further, assumption (38) is not in contradiction with the structure of separable states. In fact we have an operator identity:

$$\widehat{n}_{\mathrm{tot}_i} = \widehat{n}_{c_i}(\theta_i) + \widehat{n}_{d_i}(\theta_i), \tag{42}$$

which holds for any settings θ_i and we have

$$\langle\widehat{n}_{\mathrm{tot}_i}\rangle(\lambda) = \langle\widehat{n}_{c_i}(\theta_i)\rangle(\lambda) + \langle\widehat{n}_{d_i}(\theta_i)\rangle(\lambda), \tag{43}$$

i.e. $\langle\widehat{n}_{\mathrm{tot}_i}\rangle_\lambda$ also does not depend on the settings. Thus indeed the inequality of [17] is an entanglement indicator.

6.2. Entanglement indicators, a comparison

The inequality of [17] in the TWC version (20) can be put as the following condition for separability

$$\langle\delta\widehat{n}_1(\theta_1)\delta\widehat{n}_2(\theta_2) + \delta\widehat{n}_1(\theta_1')\delta\widehat{n}_2(\theta_2) + \delta\widehat{n}_1(\theta_1)\delta\widehat{n}_2(\theta_2') - \delta\widehat{n}_1(\theta_1')\delta\widehat{n}_2(\theta_2')\rangle_{\mathrm{sep}} \leqslant 2\langle\widehat{n}_{\mathrm{tot}_1}\widehat{n}_{\mathrm{tot}_2}\rangle_{\mathrm{sep}}, \tag{44}$$

where we introduced: $\delta\widehat{n}_i(\theta_i) = \widehat{n}_{c_i}(\theta_i) - \widehat{n}_{d_i}(\theta_i)$, and similarly for θ_i'. However, the right-hand side of this condition was derived following the additional assumption on local hidden variable models. For separable states this can be lowered, as they form a further constrained set of local hidden variable models.

We have to find its upper bound for separable states. This involves also search for optimal settings. As in the usual case of two qubits optimal violations of the CHSH inequality take place when Alice and Bob use fully complementary settings, we shall give the separability conditions for such a case. We are going to use an isomorphic mapping from entanglement witnesses for qubits, to entanglement indicators for quantum optical fields [28, 29]. We derive a separability condition based on Bell inequality for qubits and then map it to optical field operators. As we need only two pairs of settings we reduce the Bloch sphere for qubits to a circle and using the standard Pauli matrices we denote the operator basis for each of them by $\vec{\sigma}_j = (\sigma_j^x, \sigma_j^z)$, $j = 1, 2$. The optimal separability condition based on the CHSH inequality can be obtained if we choose Alice's and Bob's settings to be fully complementary. With each setting we associate a unit Bloch vector. We can put: $\vec{a} = (1, 0)$, $\vec{a}' = (0, 1)$, $\vec{b} = \frac{1}{\sqrt{2}}(1, 1)$ and $\vec{b}' = \frac{1}{\sqrt{2}}(1, -1)$. In this notation the lhs of the CHSH inequality for any pure product state of two qubits gives the following:

$$\left\langle \vec{a}\cdot\vec{\sigma}_1 \otimes (\vec{b}+\vec{b}')\cdot\vec{\sigma}_2 + \vec{a}'\cdot\vec{\sigma}_1 \otimes (\vec{b}-\vec{b}')\cdot\vec{\sigma}_2 \right\rangle_{\mathrm{prod}} \leqslant \sqrt{2}\left(\langle\sigma_1^x\rangle_{\mathrm{prod}}\langle\sigma_2^x\rangle_{\mathrm{prod}} + \langle\sigma_1^z\rangle_{\mathrm{prod}}\langle\sigma_2^z\rangle_{\mathrm{prod}}\right) \leqslant \sqrt{2}, \tag{45}$$

because $\langle\sigma_j^x\rangle^2 + \langle\sigma_j^z\rangle^2 \leqslant 1$, where $j = 1, 2$, for any qubit state. Condition (45) holds as well for all mixed separable states of two qubits as they are convex combinations of product states. It holds also for arbitrary orthogonal pairs $\vec{a}$, $\vec{a}'$ and $\vec{b}$, $\vec{b}'$. Its final form as an entanglement witness thus reads:

$$\langle\sqrt{2}\sigma_1^0\otimes\sigma_2^0 - \left[\vec{a}\cdot\vec{\sigma}_1\otimes(\vec{b}+\vec{b}')\cdot\vec{\sigma}_2 + \vec{a}'\cdot\vec{\sigma}_1\otimes(\vec{b}-\vec{b}')\cdot\vec{\sigma}_2\right]\rangle_{\mathrm{sep}} \geqslant 0, \tag{46}$$

where we have introduced identity matrices σ^0.

A method of finding an isomorphic entanglement witness given in [29] is based on replacements $\sigma_\mu \to \widehat{S}_\mu$, where the latter is a quantum Stokes operator of optical field ($\mu = 0, 1, 2, 3$). In the case of the TWC interferometric configuration $\widehat{S}_0$ can be replaced by the total intensity impinging on the detectors behind the local interferometer, here modeled by $\widehat{n}_{\mathrm{tot}_i}$, and $\widehat{S}_1$ with $\widehat{S}_2$ by respectively

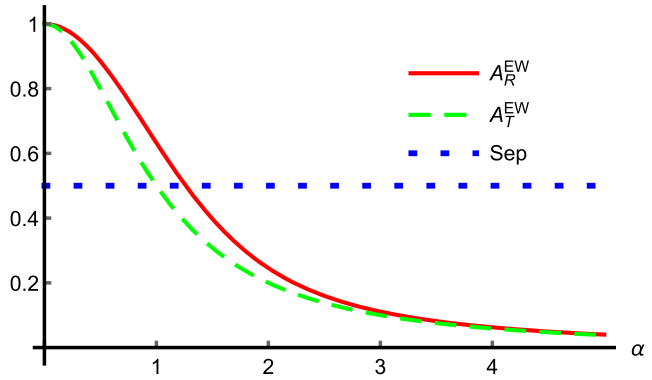

Figure 4. Comparison of amplitudes $A(\alpha)$ in function of α for CHSH based entanglement conditions for rates (47) and intensities (48). If $A(\alpha)$ exceeds $\frac{1}{2}$ we observe violation.

$\delta\widehat{n}_i(\theta_i) = \widehat{n}_{c_i}(\theta_i) - \widehat{n}_{d_i}(\theta_i)$ and $\delta\widehat{n}_i(\theta_i + \frac{\pi}{2})$. Thus the quantum optical analog for the separability condition for two qubits is given, via the isomorphism of [29], in the following form:

$$\Big\langle \sqrt{2}\widehat{n}_{\mathrm{tot}_1}\widehat{n}_{\mathrm{tot}_2} - \Big[\delta\widehat{n}_1(\theta_1)\delta\widehat{n}_2(\theta_2) + \delta\widehat{n}_1(\theta_1)\delta\widehat{n}_2(\theta_2 + \frac{\pi}{2}) + \delta\widehat{n}_1(\theta_1 + \frac{\pi}{2})\delta\widehat{n}_2(\theta_2) - \delta\widehat{n}_1(\theta_1 + \frac{\pi}{2})\delta\widehat{n}_2(\theta_2 + \frac{\pi}{2})\Big]\Big\rangle_{\mathrm{sep}} \geqslant 0. \tag{47}$$

The above condition (47) can be also transformed into the one with rates instead of intensities. This can be achieved using another isomorphism presented in [29]:

$$\Big\langle \sqrt{2}\widehat{\Pi}_1\widehat{\Pi}_2 - \Big[\delta\widehat{R}_1(\theta_1)\delta\widehat{R}_2(\theta_2) + \delta\widehat{R}_1(\theta_1 + \frac{\pi}{2})\delta\widehat{R}_2(\theta_2) + \delta\widehat{R}_1(\theta_1)\delta\widehat{R}_2(\theta_2 + \frac{\pi}{2}) - \delta\widehat{R}_1(\theta_1 + \frac{\pi}{2})\delta\widehat{R}_2(\theta_2 + \frac{\pi}{2})\Big]\Big\rangle_{\mathrm{sep}} \geqslant 0, \tag{48}$$

where $\delta\widehat{R}_i(\theta_i) = \widehat{R}_{c_i}(\theta_i) - \widehat{R}_{d_i}(\theta_i)$, and the intensity rate operators $\widehat{R}_{x_i}(\theta_i)$ are defined in equation (13).

Witnesses (47) and (48) can reveal mode entanglement of the initial state $|\Psi(\alpha)\rangle$ (3) in a certain range of the coherent field amplitudes α. Analogously to (16) we introduce $A_R^{\mathrm{EW}}(\alpha)$ that stands for the amplitude of the correlation function:

$$\frac{\langle\Psi(\alpha)|\delta\widehat{R}_1(\theta_1)\delta\widehat{R}_2(\theta_2)|\Psi(\alpha)\rangle}{\langle\Psi(\alpha)|\widehat{\Pi}_1\widehat{\Pi}_2|\Psi(\alpha)\rangle} = A_R^{\mathrm{EW}}(\alpha)\sin(\theta_1 - \theta_2), \tag{49}$$

where the amplitude is given by

$$A_R^{\mathrm{EW}}(\alpha) = \frac{\mathrm{e}^{-\alpha^2}(\mathrm{e}^{\alpha^2} - 1)}{\alpha^2}. \tag{50}$$

Condition (48) for $|\Psi\rangle$ can be put as follows:

$$A_R^{\mathrm{EW}}(\alpha)[\sin(\theta_1 - \theta_2) + \sin(\theta_1' - \theta_2) + \sin(\theta_1 - \theta_2') - \sin(\theta_1' - \theta_2')] \leqslant \sqrt{2}, \tag{51}$$

and its violation appears if $A_R^{\mathrm{EW}}(\alpha) \geqslant \frac{1}{2}$. The same holds for (47) with the difference that amplitude $A_T^{\mathrm{EW}}(\alpha) \equiv A_T(\alpha) = \frac{1}{(1+\alpha^2)}$ replaces $A_R^{\mathrm{EW}}(\alpha)$. We present entanglement detection with (48) and (47) in terms of values of $A_{R/T}^{\mathrm{EW}}(\alpha)$ in figure 4. The CHSH-based entanglement indicator involving rates (48) is more effective than the one based on CHSH-like inequalities of [17] involving intensities (47). This may seem surprising, since the CHSH-like inequalities of [17] show (spurious) violations of local realism for the TWC configuration, whereas CHSH-Bell inequality involving rates is not violated for any α. This fact shows the advantage of the rate-based approach over the intensity-based approach: it gives no spurious Bell violations and nevertheless it is more effective as an entanglement indicator.

Of course the presented entanglement indicators have two interpretations, within the context of TWC correlations. Either they detect entanglement of the state:

$$\frac{1}{\sqrt{2}}|\alpha\rangle_{a_1}(|01\rangle_{b_1b_2} + i|10\rangle_{b_1b_2})|\alpha\rangle_{a_2} \tag{52}$$

with von Neumann measurements, or entanglement of

$$\frac{1}{\sqrt{2}}(|01\rangle_{b_1b_2} + i\,|10\rangle_{b_1b_2}) \tag{53}$$

with optical homodyne based POVM measurements. In the second case the settings may depend also on varying moduli of values of local α's.

7. Discussion and conclusions

In our work we reconsidered two prototypical experimental scenarios aiming at demonstration of a single photon nonclassicality, namely the proposal of TWC [1], and the one of Hardy [2]. We have shown that if one applies an intensity-rate-based approach, without using additional assumption (9), the associated Bell-CHSH inequality for rates is not violated in the case of TWC correlations. This finding is concurrent with our previous work [19], which shows a failure of TWC setup in demonstrating nonclassicality by providing a precise local hidden variable model for the setup. Nevertheless, we have shown that the original TWC analysis can be still used as an entanglement indicator, however a weaker one than the one based on intensity rate approach. These facts are a strong premise towards treating the intensity rate-based approach to analysis of correlations of the optical fields as more appropriate from both: Bell-type perspective (as it is free of any additional assumptions) and an entanglement detection perspective (as it gives rise to more robust entanglement indicators). As a side discussion we pointed out possible threats concerning the application of a parametric approximation to a coherent light. Namely if one applies such an approximation at the same time ignoring the phase uncertainty, spurious increases of the strength of correlations may arise.

Our intensity rate-based analysis of Hardy-like scenario leads to several conclusions. First, we point out that in this approach the CH inequality for rates is strictly stronger than the CHSH one (for rates). We have shown a violation of the CH inequality for rates in Hardy-like scenario, which includes tunable amplitudes of the coherent local oscillator auxiliary fields, but also (in contrast to the original Hardy analysis) local beamsplitters with tunable transmissivities. Our approach involves modification of two further features of the Hardy scheme, namely we use just a single photon initial state as in the TWC approach ($q = 0$ in the figure 1) and do not limit the settings specified by the local oscillator strengths to the on/off detection mode. This indicates that the crucial aspect of the Hardy-like schemes which enables violation of the local realism is the tunability of the strengths of the local auxiliary fields, which need to differ from setting to setting.

Let us now discuss the physical interpretation of these observations. First, notice that the Hardy-like scenario possesses a peculiar feature untypical for Bell tests, namely that the entire initial state of the interferometric setup is different for different measurement settings. To some extent one can overcome this interpretational difficulty by treating presence of auxiliary fields as an optical implementation of a POVM. We show analytical forms of such POVMs in appendices A and B. However even such a treatment does not dispel doubts whether nonclassical correlations found in Hardy-like scenarios can be attributed solely to the single photon (excitation) state. Despite several objections discussed earlier majority of works devoted to this issue states that the sole source of correlations in such experiments is the single photon superposition. Our reconsideration of the mechanism of the nonclassical correlations in the setup indicates that such a conclusion is unfounded due to a very subtle issue, which goes beyond the duality between mode and particle entanglement in interferometric setups (see e.g. discussion in [13]). Namely, the source of observed correlations is the quantum interference, which occurs if and only if a given detected multiphoton event could have been realized in two or more genuinely indistinguishable ways. The quantum interference observed in Hardy-like schemes is based on indistinguishability of processes corresponding to detection of photons coming from the signal state and the local oscillator fields. At the detection stage due to mentioned interference all photons must be treated on equal footing, hence the distinction between the input (signal) photons and the local oscillator ones disappears. Note that such a conclusion can be drawn only for the case of homodyne measurements with weak local auxiliary fields, since then the local fields have to have a full quantum description and it is meaningful to consider them as composed of photonic excitations. Nevertheless we are not aware of any work which would show single photon Bell nonclassicality in the regime of strong-field homodyne detection.

Based on our findings, we argue that the resource behind observed nonclassical correlations in the TWC-Hardy experiments is quantum interference due to the indistinguishability of photons originating from different sources. This means that the 'nonlocality of a single photon' shares the same interpretation as the other profound interferometric nonclassical phenomena, like photonic entanglement swapping [39], or nonclassical interference for pairs of photons originating from independent sources [40–43].

Acknowledgments

We thank Łukasz Rudnicki for comprehensive discussions on the topic of mode entanglement. The work is part of the ICTQT IRAP (MAB) project of FNP, co-financed by structural funds of EU. MK acknowledges support by the Foundation for Polish Science through the START scholarship. AM acknowledges support by National Science Center through the Grant MINIATURA DEC-2020/04/X/ST2/01794.

Data availability statement

No new data were created or analysed in this study.

Appendix A. Effective POVM operators for CHSH inequality rates

We obtained the correlation coefficient (see equation (16)) for local homodyne-type measurements performed on the linear superposition of a single photon and vacuum, $|\psi\rangle_{b_1,b_2} = \frac{1}{\sqrt{2}}(|01\rangle + i\,|10\rangle)_{b_1,b_2}$, in terms of intensity rates in mode $\widehat{c}_j$ or $\widehat{d}_j$ in a symmetric beamsplitter transformation $U_{\mathrm{BS}_j}(\frac{\pi}{4},\theta_j)$, where an auxiliary coherent field $|\alpha\rangle_{a_j}$, impinges on the remaining input of the beamsplitter for $j = 1, 2$. In this section our aim is to figure out the form of the positive operators POVMs acting on the initial state $|\psi\rangle_{b_1,b_2}$, which give rise to an equivalent form of the same correlation function (18). Suppose $\mathcal{M}_{b_j}(\alpha,\theta_j)$ is the POVM operator in part of the mode b_j, for $j = 1, 2$, then we obtain the defining condition for the POVM by demanding equivalence of the two forms of the correlation coefficient (compare equations (16) and (18)):

$$\langle\Psi(\alpha)|\,\widehat{H}_1(\theta_1)\widehat{H}_2(\theta_2)\,|\Psi(\alpha)\rangle = {}_{b_1b_2}\langle\psi|\widehat{\mathcal{M}}_{b_1}(\alpha,\theta_1)\widehat{\mathcal{M}}_{b_2}(\alpha,\theta_2)|\psi\rangle_{b_1b_2}, \tag{A1}$$

where the initial state $|\Psi(\alpha)\rangle$ is defined in equation (3). Hence, the POVM operator is given by:

$$\widehat{\mathcal{M}}_{b_j}(\alpha,\theta_j) = {}_{a_j}\langle\alpha|\widehat{H}_j(\theta_j)|\alpha\rangle_{a_j} \tag{A2}$$

$$= {}_{a_j}\langle\alpha|\widehat{\Pi}_{c_jd_j}\frac{\widehat{n}_{c_j}-\widehat{n}_{d_j}}{\widehat{n}_{c_j}+\widehat{n}_{d_j}}\widehat{\Pi}_{c_jd_j}|\alpha\rangle_{a_j} \tag{A3}$$

$$= {}_{a_j}\langle\alpha|\widehat{\Pi}_{a_jb_j}\frac{\mathrm{e}^{\mathrm{i}\theta_j}\,\widehat{a}_j\widehat{b}_j^{\dagger}+\mathrm{e}^{-\mathrm{i}\theta_j}\,\widehat{a}_j^{\dagger}\widehat{b}_j}{\widehat{a}_j^{\dagger}\widehat{a}_j+\widehat{b}_j^{\dagger}\widehat{b}_j}\widehat{\Pi}_{a_jb_j}|\alpha\rangle_{a_j} \tag{A4}$$

$$= \mathrm{e}^{-\alpha^2}\sum_{n=0}^{\infty}\frac{\alpha^{2n+1}}{n!}\sum_{m=1}^{\infty}\frac{\sqrt{m}}{n+m}\left(\mathrm{e}^{\mathrm{i}\theta_j}\,|m\rangle\langle m-1|_{b_j}+\mathrm{e}^{-\mathrm{i}\theta_j}\,|m-1\rangle\langle m|_{b_j}\right). \tag{A5}$$

Appendix B. Effective POVM operators for CH inequality and tunable exit beamsplitters

In the previous section, we have calculated the POVM for the balanced beamsplitter and for the homodyne detectors $\widehat{H}_j$. Here, we will try to obtain the POVM for the correlation coefficients given in equations (30) and (31) for arbitrary beamsplitters. The construction of the POVM is shown schematically in the figure 5.

For a beamsplitter with arbitrary transitivity, the output modes are given by (see equation (5)):

$$\widehat{c}_j = \cos\,\chi_j\widehat{a}_j + \sin\,\chi_j\,\mathrm{e}^{-\mathrm{i}\theta_j}\,\widehat{b}_j, \tag{B1}$$

$$\widehat{d}_j = -\sin\,\chi_j\,\mathrm{e}^{\mathrm{i}\theta_j}\,\widehat{a}_j + \cos\,\chi_j\widehat{b}_j. \tag{B2}$$

Now we want to find out POVM elements $\widehat{\mathcal{M}}_{b_j}(\vec{v}_j), j = 1, 2$, such that the correlation coefficients and the local terms from equation (31) read $K(\vec{v}_1,\vec{v}_2) = {}_{b_1b_2}\langle\psi|\widehat{\mathcal{M}}_{b_1}(\vec{v}_1)\widehat{\mathcal{M}}_{b_2}(\vec{v}_2)|\psi\rangle_{b_1b_2}$ and $S_j(\vec{v}_j) = {}_{b_1b_2}\langle\psi|\widehat{\mathcal{M}}_{b_j}(\vec{v}_j)|\psi\rangle_{b_1b_2}$, for $j = 1, 2$.

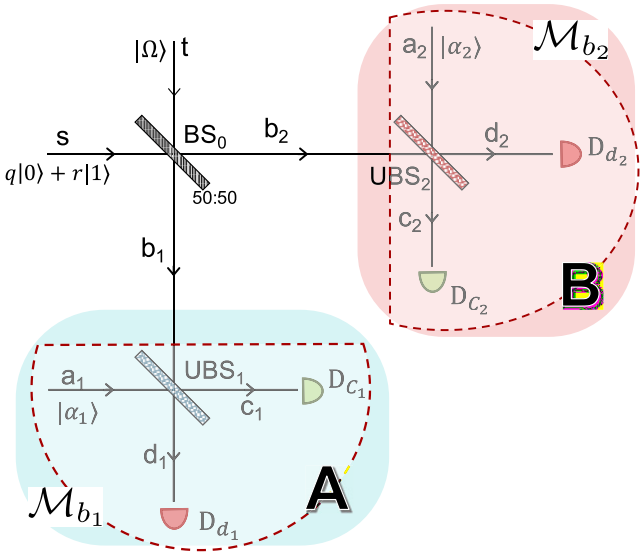

Figure 5. Schematic diagram of the effective POVM operators acting on modes $\widehat{b}_1$ and $\widehat{b}_2$ to detect the nonclassicality of a single photon. Average intensity rate $\langle \widehat{R}_{x_j} \rangle$ detected in detector D_{x_j}, for $x = c, d, j = 1, 2$, or the correlation $\langle \widehat{R}_{x_1} \widehat{R}_{x_2} \rangle$ detected in detectors D_{x_1} and D_{x_2} for $x = c, d$ on the output modes of the beamsplitters $U_{\mathrm{BS}j}, j = 1, 2$ along with an auxiliary coherent beam, can be considered as an effective POVM $\mathcal{M}_{b_j}$ acting on the modes $b_j, j = 1, 2$. The semicircular shaded region shows that the beamsplitter $U_{\mathrm{BS}j}$, the coherent field $|\alpha_j\rangle$, and detection of the Homodyne $\widehat{H}_j$ for $j = 1, 2$ are equivalent to a POVM $\mathcal{M}_{b_j}(\alpha_j, \theta_j)$, for $j = 1, 2$ is given in equation (A5) and the detection of $\widehat{R}_{d_j}$, for $j = 1, 2$ are equivalent to a POVM $\mathcal{M}_{b_j}(\vec{v_j})$, for $j = 1, 2$ is given in equation (B6).

By demanding equivalence of the two forms of correlation coefficients in equations (30) and (31) we obtain:

$$\mathcal{M}_{b_j}(\vec{v_j}) = {}_{a_j}\langle \alpha_j | \widehat{R}_{d_j}(\chi_j, \theta_j) | \alpha_j \rangle_{a_j} = {}_{a_j}\langle \alpha_j | \widehat{\Pi}_{c_j d_j} \frac{\widehat{n}_{d_j}}{\widehat{n}_{c_j} + \widehat{n}_{d_j}} \widehat{\Pi}_{c_j d_j} | \alpha_j \rangle_{a_j} \tag{B3}$$

$$= {}_{a_j}\langle \alpha_j | \widehat{\Pi}_{a_j b_j} \frac{\widehat{d}_j^\dagger \widehat{d}_j}{\widehat{a}_j^\dagger \widehat{a}_j + \widehat{b}_j^\dagger \widehat{b}_j} \widehat{\Pi}_{a_j b_j} | \alpha_j \rangle_{a_j} \tag{B4}$$

$$= {}_{a_j}\langle \alpha_j | \widehat{\Pi}_{a_j b_j} \frac{\sin^2 \chi_j \widehat{a}_j^\dagger \widehat{a}_j + \cos^2 \chi_j \widehat{b}_j^\dagger \widehat{b}_j}{\widehat{a}_j^\dagger \widehat{a}_j + \widehat{b}_j^\dagger \widehat{b}_j} \widehat{\Pi}_{a_j b_j} | \alpha_j \rangle_{a_j}$$
$$- \frac{1}{2} \sin 2\chi_{j a_j} \langle \alpha_j | \widehat{\Pi}_{a_j b_j} \frac{\mathrm{e}^{\mathrm{i}\theta_j} \widehat{a}_j \widehat{b}_j^\dagger + \mathrm{e}^{-\mathrm{i}\theta_j} \widehat{a}_j^\dagger \widehat{b}_j}{\widehat{a}_j^\dagger \widehat{a}_j + \widehat{b}_j^\dagger \widehat{b}_j} \widehat{\Pi}_{a_j b_j} | \alpha_j \rangle_{a_j} \tag{B5}$$

$$= \mathrm{e}^{-\alpha_j^2} \left(\cos^2 \chi_j \left(\mathbb{I}_{b_j} - |0\rangle \langle 0|_{b_j} \right) + \sum_{n=1}^{\infty} \frac{\alpha_j^{2n}}{n!} \frac{\sin^2 \chi_j n + \cos^2 \chi_j b_j^\dagger b_j}{n + b_j^\dagger b_j} \right.$$
$$\left. - \frac{1}{2} \sin 2\chi_j \sum_{n=0}^{\infty} \frac{\alpha_j^{2n+1}}{n!} \sum_{m=1}^{\infty} \frac{\sqrt{m}}{n+m} \left(\mathrm{e}^{\mathrm{i}\theta_j} |m\rangle \langle m-1|_{b_j} + \mathrm{e}^{-\mathrm{i}\theta_j} |m-1\rangle \langle m|_{b_j} \right) \right). \tag{B6}$$

If beamsplitters $U_{\mathrm{BS}1}$ and $U_{\mathrm{BS}2}$ have 100% transmissivity, then the above POVM reduces to $\widehat{\Pi}_{b_j} = \mathbb{I}_{b_j} - |0\rangle \langle 0|_{b_j}$, $j = 1, 2$.

ORCID iDs

Tamoghna Das https://orcid.org/0000-0002-8074-6720
Marcin Karczewski https://orcid.org/0000-0002-9120-3377
Antonio Mandarino https://orcid.org/0000-0003-3745-5204
Marcin Markiewicz https://orcid.org/0000-0002-8983-9077
Bianka Woloncewicz https://orcid.org/0000-0002-4039-9146
Marek Żukowski https://orcid.org/0000-0001-7882-7962

References

[1] Tan S M, Walls D F and Collett M J 1991 *Phys. Rev. Lett.* **66** 252
[2] Hardy L 1994 *Phys. Rev. Lett.* **73** 2279
[3] Vaidman L 1995 *Phys. Rev. Lett.* **75** 2063
[4] Hessmo B, Usachev P, Heydari H and Björk G 2004 *Phys. Rev. Lett.* **92** 180401
[5] van Enk S J 2005 *Phys. Rev.* A **72** 064306
[6] Dunningham J and Vedral V 2007 *Phys. Rev. Lett.* **99** 180404
[7] Heaney L, Cabello A, Santos M F and Vedral V 2011 *New J. Phys.* **13** 053054
[8] Jones S J and Wiseman H M 2011 *Phys. Rev.* A **84** 012110
[9] Brask J B, Chaves R and Brunner N 2013 *Phys. Rev.* A **88** 012111
[10] Morin O, Bancal J-D, Ho M, Sekatski P, D'Auria V, Gisin N, Laurat J and Sangouard N 2013 *Phys. Rev. Lett.* **110** 130401
[11] Fuwa M, Takeda S, Zwierz M, Wiseman H M and Furusawa A 2015 *Nat. Commun.* **6** 6665
[12] Lee S-Y, Park J, Kim J and Noh C 2017 *Phys. Rev.* A **95** 012134
[13] Demkowicz-Dobrzański R, Jarzyna M and Kołński J 2015 Chapter four—quantum limits in optical interferometry *Progress in Optics* vol 60 ed E Wolf (Amsterdam: Elsevier) pp 345–435
[14] Aharonov Y and Vaidman L 2000 *Phys. Rev.* A **61** 052108
[15] Gerry C C 1996 *Phys. Rev.* A **53** 4583
[16] Ashhab S, Maruyama K and Nori F 2007 *Phys. Rev.* A **76** 052113
[17] Reid M D and Walls D F 1986 *Phys. Rev.* A **34** 1260
[18] Santos E 1992 *Phys. Rev. Lett.* **68** 894
[19] Das T, Karczewski M, Mandarino A, Markiewicz M, Woloncewicz B and Żukowski M 2021 arXiv:2102.03254 [quant-ph]
[20] Żukowski M, Wieśniak M and Laskowski W 2016 *Phys. Rev.* A **94** 020102
[21] Donati G, Bartley T J, Jin X-M, Vidrighin M-D, Datta A, Barbieri M and Walmsley I A 2014 *Nat. Commun.* **5** 5584
[22] Thekkadath G S *et al* 2020 *Phys. Rev.* A **101** 031801
[23] Banaszek K and Wódkiewicz K 1999 *Phys. Rev. Lett.* **82** 2009
[24] Caspar P *et al* 2020 *Phys. Rev. Lett.* **125** 110506
[25] Munro W J 1999 *Phys. Rev.* A **59** 4197
[26] He Q Y, Reid M D, Vaughan T G, Gross C, Oberthaler M and Drummond P D 2011 *Phys. Rev. Lett.* **106** 120405
[27] He Q Y, Vaughan T G, Drummond P D and Reid M D 2012 *New J. Phys.* **14** 093012
[28] Żukowski M, Laskowski W and Wieśniak M 2017 *Phys. Rev.* A **95** 042113
[29] Yu Y, Chen X, Zhang J, Zhao C and Chen X 2019 *J. Phys.: Conf. Ser.* **1168** 032041
[30] Clauser J F and Horne M A 1974 *Phys. Rev.* D **10** 526
[31] Hardy L 1992 Nonlocality, violation of Lorentz invariance, and wave-particle duality in quantum theory *Durham Thesis* Durham University
[32] Walls D F and Milburn G J 2007 *Quantum Optics* (Berlin: Springer)
[33] Peres A 1995 *Phys. Rev. Lett.* **74** 4571
[34] Boyer T 2019 *Atoms* **7** 29
[35] Tyc T and Sanders B C 2004 *J. Phys. A: Math. Gen.* **37** 7341
[36] Garg A and Mermin N D 1987 *Phys. Rev.* D **35** 3831
[37] Santos E 1986 *Phys. Lett.* A **115** 363
[38] Das T, Karczewski M, Mandarino A, Markiewicz M, Woloncewicz B and Żukowski M 2021 in preparation.
[39] Żukowski M, Zeilinger A, Horne M A and Ekert A K 1993 *Phys. Rev. Lett.* **71** 4287–90
[40] Yurke B and Stoler D 1992 *Phys. Rev. Lett.* **68** 1251
[41] Yurke B and Stoler D 1992 *Phys. Rev.* A **46** 2229
[42] Kaltenbaek R, Blauensteiner B, Żukowski M, Aspelmeyer M and Zeilinger A 2006 *Phys. Rev. Lett.* **96** 240502
[43] Blasiak P and Markiewicz M 2019 *Sci. Rep.* **9** 20131

PAPER • OPEN ACCESS

Wave–particle complementarity: detecting violation of local realism with photon-number resolving weak-field homodyne measurements

New Journal of Physics
The open access journal at the forefront of physics

Deutsche Physikalische Gesellschaft DPG
IOP Institute of Physics

Published in partnership with: Deutsche Physikalische Gesellschaft and the Institute of Physics

OPEN ACCESS

RECEIVED
13 July 2021

REVISED
22 October 2021

ACCEPTED FOR PUBLICATION
14 February 2022

PUBLISHED
16 March 2022

PAPER

Wave–particle complementarity: detecting violation of local realism with photon-number resolving weak-field homodyne measurements

Tamoghna Das, Marcin Karczewski*, Antonio Mandarino*, Marcin Markiewicz, Bianka Woloncewicz and Marek Żukowski

International Centre for Theory of Quantum Technologies, University of Gdańsk, Wita Stwosza 63, 80-308 Gdańsk, Poland
* Authors to whom any correspondence should be addressed.

E-mail: marcin.karczewski@ug.edu.pl and antonio.mandarino@ug.edu.pl

Keywords: wave–particle complementarity, Bell's theorem, quantum optical fields

Abstract

Nowadays photon-number resolving weak-field homodyne measurements allow realization of emblematic gedankenexperiments revealing correlations of optical fields. This covers experiments on (a) excitation of a pair of spatial modes by a single photon, and (b) two spatial modes in a weakly squeezed vacuum state, involving *constant local oscillator strengths*. Proving Bell nonclassicality of such correlations demands measurements of complementary observables. We show that typical arrangement of weak-field homodyne detection with measurement settings defined by phases of local oscillators of constant strength does not provide enough complementarity for confirming Bell nonclassicality. In the case of experiment (a) we provide an exact local hidden variable model restoring all quantum probabilities, whereas in the case of experiment (b) we show that the claims of its nonclassicality are unfounded. A full complementarity of wave aspects vs particle (number) can be achieved in a measurement situation in which respectively the local oscillators are *on* or *off*. This is shown to lead to an operational scenario, in the case of both experiments (a) and (b), which reveals indisputable violations of local realism. Such schemes may find possible applications in device-independent quantum protocols.

> 'The two views of the nature of light are rather to be considered as different attempts at an interpretation of experimental evidence in which the limitation of the classical concepts is expressed in complementary ways'.
>
> 'Bohr [1]'.

1. Introduction

In one of classic textbooks on quantum optics [2], page 264, one can find the following statement at the end of the chapter devoted to Bells inequalities in Quantum Optics '[…] some of the most striking features of non-locality in quantum mechanics may be demonstrated using phase-sensitive measurements on the field produced by a single photon. These effects may not be explained classically using a particle, wave or hidden-variable theory involving local causality'. The authors meant the operational configuration of figure 1(a) presented in [3]. A statement of this kind can also be found in the monograph [4], page 606. We falsify the claim of [3], by providing an explicit local causal hidden variable model, which covers all details of the quantum predictions for the configuration. We also show arguments suggesting that another emblematic experiment [5] involving 'phase-sensitive measurements', that is homodyne measurements, figure 1(b), is not a proper Bell experiment. We show that in both cases unquestionable violations of local realism can be observed if proverbial Alice and Bob use as their alternative local settings *complementary*

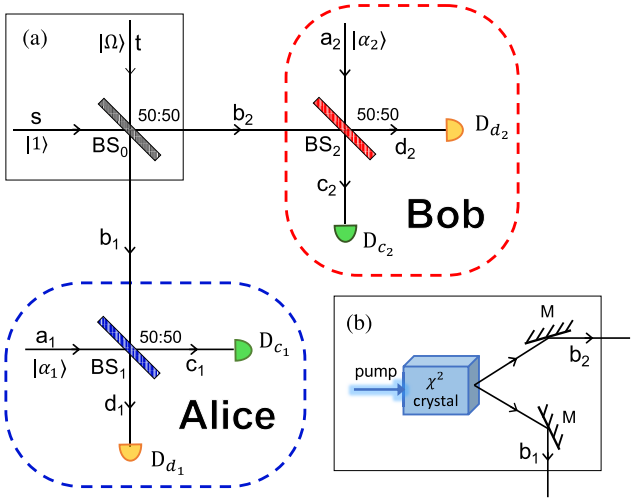

Figure 1. (a) Experimental configuration proposed by TWC, [3]. A single-photon impinges on a 50–50 beamsplitter via input *s*. We have vacuum in the input *t*. The resulting state $|\psi\rangle_{b_1,b_2}$, propagates to the laboratories of Alice and Bob, performing homodyne measurements involving weak coherent local oscillator fields (their amplitudes satisfy $|\alpha_1| = |\alpha_2|$). Following [10], detectors *D* are photon-number resolving. (b) GPY configuration: modes b_1 and b_2 are fed with radiation in two-mode squeezed state [5], and the rest of the configuration is as in (a). We show that scheme (a) of TWC in its ideal form has an explicit local realistic model, and that claims of violation of local realism by GPY scheme (b) are as yet unsubstantiated. The 'on/off' measurement scheme, which reveals violations of Bell inequalities requires operational modifications. In the 'on' case we replace the 50–50 beamsplitters with ones which optimally have transmittivity of around 80%. The 'off' setting is realized by removing the beamsplitter and blocking the input port of local detector D_{c_i}, e.g. closing a shutter.

measurement settings, which directly reflect the *wave–particle duality*: one is of the homodyne type, the other is a direct photon number measurement with the local oscillator off.

Complementarity is according to Bohr the basic feature of quantum mechanics [1]. It is behind wave–particle duality and is quantified by uncertainty relations. We know that it is also behind violations of Bell inequalities. Within the quantum theory of light Dirac [6] suggested phase vs photon-number uncertainty inequality (later formulated rigorously by [7, 8]). Recent trailblazing experiments [9–11], involving weak-field homodyne detection with photon-number resolution [12],

allow observations of new optical phenomena which exhibit both particle and wave nature of light. Thus they seem to be the perfect tool for observing the complementarity of Bohr concerning these two aspects of quantum light. A question emerges: what is the efficient operational utilization of this example of complementarity in Bell-type experiments, so that we can have unquestionable violations of local realism?

Note that homodyne measurements performed on optical beams (modes) in specific states (which we would call signal states) by their very nature blur the particle aspect of these states, as local oscillators are in coherent states, and therefore have inherently undefined number of photons. In other words, homodyning precludes photon number measurement on the signal beams, even if the final detection is photon-number-resolving. Thus, if all measurements in a Bell test are of homodyne type, they do not exploit directly photon-number wave (phase) complementarity, although they can involve mutually incompatible operational situations. That is, different phase settings defining different local measurements in Bell test.

The new technique [9–11] allows to realize emblematic gedankenexperiments, involving weak local oscillators homodyne detection, with local settings defined by the local phases, which were purported as possible Bell tests [3, 5]. We show that straight-ahead use of the photon-number vs phase complementarity, which operationally means measurement setting defined by having the local oscillator on (phase dependent measurement) or off (pure photon number measurement) leads to proper Bell tests. The other trait is that the homodyning cannot be balanced. Settings defined by phases only, and with constant oscillator strengths, lead in the case of experiment [3] to a situation, which has an explicit local realistic model. In the case of experiment [5] there exists a partial model, and there is no evidence for violations of Bell inequalities.

This suggests that such 'on/off' modifications of the discussed arrangements could be used for device-independent implementations of quantum information protocols, e.g., key distribution, or random number generation. On the contrary, the standard option to define settings by local phases and keeping local oscillator strength fixed seems out of question for device independent applications. We point out that in the device-independent version the 'on/off' arrangement should be implemented locally. We assume that an oscillator has always a constant strength α_j^2 for both observers $j = 1, 2$. Then the 'off' setting is

implemented by removing a beamsplitter BS_j and closing a shutter just before the detector D_{c_j} (see figure 1). In this way the local setting is neither revealed nor governed from the outside of the measurement station.

2. Emblematic gedankenexperiments turned real

The authors of [10] report photon-number resolving weak-field homodyne measurements in the case of the two emblematic entangled states of two spatial optical modes, namely:

(a) excitation of the modes by a single photon, first discussed in [3] by Tan, Walls and Collett (TWC),
(b) the modes in a squeezed vacuum state, first suggested in [5] by Grangier, Potasek and Yurke (GPY).

The operational schemes of the experiments are shown in figure 1. In [10] the detectors were able to distinguish photon numbers with a significant probability. State of the art techniques allow now this to up to 20 photons with approx. 90% efficiency [11].

The essential for our discussion trait of experiments (a) and (b), and their realization in [10] is that they use at the measurement stage constant local oscillator strengths and 50–50 beamsplitters.

2.1. TWC experiment (a)

TWC [3] considered the state obtained by casting a single photon on a 50–50 beamsplitter,

$$|\psi\rangle_{b_1,b_2} = \frac{1}{\sqrt{2}}\left(|01\rangle_{b_1,b_2} + \mathrm{i}|10\rangle_{b_1,b_2}\right) = \frac{1}{\sqrt{2}}(\mathrm{i}b_1^\dagger + b_2^\dagger)|00\rangle_{b_1,b_2}, \tag{1}$$

where e.g., $|10\rangle_{b_1,b_2}$, indicates one photon in exit mode b_1 and vacuum in exit mode b_2, see figure 1, and $b_i^\dagger$ are photon creation operators related with the beams i. As the experiment does not involve the polarisation degree of freedom, we assume that all photons are of the same polarisation, and thus this element is removed from the formal description. TWC suggested Bell non-classicality of $|\psi\rangle_{b_1,b_2}$ can be revealed in weak-field balanced homodyne measurements involving fixed strengths of the local oscillators.

The first form of $|\psi\rangle_{b_1,b_2}$ in (1) appears to be similar to a two-qubit Bell state. However, from the point of view of quantum optics, the fundamental theory of light, $|\psi\rangle_{b_1,b_2}$ is intrinsically different. The two states differ in the number of particles: Bell singlet is a state of two particles, while the superposition in $|\psi\rangle_{b_1,b_2}$, the second form of relation (1) is an eigenstate of the total photon number operator associated with eigenvalue 1. Bell singlet describes entanglement of two 'particles' (qubits, described using 'first quantization'), while $|\psi\rangle_{b_1,b_2}$ describes an entanglement of two spatially separated modes of the optical field, for a discussion see [13]. If one introduces a phase shift of $\frac{\pi}{2}$ in beam 1 the state transforms into

$$|\psi_S\rangle_{b_1,b_2} = \frac{1}{\sqrt{2}}\left(|01\rangle_{b_1,b_2} - |10\rangle_{b_1,b_2}\right) = \frac{1}{\sqrt{2}}(b_2^\dagger - b_1^\dagger)|00\rangle_{b_1,b_2}, \tag{2}$$

which seems to be an analog of a two-qubit singlet. However for example, a quantum optical polarization singlet in its simplest form reads

$$|\psi_{\mathrm{singlet}}\rangle_{b_1,b_2} = \frac{1}{\sqrt{2}}\left(b_{1H}^\dagger b_{2V}^\dagger - b_{1V}^\dagger b_{2H}^\dagger\right)|00\rangle_{b_1,b_2}, \tag{3}$$

where $b_{iX}^\dagger$ is a photon creation operator with $i = 1, 2$ standing for directional (spatial) modes, and $X = H, V$ for two orthogonal polarization modes. The main feature of the singlet is its rotational invariance with respect to a pair of identical local $SU(2)$ transformations of the pairs of operators $b_{iH}^\dagger$ and $b_{iV}^\dagger$. This is related to the fact that in quantum electrodynamics a singlet is a state which gives total spin angular momentum equal to zero (for electrons and also for photons, if one equates helicity with spin). This is not the case of $|\psi\rangle_{b_1,b_2}$, since there is no natural interferometric implementation of the single-mode $SU(2)$ transformation. Such an operation would demand change of the local photon number and cannot be implemented using passive linear optical devices. This can be seen most easily by noticing that a formal $SU(2)$ acting on a pair of states $|1\rangle_{b_1}$ and $|0\rangle_{b_1}$ would transform them respectively into $U_{11}|1\rangle_{b_1} + U_{21}|0\rangle_{b_1} = (U_{11}b_1^\dagger + U_{21})|0\rangle_{b_1}$ and $(U_{12}b_1^\dagger + U_{22})|0\rangle_{b_1}$. These states have different average photon number than the original ones. Therefore they are impossible with all-optical means involving passive operations only.

2.2. Experimental scheme

The state $|\psi\rangle_{b_1,b_2}$ reaches Alice (controlling the mode b_1) and Bob (b_2), see figure 1(a). They both perform local weak-field homodyne measurements. Modes b_j, where $j = 1, 2$, and the auxiliary coherent fields in state $|\alpha_j\rangle_{a_j} = |\alpha\, \mathrm{e}^{\mathrm{i}\theta_j}\rangle_{a_j}$ are fed into input ports of 50–50 beamsplitters BS_j, and end up in detectors D_{c_j} and D_{d_j}. The phases θ_j fully determine the local measurement settings, α is not varied.

3. Results

3.1. Explicit LHV model of TWC correlations

In our analysis we assume that all optical elements and detectors are perfect. We point out that any imperfections of optics that affect the interference visibility of the correlations, can be easily dealt by introducing modifications of the hidden variable model which reproduces ideal correlations. Also any inefficiency of the collection-detection in the scheme, which is assumed to be a random local process, does not change the model building scheme which we propose below. This is because the model is elastic with respect to visibilities of the various processes, and non-detection events play a crucial role in it. They occur also in the ideal case of the TWC experiment.

Quantum predictions for the TWC setup are fully characterized by the probabilities $p(\mathbf{n})$ of events consisting of registering a specific numbers of photons in the output modes: $\mathbf{n} = (k_{c_1}, l_{d_1}, r_{c_2}, s_{d_2}) \in \mathbb{N}^4$ (for readability, we omit the indices indicating the modes in further parts of this Letter). They read (see appendix A for the derivation):

$$p(\mathbf{n}) = A(\alpha, \mathbf{n}) \left[(k-l)^2 + (r-s)^2 + 2(k-l)(r-s)\sin(\theta_{12})\right], \tag{4}$$

where

$$A(\alpha, \mathbf{n}) = \frac{\mathrm{e}^{-2\alpha^2}\left(\frac{\alpha^2}{2}\right)^{k+l+r+s}}{2\alpha^2 k!\ l!\ r!\ s!}$$

and $\theta_{12} = \theta_1 - \theta_2$.

Note that, whenever both detectors of Alice *or* Bob register the same number of photons, the probability does not depend on θ_{12}. Let us denote the set of these events as $\mathcal{N} := \{\mathbf{n} : k = l \text{ or } r = s\}$. We cover them by a family of trivial LHV submodels assigning fixed outcomes to Alice and Bob, see further.

The probabilities that do depend on θ_{12} are of the form $p(\mathbf{n}|\theta_{12}) = B(\alpha, \mathbf{n})(1 + \mathcal{V}_{\mathbf{n}}\ \sin(\theta_{12}))$, where $B(\alpha, \mathbf{n}) = A(\alpha, \mathbf{n})\left[(k-l)^2 + (r-s)^2\right]$ and $\mathcal{V}_{\mathbf{n}} = \frac{2(k-l)(r-s)}{(k-l)^2+(r-s)^2}$. To reproduce them, we adapt a model by Larsson [14, 15], which emulates quantum predictions for the two-qubit singlet state, for detection efficiency lower than $2/\pi$.

Our model $\mathcal{M}$ is a convex combination of submodels $\mathcal{M}_{\mathbf{n}}$, each chosen with probability $P(\mathcal{M}_{\mathbf{n}})$. The submodels belong to two infinite families: the trivial $\{\mathcal{M}_{\mathbf{n}}\}_{\mathbf{n}\in\mathcal{N}}$ and Larsson-like one $\{\mathcal{M}_{\mathbf{n}}\}_{\mathbf{n}\in\tilde{\mathcal{N}}}$, where $\tilde{\mathcal{N}} := \{\mathbf{n} : k > l \text{ and } r > s\}$. We focus on the latter first.

We group the probabilities that depend on the local settings θ_j with ones corresponding to events of class $\mathcal{O}$ in the case of which (perfect) detectors of either Alice or Bob do not register any photons. Formally we have $\mathcal{O} := \{\mathbf{n} \in \mathcal{N} : \text{either } k = l = 0, \text{ or } r = s = 0\}$.

Each Larsson-like submodel $\{\mathcal{M}_{(k,l,r,s)}\}$ is going to predict eight events resulting from applying (or not) the swaps $k \leftrightarrow l$ and $r \leftrightarrow s$ to events $(0, 0, r, s)$, $(k, l, 0, 0)$ and (k, l, r, s). Notice that only one of the above matches the *index* $(k, l, r, s) \in \tilde{\mathcal{N}}$ of the model. To construct it, we take a uniformly distributed continuous hidden variable $\lambda \in [0, 2\pi]$ and a coin toss one $x \in \{0, 1\}$.

Specifically, for $x = 0$ Alice can register the event $(c, d) \in \{(k, l), (l, k)\}$ with probability

$$P^{\mathrm{A}}_{\mathbf{n}}(c, d|\theta_1, \lambda, 0) = R_{\mathbf{n}}(c, d|\theta_1, \lambda) = \frac{1}{\pi}(1 - \mathcal{V}_{\mathbf{n}}) + \mathcal{V}_{\mathbf{n}}|\sin(\theta_1 - \lambda)|H\left((c - d)\sin(\theta_1 - \lambda)\right), \tag{5}$$

where H is the Heaviside function, and for $(0, 0)$ event we put

$$P^{\mathrm{A}}_{\mathbf{n}}(c = 0, d = 0|\theta_1, \lambda, 0) = R_{\mathbf{n}}(0, 0|\theta_1, \lambda) = 1 - \sum_{(e,f)\in\{(k,l),(l,k)\}} R_{\mathbf{n}}(e, f|\theta_1, \lambda). \tag{6}$$

Note that the sets of possible outcomes depend on the submodel $\mathcal{M}_{\mathbf{n}}$. However, within each submodel the definitions of local probabilities of one party do not depend on the outcomes of the other, as the visibility $\mathcal{V}_{\mathbf{n}}$ is fixed for a given index $\mathbf{n}$. Bob detects $(c', d') \in \{(r, s), (s, r)\}$ with probabilities

$$P^{\mathrm{B}}_{\mathbf{n}}(c', d'|\theta_2, \lambda, 0) = Q_{\mathbf{n}}(c', d'|\theta_2, \lambda) = H\left((c' - d')\cos(\theta_2 - \lambda)\right). \tag{7}$$

For $x = 1$ we put $P^{\mathrm{A}}_{\mathbf{n}}(c, d|\theta_1, \lambda, 1) = Q_{\mathbf{n}}(c, d|\theta_1, \lambda)$, and $P^{\mathrm{B}}_{\mathbf{n}}(c', d'|\theta_2, \lambda, 1) = R_{\mathbf{n}}(c', d'|\theta_2, \lambda)$. This symmetrizes the model.

The joint probabilities for each submodel are given by:

$$P^{\mathrm{AB}}_{\mathbf{n}}(c, d, c', d'|\theta_1, \theta_2) = \frac{1}{4\pi}\sum_{x=0}^{1}\int_0^{2\pi} \mathrm{d}\lambda\, P^{\mathrm{A}}_{\mathbf{n}}(c, d|\theta_1, \lambda, x)P^{\mathrm{B}}_{\mathbf{n}}(c', d'|\theta_2, \lambda, x). \tag{8}$$

To get the probability that the submodel $\mathcal{M}_{\mathbf{n}}$ predicts event $\mathbf{n} = (k, l, r, s)$, in the simplest case of $\pi/2 > \theta_1 > \theta_2 > 0$, $k > l$ and $r > s$, is elementary. It reads: $\frac{1}{2\pi}(1 + \mathcal{V}_{\mathbf{n}} \sin\theta_{12})$. Generally, for events (k, l, r, s), (l, k, r, s), (k, l, s, r) and (l, k, s, r) we get:

$$P^{\mathrm{AB}}_{\mathbf{n}}(c, d, c', d'|\theta_1, \theta_2) = \frac{1 + \mathcal{V}_{\mathbf{n}} \operatorname{sgn}\left((c-d)(c'-d')\right) \sin(\theta_{12})}{2\pi}. \tag{9}$$

In the case of the $\mathcal{O}$-events $(0, 0, r, s)$, $(0, 0, s, r)$, $(k, l, 0, 0)$ and $(l, k, 0, 0)$, the probability is flat and reads $\frac{1}{4} - \frac{1}{2\pi}$, which follows directly from the normalisation condition in (6). Comparing (9) with the corresponding quantum probabilities $p(\mathbf{n}|\theta_{12})$, we see that each Larsson-like submodel $\mathcal{M}_{\mathbf{n}}$ must appear in the full model $\mathcal{M}$ with probability $P(\mathcal{M}_{\mathbf{n}}) = 2\pi B(\alpha, \mathbf{n})$.

The overall model reproduces all probabilities which reveal interference. However a *condicio sine qua non* for consistency of the full model is to properly describe also events $\mathcal{O}$. The construction, due to the Larsson-like submodels, ascribes probability $(\frac{\pi}{2} - 1)B(\alpha, (k, l, c', d'))$ to the event $(k, l, 0, 0)$ and $(l, k, 0, 0)$. This is so, because for each of the submodels $\mathcal{M}_{(k,l,c',d')}$, a fraction $\frac{1}{4} - \frac{1}{2\pi}$ of it covers these events from $\mathcal{O}$, and the sub-model as a whole appears with probability $2\pi B(\alpha, \mathbf{n})$.

The sum of all such contributions cannot be greater than the quantum probability $p(k, l, 0, 0)$. It can be lower since the difference can be described by trivial models. This gives the following consistency conditions:

$$\Delta_{(k,l,0,0)} = p(k, l, 0, 0) - \left(\frac{\pi}{2} - 1\right) \sum_{c'>d'} B(\alpha, (k, l, c', d')) \geqslant 0, \tag{10}$$

which must hold for any $k \neq l$. Due to the symmetrization an analogous constraint holds for events of $(0, 0, r, s)$.

In appendix A.3 we show that the condition in equation (10) is satisfied for *any* (k, l) and (r, s), whenever $\alpha^2 < 0.87$. The model can be completed using a family of trivial submodels $\mathcal{M}_{\mathbf{n}}$ for events $\mathbf{n} \in \mathcal{N}$. They predict fixed outcomes for Alice and Bob, $P^{\mathrm{A}}_{\mathbf{n}}(k, l) = P^{\mathrm{B}}_{\mathbf{n}}(r, s) = 1$, which lead to $P^{\mathrm{AB}}_{\mathbf{n}}(k, l, r, s) = 1$. For events $\mathbf{n} \in \mathcal{N}\backslash\mathcal{O}$, we choose each corresponding trivial model $\mathcal{M}_{\mathbf{n}}$ with probability $p(\mathbf{n})$. Finally, for events $\mathbf{n} \in \mathcal{O}$ we might need to compensate the potential difference $\Delta_{(k,l,0,0)} > 0$ between the quantum predictions for the $\mathcal{O}$-events and the predictions specified by the Larsson-like models. To this end, we use an additional trivial submodel for event $(k, l, 0, 0)$, which appears in the full model with probability $P(\mathcal{M}_{(k,l,0,0)}) = \Delta_{(k,l,0,0)}$. The case of $\Delta_{(0,0,r,s)} > 0$ is treated the same way.

One can build a version of the model holding for slightly higher values of α. We were not able to find a model which has an unconstrained validity, and we conjecture that the Larsson-like approach cannot lead to such. Still, our model fully covers the range of α for which TWC predicted a violation of local realism: $\alpha^2 < \sqrt{2} - 1$ [3]. Thus, this claim is fully revoked, and this is done for, finer than in TWC proposal, photon-number resolving measurements. The model works for the intensities of the local oscillators used in [10], figure 3 there, corresponding to $\alpha \approx 0.55$.

3.2. GPY experiment (b)

The setup proposed in [5], and realised in [10] in a weak-field homodyne photon-number resolving version, is presented in figure 1(b). The source is a parametric down conversion process, in which a non-linear crystal transforms part of the pumping light into pairs of photons, fed into two output modes, b_1, b_2. The photons are sent to two measurement stations which perform weak-field homodyne measurements. The state is a two mode squeezed vacuum, $|\sigma_v\rangle_{b_1 b_2} = \sqrt{1-\gamma^2}\sum_{k=0}^{+\infty} \gamma^k |k, k\rangle_{b_1, b_2}$, where γ is for simplicity assumed to be real. As before, Alice and Bob mix $|\sigma_v\rangle_{b_1 b_2}$ with two weak coherent states in modes a_1 and a_2, namely $|\alpha_j\rangle_{a_j} = |\alpha\, \mathrm{e}^{\mathrm{i}\theta_j}\rangle_{a_j}$ using local beamsplitters.

3.3. Is this a Bell experiment?

We show an explicit model for a subset of correlations appearing in the GPY setup with photon-number resolution, which is inspired by the model for the TWC correlations. It covers events with maximally one photon detected on one side, and maximally three on the other one. They depend only on θ_{12}. We call them *class 1* events. We were not able to find an explicit Larsson-model for the *class 2* events with two photons detected on both sides, as they depend also on $2\theta_{12}$. We show that there is no evidence that such a model does not exist, showing that CGLMP inequalities [16] cannot be violated by this subset of events. For all events with altogether up to four detected photons there is no evidence for violation of local realism. As these events definitely are most frequent, this constitutes a strong argumentation toward showing that the GPY configuration (with constant local oscillator strengths) does not constitute a proper Bell test. Our additional partial analysis, not to be presented here, seems to indicate that violation of local realism cannot be shown also for other events not restricted to altogether up to four photons.

Class 1 events follow a pattern: one party registers a local event (k, l), $k \neq l$, while the other detects a single photon. Their probabilities are of the form

$$p(\mathbf{n}) = A(\mathbf{n})\left(\alpha^4 + c_1(\mathbf{n})\gamma^2 \pm c_2(\mathbf{n})\alpha^2\gamma\,\cos\,\theta_{12}\right), \tag{11}$$

see the appendix B.1 for the exact form of the coefficients. Larrson-like models exist in this case. In each of them, one party predicts local events $(0, 0)$, (k, l), and (l, k). The last two, denoted '+' and '−' according to the sign of $k - l$, occur with probability

$$R(c_1(\mathbf{n}), c_2(\mathbf{n}), \pm) = \frac{1 - c_2\alpha^2\gamma}{\pi(\alpha^4 + c_1\gamma^2)} + \frac{c_2\alpha^2\gamma}{(\alpha^4 + c_1\gamma^2)}|\cos(\theta_i - \lambda)|H\left(\pm\cos(\theta_i - \lambda)\right), \tag{12}$$

where θ_i is θ_1 for Alice and θ_2 for Bob. The remaining probability $1 - R(c_1(\mathbf{n}), c_2(\mathbf{n}), +) - R(c_1(\mathbf{n}), c_2(\mathbf{n}), -)$ is assigned to the event $(0, 0)$. The other party predicts $(1, 0)$ and $(0, 1)$ with probability $H\left(\pm\cos(\theta_i + \lambda)\right)$.

Submodels are chosen with probability $2\pi A(\mathbf{n})\,(\alpha^4 + c_1(\mathbf{n})\gamma^2)$. The events whose probabilities do not depend on local settings are covered by trivial models, with the exception of single-photon events. This is because the submodels corresponding to *class 1* events contribute to their probabilities. Just as in the TWC case, we need to check if the sum of these contributions does not exceed the quantum probabilities. This provides a condition for the validity of the model. In the case of $\gamma \leqslant \alpha^2$ it restricts the model to $\alpha^2 < 0.58$, but this does not characterize its full range, which is broader as shown in appendix B.

Class 2 events with two photons registered on both sides, which we shall denote as $(2\,\&\,2)$, come from the following term of the expansion of the overall state (PDC modes plus local oscillators),

$$|\xi_{2\,\&\,2}\rangle = Z\left(\frac{\alpha_1^2\alpha_2^2}{4}a_1^{\dagger 2}a_2^{\dagger 2} + \gamma\alpha_1\alpha_2 a_1^\dagger a_2^\dagger b_1^\dagger b_2^\dagger + \frac{\gamma^2}{2}b_1^{\dagger 2}b_2^{\dagger 2}\right)|\Omega\rangle, \tag{13}$$

where Z is the overall normalization constant of the entire state. The overall probabilistic weight of this term is thus $p(2\,\&\,2) = \frac{Z^2}{4}(\alpha^8 + 4\gamma^4 + 4\gamma^2\alpha^4)$. The events in the case of which two photons are registered on one side and on the other side no photons, denoted by $(2\,\&\,0)$, come from the component $|\xi_{2\,\&\,0}\rangle = \frac{Z}{2}\left(\alpha_1^2 a_1^{\dagger 2} + \alpha_2^2 a_2^{\dagger 2}\right)|\Omega\rangle$. Its overall probabilistic weight is $p(2\,\&\,0) = Z^2\alpha^4$.

$|\xi_{2\,\&\,2}\rangle$, after normalization, is a proper $3 \otimes 3$ dimensional state, and thus predictions for it can be put into a CGLMP inequality for $d \geqslant 3$ (see appendix C for an explicit form of the inequality). We choose $d = 4$ because we want to analyze it together with $|\xi_{2\,\&\,0}\rangle$, as such would have been the case had we managed to construct a Larsson like submodel for this specific set of events. We ascribe the following numeric values to the results: for Alice and Bob counts 00, 02, 20, 11, are assigned values $a, b = 0, 1, 2, 3$. The optimal way of ascribing these values is given below.

The overall probability of events $(2\,\&\,2)$ and $(0\,\&\,2)$ is a convex combination of the two cases: $p(a, b|class\ 2) = \lambda p(a, b|2\,\&\,2) + (1 - \lambda)p(a, b|0\,\&\,2)$, with $\lambda = \frac{p(2\,\&\,2)}{p(2\,\&\,2)+p(0\,\&\,2)}$. The CGLMP expression is linear, thus its value, $W[p(\cdot|class\ 2)]$, reads $\lambda W[p(\cdot|2\,\&\,2)] + (1 - \lambda)W[p(\cdot|0\,\&\,2)]$. The maximal possible *algebraic* value of the CGLMP expression is 4. Thus $W[p(\cdot|2\,\&\,2)] \leqslant 4$. As probabilities $p(a, b|0\,\&\,2)$ are independent of settings, for them settings become irrelevant in the inequality. By looking at the CGLMP inequality, (see equation (C1)) of appendix C) we notice that the value for $W[p(\cdot|0\,\&\,2)]$ is $2\left[p(a = b|0\,\&\,2) - \frac{1}{3}p(a \neq b|0\,\&\,2)\right] = \frac{8}{3}p(a = b|0\,\&\,2) - \frac{2}{3}$. We must seek a function relating photon counts 00, 02, 20, 11 with values a, b, such that the value of $W[p(\cdot|0\,\&\,2)]$ is highest. This is so when e.g., 00 result on Alice's side is ascribed 0 and 11 on Bob's side is also 0, and 11 on Alice's is given 1 and 00 on Bob's also 1, see formulas of Methods section. Because then $p(a = b|0\,\&\,2) = \frac{1}{2}$, and $W[p(\cdot|0\,\&\,2)] = \frac{2}{3}$. Thus the value of the CGLMP expression cannot be higher than $W[p(\cdot|S)] = 4\lambda + \frac{2}{3}(1 - \lambda) = \frac{10}{3}\lambda + \frac{2}{3}$. As the local realistic bound is $W[p(\cdot|S)] \leqslant 2$, *a* threshold necessary condition for having a local realistic description for *class 2* is $2 = \frac{10}{3}\lambda + \frac{2}{3}$,, i.e. we must have $\lambda \leqslant \frac{2}{5}$. Thus if $\alpha^2 = \gamma$, we must have approximately $\alpha^2 < 0.54$. Since $\lambda(\gamma^2)$ increases together with γ^2, this holds also for all $\gamma < \alpha^2 < 0.54$. This range is consistent with the range of the Larsson like models. Still, one definitely must have $W[p(\cdot|2\,\&\,2)]$ much below 4, since the Tsirelson bound for $d = 4$ CGLMP inequality is much less than 4. In [17] it is estimated to be around 3.1. This gives $\lambda \leqslant \frac{4}{7.3}$, and $\alpha^2 \leqslant 0.73$.

Thus, there is *no evidence* in terms of a violation of CGLMP Bell inequality that *there is no local realistic model* for experiments of the type [10], and their precursors like [18], for the situation in which up to altogether four photon counted. We conjecture that this can be extended to more photon events. We have chosen the CGLMP inequality as it appears in [10] in an argument on Bell nonclassicality of the correlations. Of course, our claim is not that the model exists, but that there is currently no evidence that it does not exist, while a partial explicit model does exist. Thus, for GPY experiment with weak photon-number resolving homodyne measurements of constant strengths of local oscillators seems not to

lead to indisputable violations of local realism, even in the idealized case. Below we show how to modify the operational situation to get the violations, in the case of both TWC and GPY schemes.

4. On/off unbalanced homodyne measurements as a solution

The ramifications of the results of the previous section are as follows. TWC experiment involving balanced homodyne measurements with fixed local oscillator strengths does not lead to violations of local realism. Showing that an LHV model exists for a specific interference experiment is a no-go theorem for all the possible experimental realizations of device independent secure quantum communication protocols based on such an experiment. Such protocols, to be certified, require that every possible classical-like description is ruled out. Moreover, as the TWC experiment inspired many research articles, e.g. [19–24], and is even used as a paradigmatic textbook example of violation of local realism [2, 4, 25], this situation had to be clarified.

Similar ramifications follow from our analysis of the GPY experiment, however we cannot claim that a consistent LHV model for all detection events exists. Nevertheless, we show that previous claims concerning violations of local realism with balanced homodyne measurements with fixed oscillator strength are not substantiated, and additionally the dominant detection events do have a local realistic model. Thus currently there is no reason to think that the GPY correlations could be useful in device independent secure communication schemes.

The following question emerges: if we allow the local oscillator strengths to vary between the settings, does this lead to an unquestionable Bell test? In the case of the single photon experiment, one may think that the paper of Hardy [19] gives a positive answer. However, the reasoning presented in [19] works only in the case of a superposition of a single photon state and the vacuum in the input mode of the state preparing beamsplitter BS_0, see figure 1, namely $c|0\rangle_s + \sqrt{1-|c|^2}|1\rangle_s$. And most importantly one can show that if the amplitude of vacuum satisfies $|c| < 0.28$ then violation of the Hardy's condition for local realism is prohibitively small, from the experimental perspective. Thus Hardy's reasoning absolutely does not apply in the case of the single photon input, $c = 0$.

Below, we shall show that in the case of the experiment (a), if one goes effectively to the extreme in variation of the local oscillator strength (as in [19]) and additionally necessarily uses unbalanced beamsplitters at the measurement stations, see the caption of figure 1, then one can observe a violation of local realism. Interestingly, at each local station we exploit here a form of the wave–particle duality. In the 'off' situation, we just collect the photon at a detector—the particle aspect, and in the 'on' situation we detect photons which interfered at the beamsplitter, and the indistinguishability of photons from the local oscillators and the signal photon is the reason of the interference—the wave aspect involving the bosonic nature of photons. Interestingly this method also works in the case of the GPY configuration.

We will utilise the simplest Bell inequality based on probabilities of specific events, namely the *CH* inequality [26]:

$$-1 \leqslant P(A,B) + P(A,B') + P(A',B) - P(A',B') - P(A) - P(B) = CH \leqslant 0. \tag{14}$$

As the events in (14) we shall take specific photon counts at the local detectors, and we will use the on/off scheme for the settings. The unprimed settings correspond to the *off* case (local oscillator is turned off) and the primed ones to the *on* case (local oscillator is present). By event A' we denote a single photon detected in mode d_1 and no-photon in mode c_1 in the case we have a beamsplitter with an optimized transmittivity T and the local oscillator field on ('on' setting), and by A we denote a single photon count at d_1 and no count at c_1 when the local oscillator is off, or detector c_1 is blocked ('off' setting), and the beamsplitter is removed. Events B and B' play the same role for Bob. In our following calculations we have assumed that the intensity of the local oscillator and the transmittivity of the tunable local beamsplitters are in the case of the 'on' setting the same for both Alice and Bob. An overall optimization certifies that it is fulfilled by the optimal settings.

The reason behind choosing such a photonic detection event is that for experiment (a) we have numerically checked that there are no other events which show violation. However, for experiment (b), there are other events, which show a violation, but the values of the violation are minuscule. For example if one consider the event of detecting no photon in mode c_j and two photons in mode d_j for both $j = 1, 2$, then the $CH_{\max}$ decreases one more order of magnitude, see appendix E for further clarification. Thus for the operational situations of figure 1, and the on–off approach, events with just one photon detected only in path d_i are optimal.

4.1. Experiment (a)

For the single photon input state impinging on a balanced beamsplitter, the joint probability $P(A', B')$, when both the local oscillators are 'on', is given by

$$P(A', B') = |_{c_1,d_1,c_2,d_2}\langle 0, 1, 0, 1|\Psi\rangle|^2 = \alpha^2\, \mathrm{e}^{-2\alpha^2} T(1-T)(1+\sin(\theta_1-\theta_2)), \tag{15}$$

where $|\Psi\rangle = |\alpha\, \mathrm{e}^{\mathrm{i}\theta_1}\rangle_{a_1}|\psi\rangle_{b_1,b_2}|\alpha\, \mathrm{e}^{\mathrm{i}\theta_2}\rangle_{a_2}$. The probabilities with 'on' stetting on one side are $P(A', B) = P(A, B') = \frac{1}{2}\alpha^2\, \mathrm{e}^{-\alpha^2}(1-T)$. One can easily check that when the beamsplitter is absent and the local oscillator is turned off, then detecting single photon in mode d_j, (effectively equivalent with mode b_j) and no photon in mode c_j (equivalent to mode a_j), for both $j = 1, 2$ is the only event which has a non-zero probability. The case of off settings on both sides gives $P(A, B) = 0$, and $P(A) = P(B) = \frac{1}{2}$, see appendix D for the derivation. With all that the Clauser–Horne expression CH in (14) reduces to

$$CH = \mathrm{e}^{-2\alpha^2}\alpha^2(1-T)\left(\mathrm{e}^{\alpha^2} - T\,(1+\sin\,(\theta_1-\theta_2))\right) - 1. \tag{16}$$

We have $CH < -1$ provided $\mathrm{e}^{\alpha^2}/(1+\sin\,(\theta_1-\theta_2)) < T < 1$, and the range and the violation is maximal for $\theta_1 - \theta_2 = \frac{\pi}{2}$. An optimization results in $CH_{\min} \approx -1.010$, for $\alpha^2 \approx 0.196$, $T \approx 0.804$, and $\theta_1 - \theta_2 = \frac{\pi}{2}$. The violation is quite robust as the probabilities for the non-trivial case read only $P(A', B) = 0.0157$, $P(A', B') = 0.0417$.

4.2. Experiment (b)

For two mode squeezed vacuum state, when both the observers choose 'on' settings, we have $P(A', B') = \mathrm{e}^{-2\alpha^2}(1-\gamma^2)(T\gamma - \alpha^2(1-T))^2$, whereas for the on situation on one side and off one the other one has $P(A', B) = P(A, B') = \mathrm{e}^{-\alpha^2}\gamma^2(1-\gamma^2)T$. In this calculation we have assumed that $\theta_1 = -\theta_2$, as it is true for optimum violation of CH inequality. Finally $P(A, B) = P(A) = P(B) = \gamma^2(1-\gamma^2)$. The CH expression now reads as

$$CH = \mathrm{e}^{-\alpha^2}\left(1-\gamma^2\right)\left(\gamma^2\left(2T - \mathrm{e}^{\alpha^2}\right) - \mathrm{e}^{-\alpha^2}\left(\gamma T - \alpha^2(1-T)\right)^2\right). \tag{17}$$

The sufficient condition for $CH > 0$ reads as $T = \frac{\alpha^2}{\gamma+\alpha^2} > \frac{1}{2}\,\mathrm{e}^{\alpha^2}$. Optimization of the CH expression yields $CH_{\max} \approx 0.0027$ for $\alpha^2 \approx 0.200$, $\gamma \approx 0.175$ and $T \approx 0.799$. The violation is quite robust as $P(A, B) \approx 0.0299$, $P(A, B') \approx 0.0196$ and $P(A', B') \approx 0.0065$.

5. Discussion and outlook

The original TWC configuration and most probably the GPY scheme are not proper Bell experiments. We construct an explicit LHV model for the ideal predictions of experiment (a), and show that the hope for a violation of local realism in experiment (b), in [5, 10] is not substantiated (a partial LHV model exists, claims about violation of Bell inequalities are at least premature). On the positive note, we show that Bell-type experiments on the signal states $|\psi\rangle_{b_1b_2}$ and $|\sigma_v\rangle_{b_1b_2}$ with each observer switching the local oscillator on (setting 1) or off (setting 2), and involving (non 50–50) optimized beamsplitters, do violate a Bell inequality. Thus, such seems to be the proper operational scenario in this context.

The on/off scheme represents a version of complementarity between measuring wave vs particle aspects of the state of the modes. It seems that quantum optical Bell tests with weak homodyne measurements must involve local situations in which photon counting replaces weak-field homodyne measurements. This does work also when the local oscillator is almost off, see [27] for the TWC case. On/off situation leads to a violation of local realism in [19, 28], albeit in a slightly different situations: modification of the signal state in beam s in [19], and a displacement procedure in [28]. Our results suggest that this is not a peculiarity, but seems to be a rule for Bell tests involving homodyne photon number resolving measurements.

Our exact model closes the long standing dispute on whether the 1991 gedankenexperiment TWC [3] reveals 'nonlocality of a single photon'. Moreover, we show that thus far *there is no evidence* that the 1988 proposal of GPY [5] involving parametric down conversion (an emblematic source of entanglement) and weak-field homodyning (with constant local oscillator strengths, and 50–50 beamsplitters) constitutes a valid Bell-type experiment. We conjecture that this claim is unfounded.

5.1. Ramifications concerning the claims on 'non-locality of a single photon'

The TWC experiment was supposed to imply 'nonlocality of a single photon'. TWC use the run-of-the-mill of the time approach to photodetection: the probability of a detector to fire is proportional to the intensity of the impinging light, e.g. [29]. The joint probability of having a coincidence of firings for detectors D_{x_1}

and D_{y_2} is put as $P_f(x_1, y_2|\theta_1, \theta_2) \approx \langle I_{x_1}(\theta_1) I_{y_2}(\theta_2)\rangle$, where $I_{x_j}(\theta_j)$ is the intensity at output $x = c, d$, and the averaging is done, depending on the context, over local hidden variables (LHVs), or within quantum formalism. The probability of a single firing is: $P_f(x_j|\theta) \approx \left\langle I_{x_j}(\theta)\right\rangle$. They model the quantum intensity observable by the photon number operator.

To show a violation of local realism, TWC use Bell-like inequalities derived in [30], of the well known CHSH form [31]. The local settings were defined by the local phases θ_j and θ'_j. For (constant) amplitudes of the local oscillators satisfying $\alpha^2 < \sqrt{2} - 1 \approx 0.41$, they show a violation of the CHSH-like inequality, and conclude that the state $|\psi\rangle_{b_1,b_2}$ is 'nonlocal'. The inequality of [30], rests on an *additional* assumption: in LHV models the total intensity for each observer j does *not* depend on θ_j: $I_j(\lambda) = I_{c_j}(\theta_j, \lambda) + I_{d_j}(\theta_j, \lambda)$, where λ symbolizes the hidden variables. The condition is justified in classical optics, but constrains possible LHV models, see [32, 33].

In [32] Santos suggested that the correlations of firings $P_f(x_1, y_2|\theta_1, \theta_2)$ in the TWC scheme *could be* explainable with LHVs [32] and therefore cannot be used to convincingly demonstrate 'nonlocality' of a single photon. However, his LHV model reproduced only the correlations of firings, and not the full quantum predictions, failing completely to recover quantum predictions for $P(x_j|\theta) \approx \left\langle I_{x_j}(\theta)\right\rangle$. Thus, this was not an LHV model of the quantum predictions, but rather a hint that there is something wrong in the TWC analysis. Santos suggested that the additional assumption is violated rather than local realism. Santos did *not* model photon number resolving detection.

Other works challenge the single-photon nature of the effect [34, 35], or suggest *modifications* of the experiment which allow provable violations of local realism [19, 28, 36], while keeping the experiment all-optical. Thus far, no definite answer was given to the problem whether the TWC effect, which seemingly violates local realism, admits an exact local realistic model, or not. Papers describing the experimental realizations of variants of this scheme [18, 21, 22] claim violations of a Bell inequality. However, the claims are presented with caution, e.g., as in [22] where it is stated that the results are no better than for conventional Bell tests with the efficiency loophole.

Several proposals [20, 37, 38] show how the single-photon superposition can be used to generate an entangled state of a couple of two-level systems, e.g. two atoms in a cavity. The reduction to a state of a pair of entangled atoms straightforwardly leads to a violation of local realism, as discussed in [39–41]. Moreover, exploiting the single-photon superposition to induce entanglement between two different objects has also been proposed in the context of teleportation protocols, for instance [24]. Anyway all these efforts reduce to the well known case of the two-qubit entanglement. No conclusion can be drawn about the violation of local realism by optical fields containing only a single photon with all-optical setups involving only passive elements. Note that a recent proposal to reveal the violation of local realism with multiple copies of the single photon state has been put forward in [42].

We show an LHV model which reproduces precisely quantum predictions for the original TWC setup (a), even in the case of photon number resolving detection. This obviously covers the course-grained description in terms of the probabilities of firings of detectors whose response is proportional to the number of impinging photons. Its applicability is limited by the strength of the local oscillators, but covers the range reported in [3] as revealing the 'nonlocality of the single-photon'. The result closes the case and precludes any attempt to implement device-independent protocols using original TWC correlations.

This signals once more that a great care must be taken when claiming Bell non-classicality (for earlier controversies of this type involving other experiments see e.g. [15, 43–45]).

Finally, let us mention that the paper [23], which seemed to elucidate the question of violations of local realism in an extended version of the TWC experiment (with local settings defined by beamsplitters of tunable transmittivity-reflectivity), and thus seemingly was a non-controversial demonstration of 'non-locality' of the single photon state behind 50–50 beamsplitter (1), contains an erroneous claim, formula (20) therein, that the CHSH-Bell inequality is violated. Our detailed analysis of the experiment in reference [23] shows, that the purported CHSH inequality violation never occurs for the measurement setup proposed by the authors. This would be explicitly discussed in a forthcoming comment [46].

Acknowledgments

Work supported by Foundation for Polish Science (FNP), IRAP Project ICTQT, Contract No. 2018/MAB/5, co-financed by EU Smart Growth Operational Programme. MK is supported by FNP START scholarship. AM is supported by (Polish) National Science Center (NCN): MINIATURA DEC-2020/04/X/ST2/01794.

Data availability statement

No new data were created or analysed in this study.

Appendix A. Experiment (a): quantum photodetection probabilities

In this section, we calculate the probability of detecting the event $\mathbf{n} = (k_{c_1}, l_{d_1}, r_{c_2}, s_{d_2})$, of registering specific numbers of photons in the output modes, of the Tan–Walls–Collett setup (experiment (a) in the main text).

The initial state in the TWC scheme, obtained by transforming a single photon with a balanced beamsplitter and adding two coherent states of the local oscillators

$$|\Psi\rangle = \frac{1}{\sqrt{2}}\left|\alpha\, e^{i\theta_1}\right\rangle_{a_1}\left(|01\rangle + i\,|10\rangle\right)_{b_1 b_2}\left|\alpha\, e^{i\theta_2}\right\rangle_{a_2}. \tag{A1}$$

We show how the state (A1) transforms on the following 50–50 beamsplitters which link the output and input modes via

$$\hat{c}_j = \frac{1}{\sqrt{2}}(\hat{a}_j + i\hat{b}_j) \quad \text{and} \quad \hat{d}_j = \frac{1}{\sqrt{2}}(i\hat{a}_j + \hat{b}_j). \tag{A2}$$

Applying (A2) to the state (A1) we get

$$\begin{aligned}
|\Psi\rangle &= e^{-\alpha^2}\sum_{j=0}^{\infty}\frac{(\alpha\, e^{i\theta_1})^j}{j!}(\hat{a}_1^\dagger)^j\frac{1}{\sqrt{2}}(i\hat{b}_1^\dagger + \hat{b}_2^\dagger)\sum_{k=0}^{\infty}\frac{(\alpha\, e^{i\theta_2})^k}{k!}(\hat{a}_2^\dagger)^k \\
&= e^{-\alpha^2}\sum_{j,k=0}^{\infty}2^{-\frac{j+k}{2}}\frac{(\alpha\, e^{i\theta_1})^j}{j!}\frac{(\alpha\, e^{i\theta_2})^k}{k!}\left(\hat{c}_1^\dagger + i\hat{d}_1^\dagger\right)^j\frac{1}{2}\left(-\hat{c}_1^\dagger + i\hat{d}_1^\dagger + i\hat{c}_2^\dagger + \hat{d}_2^\dagger\right)\left(\hat{c}_2^\dagger + i\hat{d}_2^\dagger\right)^k|\Omega\rangle \\
&= e^{-\alpha^2}\sum_{j,k=0}^{\infty}2^{-\frac{j+k}{2}}\frac{(\alpha\, e^{i\theta_1})^j}{j!}\frac{(\alpha\, e^{i\theta_2})^k}{k!}\sum_{p=0}^{j}\binom{j}{p}(\hat{c}_1^\dagger)^{j-p}(i\hat{d}_1^\dagger)^p \\
&\quad\times\frac{1}{2}\left(-\hat{c}_1^\dagger + i\hat{d}_1^\dagger + i\hat{c}_2^\dagger + \hat{d}_2^\dagger\right)\sum_{q=0}^{k}\binom{k}{q}(\hat{c}_2^\dagger)^{k-q}(i\hat{d}_2^\dagger)^q|\Omega\rangle, \\
&= \sum_{j,k=0}^{\infty}\sum_{p=0}^{j}\sum_{q=0}^{k}f(j,p,k,q)(\hat{c}_1^\dagger)^{j-p}(\hat{d}_1^\dagger)^p\left(-\hat{c}_1^\dagger + i\hat{d}_1^\dagger + i\hat{c}_2^\dagger + \hat{d}_2^\dagger\right)(\hat{c}_2^\dagger)^{k-q}(\hat{d}_2^\dagger)^q|\Omega\rangle, \qquad \text{(A3)} \\
&= \sum_{j,k=0}^{\infty}\sum_{p}^{j}\sum_{q=0}^{k}f(j,p,k,q)\Big[-\sqrt{(j-p+1)!p!(k-q)!q!}|j-p+1\rangle_{c_1}|p\rangle_{d_1}|k-q\rangle_{c_2}|q\rangle_{d_2} \\
&\quad + i\sqrt{(j-p)!(p+1)!(k-q)!q!}|j-p\rangle_{c_1}|p+1\rangle_{d_1}|k-q\rangle_{c_2}|q\rangle_{d_2} \\
&\quad + i\sqrt{(j-p)!p!(k-q+1)!q!}|j-p\rangle_{c_1}|p\rangle_{d_1}|k-q+1\rangle_{c_2}|q\rangle_{d_2} \\
&\quad + \sqrt{(j-p)!p!(k-q)!(q+1)!}|j-p\rangle_{c_1}|p\rangle_{d_1}|k-q\rangle_{c_2}|q+1\rangle_{d_2}\Big], \qquad \text{(A4)}
\end{aligned}$$

where

$$f(j,p,k,q) = e^{-\alpha^2}2^{-\frac{j+k}{2}-1}\frac{(\alpha, e^{i\theta_1})^j}{j!}\frac{(\alpha\, e^{i\theta_2})^k}{k!}\binom{j}{p}\binom{k}{q}(i)^{p+q}, \quad \forall\ p \leqslant j,q \leqslant k. \tag{A5}$$

Finally, we obtain the expression for the probability that reads:

$$\begin{aligned}
p(k,l;r,s) \equiv p(\mathbf{n}) = |\langle k,l,r,s|\Psi\rangle|^2 &= \Big|-f(k+l-1,l,r+s,s) + if(k+l-1,l-1,r+s,s) \\
&\quad + if(k+l,l,r+s-1,s) + f(k+l,l,r+s-1,s-1)\Big|^2 k!\ l!\ r!\ s! \\
&= \frac{e^{-2\alpha^2}}{k!\ l!\ r!\ s!}\left(\frac{\alpha^2}{2}\right)^{k+l+r+s}\frac{1}{2\alpha^2}\left[(k-l)^2 + (r-s)^2 + 2(k-l)(r-s)\sin(\theta_1-\theta_2)\right]. \qquad \text{(A6)}
\end{aligned}$$

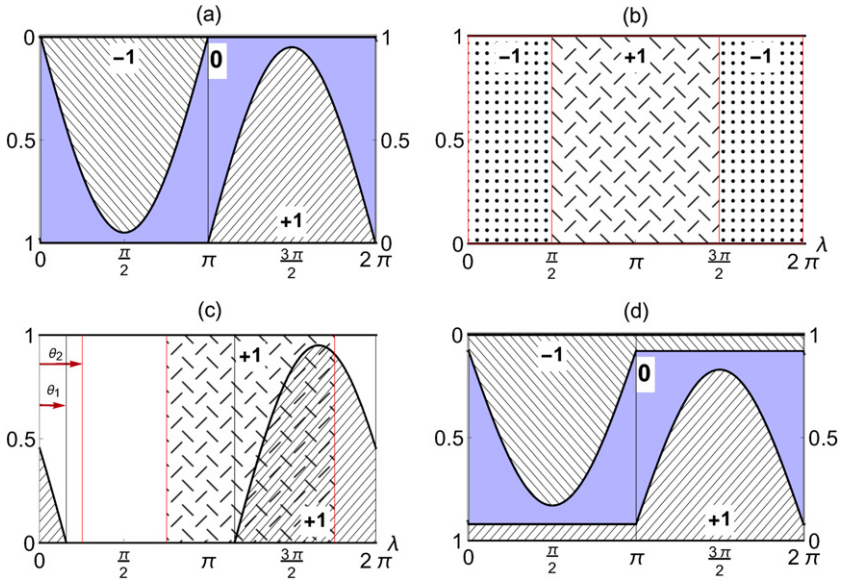

Figure 2. It is useful to picture local probabilities of Alice and Bob as regions on two plots, (a) and (b). If these plots were printed on transparencies and overlapped, one could easily obtain the joint probabilities as regions of specific colors. To reflect the choices of local angles θ_1 and θ_2, the transparencies should be shifted, (c). In case of imperfect visibility, local probabilities of Alice need to be modified, (d).

For the case of different intensities of the local oscillator fields, namely when the moduli of the amplitudes $\alpha_1 \neq \alpha_2$, the formula for the coincidence probabilities is obtainable via a similar calculation, and reads

$$p(k,l;r,s) = \frac{\mathrm{e}^{-(\alpha_1^2+\alpha_2^2)}}{k!\ l!\ r!\ s!}\frac{\alpha_1^{2(k+l-1)}\alpha_2^{2(r+s-1)}}{2^{k+l+r+s+1}}\left[\alpha_1^2(k-l)^2+\alpha_2^2(r-s)^2+2\alpha_1\alpha_2(k-l)(r-s)\sin(\theta_1-\theta_2)\right]. \tag{A7}$$

As we see we have the same sinusoidal dependence on the difference of phases, and the most important fact, from the interferometric point of view, is that the visibility is changed. No new interference effects pop up. This clearly implies that one can repeat the steps for building the LHV model to get one which is a modification of the construction presented in the main text.

A.1. Experiment (a): local hidden variable models

In this section we illustrate the idea behind the construction of our LHV models, based on the model of Larsson in [14]. To do that we first consider a simple scenario, in which the photon numbers detected by Alice and Bob can only be (0, 1), (1, 0) or (0, 0). We label these outcomes -1, $+1$, and 0 respectively. The probabilities we want to replicate are of the form

$$p(-1,-1) = p(+1,+1) = a(1+\sin\theta_{12}) \tag{A8}$$

$$p(+1,-1) = p(-1,+1) = a(1-\sin\theta_{12}) \tag{A9}$$

$$p(0,\pm1) = p(\pm1,0) = \frac{1}{4} - a \tag{A10}$$

$$p(0,0) = 0, \tag{A11}$$

where θ_{12} is the difference of the local parameters θ_1 and θ_2, controlled by each party. A simple LHV model, adapted from the one presented by Larsson [14], leads to the same structure of probabilities, see figure 2 for a pictorial representation.

It assigns probabilities to local events of Alice and Bob via functions P^{A} and P^{B}. The joint probability reads

$$P^{\mathrm{AB}}(i,j|\theta_1,\theta_2) = \frac{1}{2\pi}\int_0^{2\pi} \mathrm{d}\lambda P^{\mathrm{A}}(i|\theta_1,\lambda)P^{\mathrm{B}}(j|\theta_2,\lambda), \tag{A12}$$

where $i,j = \pm1, 0$, and λ is a hidden variable.

Local probabilities P^{A} are

$$P^{\mathrm{A}}(\pm 1|\theta_1,\lambda) = C|\sin(\theta_1-\lambda)|h(\pm\sin(\theta_1-\lambda)), \tag{A13}$$

$$P^{\mathrm{A}}(0|\theta_1,\lambda) = 1 - P^{\mathrm{A}}(+1|\theta_1,\lambda) - P^{\mathrm{B}}(-1|\theta_1,\lambda), \tag{A14}$$

where $h(x)$ is the Heaviside function and $0 \leqslant A \leqslant 1$. For Bob's observations we have

$$P^{\mathrm{B}}(\pm 1|\theta_2,\lambda) = h(\mp\cos(\theta_2-\lambda)), \tag{A15}$$

Note that this means that, in contrast to the quantum predictions, Bob sees no 0 events. This issue is fixed by swapping the roles of Alice and Bob according to a coin toss, i.e. taking the equal mixture of the model presented above and the one with $P^{\mathrm{A}} \leftrightarrow P^{\mathrm{B}}$.

To quickly check the predictions of the model it is enough to consider $P^{\mathrm{AB}}(+1,+1|\theta_1,\theta_2)$ and assume the simplest case of $2\pi > \theta_1 > \theta_2 > \pi$. Then

$$P^{\mathrm{AB}}(+1,+1|\theta_1,\theta_2) = \int_{\theta_2+\pi/2}^{\theta_1+2\pi} \mathrm{d}\lambda \frac{C}{2\pi}\sin(\theta_1-\lambda) = \frac{C}{2\pi}[1+\sin(\theta_{12})]\,. \tag{A16}$$

By performing the integrations for the remaining cases, one can verify that the model yields

$$P^{\mathrm{AB}}(i,j|\theta_1,\theta_2) = \frac{C}{2\pi}[1+ij\,\sin(\theta_{12})], \tag{A17}$$

$$P^{\mathrm{AB}}(i,0|\theta_1,\theta_2) = P^{\mathrm{AB}}(0,i|\theta_1,\theta_2) = \frac{1}{4} - \frac{C}{2\pi}, \tag{A18}$$

where $i,j = \pm 1$. Thus, for $C = 2\pi a$ we obtain the probabilities given in equation (A8)–(A11), *provided that* $a \leqslant \frac{1}{2\pi}$, as otherwise the local probabilities in our model are not well-defined.

A.1.1. Extension to imperfect visibility

Now we would like to extend the basic model so that it covers arbitrary visibility of interference, $\mathcal{V} \leqslant 1$. In other words, we want to replicate the following set of probabilities

$$p(-1,-1) = p(+1,+1) = a(1+\mathcal{V}\,\sin\theta_{12}) \tag{A19}$$

$$p(+1,-1) = p(-1,+1) = a(1-\mathcal{V}\,\sin\theta_{12}) \tag{A20}$$

$$p(0,\pm 1) = p(\pm 1,0) = \frac{1}{4} - a \tag{A21}$$

$$p(0,0) = 0. \tag{A22}$$

To do that, we only need to change the local probabilities $P^{\mathrm{A}}(\pm 1|\theta_1,\lambda)$ (compare with equation (A13))

$$P^{\mathrm{A}}(\pm 1|\theta_1,\lambda) = C\mathcal{V}|\sin(\theta_1-\lambda)|h(\pm\sin(\theta_1-\lambda)) + C\frac{1-\mathcal{V}}{\pi}. \tag{A23}$$

Then, the calculation of the joint probability $P^{\mathrm{AB}}(+1,+1|\theta_1,\theta_2)$ in the case of $2\pi > \theta_1 > \theta_2 > \pi$ gives

$$\begin{aligned} P^{\mathrm{AB}}(+1,+1|\theta_1,\theta_2) &= \int_{\theta_2+\pi/2}^{\theta_2+3\pi/2} \mathrm{d}\lambda C\frac{1-\mathcal{V}}{2\pi^2} + \int_{\theta_2+\pi/2}^{\theta_1+2\pi} \mathrm{d}\lambda \frac{C\mathcal{V}}{2\pi}\sin(\theta_1-\lambda) \\ &= C\frac{1-\mathcal{V}}{2\pi} + \frac{C\mathcal{V}}{2\pi}[1+\sin(\theta_{12})] = \frac{C}{2\pi}(1+\mathcal{V}\,\sin\,\theta_{12}). \end{aligned} \tag{A24}$$

All the other reasoning stays the same as in the basic model.

A.2. Experiment (a): explicit calculation of the sum of probabilities of all submodels $\mathcal{M}_{\mathbf{n}}$

In this section we prove that the probabilities $P(\mathcal{M}_{\mathbf{n}})$ of choosing specific submodels are properly normalized. We have

$$\sum_{\mathbf{n}\in\mathcal{N}\cap\tilde{\mathcal{N}}} P(\mathcal{M}_{\mathbf{n}}) = \sum_{\mathbf{n}\in\mathcal{N}\setminus\mathcal{O}} B(\alpha,\mathcal{M}_{\mathbf{n}}) + \sum_{\mathbf{n}\in\tilde{\mathcal{N}}} 2\pi B(\alpha,\mathcal{M}_{\mathbf{n}}) + \sum_{\mathbf{n}\in\mathcal{O}} \Delta_{\mathbf{n}}, \tag{A25}$$

where

$$\begin{aligned}\sum_{\mathbf{n}\in\mathcal{O}}\Delta_{\mathbf{n}} &= \sum_{k\neq l}\left(p((\mathbf{k},\mathbf{l},0,0)) - \left(\frac{\pi}{2}-1\right)\sum_{c'>d'} B(\alpha,(k,l,c',d'))\right)\\ &\quad + \sum_{r\neq s}\left(p((0,0,\mathbf{r},\mathbf{s})) - \left(\frac{\pi}{2}-1\right)\sum_{c>d} B(\alpha,(c,d,r,s))\right) \qquad \text{(A26)}\\ &= \sum_{\mathbf{n}\in\mathcal{O}} B(\alpha,\mathcal{M}_{\mathbf{n}}) - 4\left(\frac{\pi}{2}-1\right)\sum_{\mathbf{n}\in\tilde{\mathcal{N}}} B(\alpha,\mathcal{M}_{\mathbf{n}}) = \sum_{\mathbf{n}\in\mathcal{O}} B(\alpha,\mathcal{M}_{\mathbf{n}}) - (2\pi-4)\sum_{\mathbf{n}\in\tilde{\mathcal{N}}} B(\alpha,\mathcal{M}_{\mathbf{n}}). \qquad \text{(A27)}\end{aligned}$$

Moreover, notice that

$$\sum_{\mathbf{n}\in\tilde{\mathcal{N}}} B(\alpha,\mathcal{M}_{\mathbf{n}}) = \frac{1}{4}\sum_{\substack{\mathbf{n}\in\mathbb{N}^4\\ c\neq d,\, c'\neq d'}} B(\alpha,\mathcal{M}_{\mathbf{n}}). \tag{A28}$$

Plugging equations (A26) and (A28) into equation (A25) we get

$$\begin{aligned}\sum_{\mathbf{n}\in\mathcal{N}\cap\tilde{\mathcal{N}}} P(\mathcal{M}_{\mathbf{n}}) &= \sum_{\mathbf{n}\in\mathcal{N}\setminus\mathcal{O}} B(\alpha,\mathcal{M}_{\mathbf{n}}) + 2\pi\sum_{\mathbf{n}\in\tilde{\mathcal{N}}} B(\alpha,\mathcal{M}_{\mathbf{n}})\\ &\quad + \sum_{\mathbf{n}\in\mathcal{O}} B(\alpha,\mathcal{M}_{\mathbf{n}}) - (2\pi-4)\sum_{\mathbf{n}\in\tilde{\mathcal{N}}} B(\alpha,\mathbf{n}) = \sum_{\mathbf{n}\in\mathbb{N}^4} B(\alpha,\mathbf{n}) = 1. \qquad \text{(A29)}\end{aligned}$$

A.3. Experiment (a): threshold intensity of local oscillators for the validity of the LHV model for the TWC scheme

In this section we prove that if $\alpha^2 < 0.87$, the probabilities of choosing a specific submodel $P(\mathcal{M}_{\mathbf{n}})$ are non-negative. To do that, we only need to consider $\mathbf{n_0}\in\mathcal{O}$, for which $P(\mathcal{M}_{\mathbf{n_0}}) = \Delta_{\mathbf{n_0}}$. Let us fix $\mathbf{n_0} = (k,l,0,0)$, $k\neq l$, as the reasoning for $\mathbf{n_0} = (0,0,r,s)$ is fully analogous. We need to check the conditions in which

$$\Delta_{\mathbf{n_0}} = B(\alpha,(\mathbf{k},\mathbf{l},0,0)) - \left(\frac{\pi}{2}-1\right)\sum_{c'>d'} B\left(\alpha,(k,l,c',d')\right) \geqslant 0. \tag{A30}$$

We plug the definition of the function $B(\alpha,\mathbf{n})$ from the main text into (A30) and obtain, after some transformations,

$$\Delta_{\mathbf{n_0}} = \frac{\mathrm{e}^{-2\alpha^2}2^{-k-l-3}\left(\alpha^2\right)^{k+l-1}\left(-(\pi-2)\mathrm{e}^{\alpha^2}\left(\alpha^2+(k-l)^2\right)+(\pi-2)I_0\left(\alpha^2\right)(k-l)^2+4(k-l)^2\right)}{k!l!}. \tag{A31}$$

It is easy to see that the condition $\Delta_{\mathbf{n_0}} \geqslant 0$ is equivalent to

$$-(\pi-2)\mathrm{e}^{\alpha^2}\left(\alpha^2+(k-l)^2\right)+(\pi-2)I_0\left(\alpha^2\right)(k-l)^2+4(k-l)^2 \geqslant 0. \tag{A32}$$

As the Bessel function I_0 satisfies $I_0\left(\alpha^2\right) \geqslant 1$, the inequality (A32) can be approximated by a slightly stricter

$$\begin{aligned} &-(\pi-2)\mathrm{e}^{\alpha^2}\left(\alpha^2+(k-l)^2\right)+(\pi-2)(k-l)^2+4(k-l)^2 \\ &=\left((\pi-2)\left(-\mathrm{e}^{\alpha^2}\right)+\pi+2\right)(k-l)^2-(\pi-2)\alpha^2\,\mathrm{e}^{\alpha^2}\geqslant 0. \end{aligned} \tag{A33}$$

For $\alpha<1$, the coefficient $\left((\pi-2)\left(-\mathrm{e}^{\alpha^2}\right)+\pi+2\right)$ standing in front of $(k-l)^2$ is positive. This means that the critical case we need to consider is $(k-l)^2=1$. Thus, we arrive at

$$\left((\pi-2)\left(-\mathrm{e}^{\alpha^2}\right)+\pi+2\right)-(\pi-2)\alpha^2\,\mathrm{e}^{\alpha^2}\geqslant 0. \tag{A34}$$

It can be shown that the inequality (A34) is satisfied for

$$\alpha^2 \leqslant W\left(\frac{2e+e\pi}{\pi-2}\right)-1\approx 0.87, \tag{A35}$$

where W denotes the Lambert W function ($W(z)$ returns the principal solution for w in $z=we^w$).

Appendix B. Experiment (b): threshold intensity for the validity of the partial LHV model for the GPY scheme

The presented model definitely reproduces all probabilities of events other than (0, 0, 0, 1), (0, 0, 1, 0), (0, 1, 0, 0) and (1, 0, 0, 0). We need to check if the probabilities of the single-photon events can also be recovered. To this end, we need to calculate the sum of all the contributions to these probabilities stemming from the nontrivial submodels. It cannot be greater than the quantum probability for these event, but can be lower since the difference can be compensated by the trivial models. This gives the following consistency condition

$$\begin{aligned} \Delta_{(0,0,0,1)}(\alpha^2,\gamma) &= p(0,0,0,1)-(\pi-2)\sum_{\text{relevant submodels}} A(\alpha^4+c_1\gamma^2) \\ &= \frac{\alpha^2}{2}-\frac{1}{48}(\pi-2)\left(2\alpha^8+3\alpha^6+6\alpha^4\left(\gamma^2+2\right)+12\alpha^2\gamma^2+12\gamma^2\right)\geqslant 0. \end{aligned} \tag{B1}$$

Obviously a similar condition could be presented for other single-photon events. However, the one above is the most strict of them all.

Under the assumption $\gamma=\alpha^2$, the condition (B1) simplifies to

$$\alpha^2 \geqslant \frac{1}{24}(\pi-2)\alpha^4\left(8\alpha^4+15\alpha^2+24\right). \tag{B2}$$

It is satisfied for approximately $\alpha^2<0.58$.

Finally, notice that the value of $\Delta_{(0,0,0,1)}(\alpha^2,\gamma)$ given by equation (B1) decreases with the growth of γ. Thus, the model works for all $\gamma\leqslant\alpha^2<0.58$. Of course, this not the full range of the model in the parameter space of α and γ.

B.1. Experiment (b): quantum probabilities of four-photon events registered in the GPY scheme

In this section, we are going to calculate the probability of detecting of detecting k, l, r, s photons respectively in modes c_1, d_1, c_2, d_2, in the (b) configuration of the experimental setup outlined in the main text. It is given by:

$$P(k,l;r,s)=\mathrm{e}^{-(\alpha_1^2+\alpha_2^2)}(1-\gamma^2)\left|\sum_{q=0}^{k}\sum_{p=0}^{r}\sum_{t=0}^{N}\binom{k}{q}\binom{l}{q'}\binom{r}{p}\binom{s}{p'}\frac{\gamma^t(-1)^{q+p}\alpha_1^{k+l-t}\alpha_2^{r+s-t}t!}{\sqrt{2^{klrs}}\sqrt{k!l!r!s!}}\right|^2, \tag{B3}$$

where the upper bound in the last sum, $N=\min(k+l,r+s)$, is a condition imposed by the expansion of the twin beam state in the Fock basis.

The table below gives probabilities of the *class 1* events reproduced by the LHV model in the main text.

Events	Probabilities divided by $P(0,0,0,0) = e^{-2\alpha^2}(1-\gamma^2)$	$\{A(\mathbf{n})/P(0,0,0,0), c_1(\mathbf{n}), c_2(\mathbf{n})\}$
$\begin{Bmatrix}(0&1&0&1)\\(1&0&1&0)\end{Bmatrix}$	$\frac{1}{4}\left(\alpha^4+2\alpha^2\gamma\,\cos(\theta_1+\theta_2)+\gamma^2\right)$	$\left\{\frac{1}{4},\,2,\,1\right\}$
$\begin{Bmatrix}(0&1&0&2)\\(0&2&0&1)\\(1&0&2&0)\\(2&0&1&0)\end{Bmatrix}$	$\frac{1}{16}\alpha^2\left(\alpha^4+4\gamma\left(\alpha^2\,\cos(\theta_1+\theta_2)+\gamma\right)\right)$	$\left\{\frac{a^2}{16},\,4,\,4\right\}$
$\begin{Bmatrix}(0&1&0&3)\\(0&3&0&1)\\(1&0&3&0)\\(3&0&1&0)\end{Bmatrix}$	$\frac{1}{96}\alpha^4\left(\alpha^4+6\alpha^2\gamma\,\cos(\theta_1+\theta_2)+9\gamma^2\right)$	$\left\{\frac{a^4}{96},\,6,\,9\right\}$
$\begin{Bmatrix}(0&1&1&0)\\(1&0&0&1)\end{Bmatrix}$	$\frac{1}{4}\left(\alpha^4-2\alpha^2\gamma\,\cos(\theta_1+\theta_2)+\gamma^2\right)$	$\left\{\frac{1}{4},\,-2,\,1\right\}$
$\begin{Bmatrix}(0&1&1&2)\\(1&0&2&1)\\(1&2&0&1)\\(2&1&1&0)\end{Bmatrix}$	$\frac{1}{32}\alpha^4\left(\alpha^4+2\alpha^2\gamma\,\cos(\theta_1+\theta_2)+\gamma^2\right)$	$\left\{\frac{a^4}{32},\,2,\,1\right\}$
$\begin{Bmatrix}(0&1&2&0)\\(0&2&1&0)\\(1&0&0&2)\\(2&0&0&1)\end{Bmatrix}$	$\frac{1}{16}\alpha^2\left(\alpha^4+4\gamma\left(\gamma-a^2\,\cos(\theta_1+\theta_2)\right)\right)$	$\left\{\frac{a^2}{16},\,-4,\,4\right\}$
$\begin{Bmatrix}(0&1&2&1)\\(1&0&1&2)\\(1&2&1&0)\\(2&1&0&1)\end{Bmatrix}$	$\frac{1}{32}\alpha^4\left(\alpha^4-2\alpha^2\gamma\,\cos(\theta_1+\theta_2)+\gamma^2\right)$	$\left\{\frac{a^4}{32},\,-2,\,1\right\}$
$\begin{Bmatrix}(0&1&3&0)\\(0&3&1&0)\\(1&0&0&3)\\(3&0&0&1)\end{Bmatrix}$	$\frac{1}{96}\alpha^4\left(\alpha^4-6\alpha^2\gamma\,\cos(\theta_1+\theta_2)+9\gamma^2\right)$	$\left\{\frac{a^4}{96},\,-6,\,9\right\}$

The LHV model does not reproduce the following probabilities of events that belong to the (2 & 2) subspace.

Events	Probabilities divided by $P(0,0,0,0) = e^{-2\alpha^2}(1-\gamma^2)$
$\begin{Bmatrix}(0&2&1&1)\\(1&1&0&2)\\(1&1&2&0)\\(2&0&1&1)\end{Bmatrix}$	$\frac{1}{32}\left(\alpha^8-4\alpha^4\gamma^2\,\cos(2(\theta_1+\theta_2))+4\gamma^4\right)$
$\begin{Bmatrix}(0&2&0&2)\\(2&0&2&0)\end{Bmatrix}$	$\frac{1}{64}\left(\alpha^8+16\alpha^4\gamma^2+4\alpha^4\gamma^2\,\cos(2(\theta_1+\theta_2))+8\alpha^2\gamma\left(\alpha^4+2\gamma^2\right)\cos(\theta_1+\theta_2)+4\gamma^4\right)$
$\begin{Bmatrix}(0&2&2&0)\\(2&0&0&2)\end{Bmatrix}$	$\frac{1}{64}\left(\alpha^8+16\alpha^4\gamma^2+4\alpha^4\gamma^2\,\cos(2(\theta_1+\theta_2))-8\alpha^2\gamma\left(\alpha^4+2\gamma^2\right)\cos(\theta_1+\theta_2)+4\gamma^4\right)$
$\{(1\quad 1\quad 1\quad 1)\}$	$\frac{1}{16}\left(\alpha^8+4\alpha^4\gamma^2\,\cos(2(\theta_1+\theta_2))+4\gamma^4\right)$

Appendix C. CGLMP inequality for four outcomes per observer

The CGLMP inequality (see reference [16]) of the main manuscript) is a Bell inequality for a scenario with two observers, two settings per observer and arbitrary number of local outcomes. We utilize the case of four outcomes per observer, for which the inequality reads:

$$\sum_{k=0,1}\left(1-\frac{2k}{3}\right)\big[p(a=b+k|11)+(a=b-k-1|21)+p(a=b+k|22)$$
$$+p(a=b-k|12)-p(a=b-k-1|11)-p(a=b+k|21)$$
$$-p(a=b-k-1|22)-p(a=b+k+1|12)\big]\leqslant 2, \tag{C1}$$

where the convention is that the local outcomes a and b for Alice and Bob take values $a, b = 0, 1, 2, 3$, and the settings are labeled by numbers 1, 2. For example the expression $p(a = b + k|11)$ denotes the probability that the outcomes of Alice and Bob fulfill $a - b = k$ for the choice of first setting at each side.

The probabilities for the $(2\,\&\,0)$ and $(0\,\&\,2)$ events (divided by $P(0,0,0,0)$) are given by:

$$P(2,0,0,0) = P(0,2,0,0) = P(0,0,2,0) = P(0,0,0,2) = \frac{\alpha^4}{8}, \tag{C2}$$

$$P(1,1,0,0) = P(0,0,1,1) = \frac{\alpha^4}{4}. \tag{C3}$$

Appendix D. A simple calculation of *CH* inequality violation by on/off version of the TWC experiment (a) for very weak local oscillators

In this section we show the *method* of the derivation of the probabilities appearing in equation (10) of the main text. We present this for an approximation in which the coherent local oscillator fields are replaced by their first two terms. Thus what we present here is just illustrative. We want to avoid unnecessary technicalities.

For simplicity we take the single photon state as $\frac{1}{\sqrt{2}}(b_1^\dagger + b_2^\dagger)$. We have the following initial state:

$$\frac{1}{\sqrt{2}}(b_1^\dagger + b_2^\dagger)\frac{1}{1+\alpha^2}(1+\alpha_1 a_1^\dagger)(1+\alpha_2 a_2^\dagger)|\Omega\rangle. \tag{D1}$$

When the state in (D1) impinges on the beamsplitters of transitivity T, and reflectively R, it transforms to

$$\frac{1}{\sqrt{2}}\left(\sqrt{T}d_1^\dagger + \mathrm{i}\sqrt{R}c_1^\dagger + \sqrt{T}d_2^\dagger + \mathrm{i}\sqrt{R}c_2^\dagger\right)\frac{1}{1+\alpha^2}\left[1+\alpha_1(\sqrt{T}c_1^\dagger + \mathrm{i}\sqrt{R}d_1^\dagger)\right]\left[1+\alpha_2(\sqrt{T}c_2^\dagger + \mathrm{i}\sqrt{R}d_2^\dagger)\right)\Big]|\Omega\rangle. \tag{D2}$$

The probability $P(A',B')$ is related to the amplitude of detecting a photon in both detectors D_{d_1} and D_{d_2}, namely to the amplitude $\frac{1}{\sqrt{2}(1+\alpha^2)}\left(\sqrt{T}\mathrm{i}\sqrt{R}\alpha_1 + \sqrt{T}\mathrm{i}\sqrt{R}\alpha_2\right)$. That gives the probability $P(A',B') = \frac{TR}{2}\frac{|\alpha_1+\alpha_2|^2}{(1+\alpha^2)^2}$.

The event A (B) is defined as the firing of any local detector when the local oscillator is off, that gives the trivial probabilities $P(A) = 1/2 = P(B)$ and $P(A,B) = 0$. While, the probability of the event pair $P(A,B')$ is related to the final state

$$\frac{1}{\sqrt{2}}\left(b_1^\dagger + \sqrt{T}d_2^\dagger + \mathrm{i}\sqrt{R}c_2^\dagger\right)\frac{1}{\sqrt{1+\alpha^2}}\left[1+\alpha_2(\sqrt{T}c_2^\dagger + \mathrm{i}\sqrt{R}d_2^\dagger)\right]|\Omega\rangle. \tag{D3}$$

The amplitude of $b_1^\dagger d_2^\dagger|\Omega\rangle$ is $\frac{\mathrm{i}}{\sqrt{2}}\frac{\sqrt{R}\alpha_2}{\sqrt{1+\alpha^2}}$. Thus, $P(A,B') = \frac{R\alpha^2}{2(1+\alpha^2)}$ and so is $P(A',B)$.

We take the left-hand side *CH* inequality

$$-1 \leqslant P(A,B) + P(A,B') + P(A',B) - P(A',B') - P(A) - P(B) = CH \leqslant 0, \tag{D4}$$

and put the values of the probabilities, results: $0 + \frac{\alpha^2}{1+\alpha^2}R - \frac{1}{2}TR|\alpha_1+\alpha_2|^2\frac{1}{(1+\alpha^2)^2} - 1/2 - 1/2$. We choose the phases of the coherent states to be identical to get $\frac{\alpha^2}{1+\alpha^2}R - 2TR\alpha^2\frac{1}{(1+\alpha^2)^2} - 1 = \frac{\alpha^2}{1+\alpha^2}R\left(1 - 2T\frac{1}{1+\alpha^2}\right) - 1$, which obviously can be less that -1, with a proper choice of T. The *CH* inequality will be violated when $T > \frac{1+\alpha^2}{2} > \frac{1}{2}$.

Note that the situation with balanced beamsplitters, $T = 1/2$, does not violate the *CH* inequality.

To get the formulas used in the main text, which are for full coherent states of the local oscillators, only minor modifications of the above are needed. In situation (b) the calculation follows a similar path.

Appendix E. Comparison of Clauser–Horne inequality for higher number of photon detection

In this section, we will show that for the two-mode squeezed vacuum state the maximal violation of Clauser–Horne inequality is substantially low if one considers the photodetection event, in which two photons have been detected in mode d_j and no photon in mode c_j.

When both the observers are using the 'on' settings, then the joint probability, $P(A',B')$, is given by,

$$P(A',B') = |_{c_1,d_1,c_2,d_2}\langle 0,2,0,2|\Psi\rangle|^2 = \mathrm{e}^{-2\alpha^2}\left(1-\gamma^2\right)\left(\frac{1}{2}\alpha^4(1-T)^2 - 2\alpha^2\gamma(1-T)T + \gamma^2T^2\right)^2, \tag{E1}$$

where $|\Psi\rangle = |\alpha\,\mathrm{e}^{\mathrm{i}\theta_1}\rangle_{a_1}|\sigma_v\rangle_{b_1,b_2}|\alpha\,\mathrm{e}^{\mathrm{i}\theta_2}\rangle_{a_2}$. We have assumed that the intensity of the local oscillator and the transmittivity of the tunable local beamsplitters are the same for both Alice and Bob for the 'on' settings,

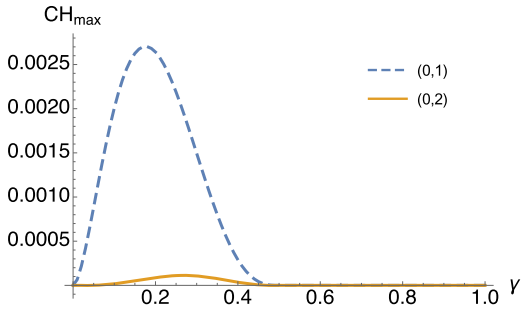

Figure 3. Plot of optimal *CH* violation $CH_{\max}$ as a function of γ, for our proposed measurement settings, given in section 4.2, for two symmetric events namely $(0,1)$ and $(0,2)$. By $(0,x)$, we mean no photon detected in mode c_j and $x \in \{1,2\}$ number of photon(s) detected in mode d_j, for both $j = 1,2$.

and $\theta_1 = -\theta_2$. Similarly the other probabilities are $P(A,B') = P(A',B) = \mathrm{e}^{-\alpha^2}\gamma^4\left(1-\gamma^2\right)T^4$, and $P(A,B) = P(A) = P(B) = \gamma^4\left(1-\gamma^2\right)$.

An optimization of *CH* expression, over T and α^2, for each γ has been plotted in figure 3 by the orange solid curve. The blue dashed line is the same optimal *CH* expression for the other event described in section 4.2. This two plots show that in order to confirm the non-classical feature of the squeezed vacuum state one should not consider the other set of photodetection events.

ORCID iDs

Tamoghna Das https://orcid.org/0000-0002-8074-6720
Marcin Karczewski https://orcid.org/0000-0002-9120-3377
Antonio Mandarino https://orcid.org/0000-0003-3745-5204
Marcin Markiewicz https://orcid.org/0000-0002-8983-9077
Bianka Woloncewicz https://orcid.org/0000-0002-4039-9146
Marek Żukowski https://orcid.org/0000-0001-7882-7962

References

[1] Bohr N 1928 The quantum postulate and the recent development of atomic theory *Nature* **121** 580–90
[2] Walls D F and Milburn G J 2007 *Quantum Optics* (Berlin: Springer)
[3] Tan S M, Walls D F and Collett M J 1991 *Phys. Rev. Lett.* **66** 252
[4] Auletta G, Fortunato M and Parisi G 2012 *Quantum Mechanics* (Cambridge: Cambridge University Press)
[5] Grangier P, Potasek M J and Yurke B 1988 *Phys. Rev.* A **38** 3132
[6] Dirac P A M 1927 *Proc. R. Soc.* A **114** 243 Containing papers of a mathematical and physical character
[7] Susskind L and Glogower J 1964 *Phys. Phys. Fiz.* **1** 49
[8] Pegg D T and Barnett S M 1989 *Phys. Rev.* A **39** 1665
[9] Puentes G, Lundeen J S, Branderhorst M P A, Coldenstrodt-Ronge H B, Smith B J and Walmsley I A 2009 *Phys. Rev. Lett.* **102** 080404
[10] Donati G, Bartley T J, Jin X-M, Vidrighin M-D, Datta A, Barbieri M and Walmsley I A 2014 *Nat. Commun.* **5** 5584
[11] Thekkadath G S *et al* 2020 *Phys. Rev.* A **101** 031801
[12] Wallentowitz S and Vogel W 1996 *Phys. Rev.* A **53** 4528
[13] Demkowicz-Dobrzański R, Jarzyna M and Kołodyński J 2015 *Chapter Four-Quantum Limits in Optical Interferometry* (*Progress in Optics* vol 60) (Amsterdam: Elsevier) http://sciencedirect.com/science/article/pii/S0079663815000049
[14] Larsson J-Å 1999 *Phys. Lett.* A **256** 245
[15] Aerts S, Kwiat P, Larsson J-Å and Żukowski M 1999 *Phys. Rev. Lett.* **83** 2872
[16] Collins D, Gisin N, Linden N, Massar S and Popescu S 2002 *Phys. Rev. Lett.* **88** 040404
[17] Gruca J, Laskowski W and Żukowski M 2012 *Phys. Rev.* A **85** 022118
[18] Kuzmich A, Walmsley I A and Mandel L 2000 *Phys. Rev. Lett.* **85** 1349
[19] Hardy L 1994 *Phys. Rev. Lett.* **73** 2279
[20] van Enk S J 2005 *Phys. Rev.* A **72** 064306
[21] Hessmo B, Usachev P, Heydari H and Björk G 2004 *Phys. Rev. Lett.* **92** 180401
[22] Babichev S A, Appel J and Lvovsky A I 2004 *Phys. Rev. Lett.* **92** 193601
[23] Cooper J J and Dunningham J A 2008 *New J. Phys.* **10** 113024
[24] Lombardi E, Sciarrino F, Popescu S and De Martini F 2002 *Phys. Rev. Lett.* **88** 070402
[25] Vanderwerf D 2017 *The Story of Light Science: From Early Theories to Today's Extraordinary Applications* (Berlin: Springer) https://books.google.it/books?id=2BUwDwAAQBAJ
[26] Clauser J F and Horne M A 1974 *Phys. Rev.* D **10** 526
[27] Das T, Karczewski M, Mandarino A, Markiewicz M, Woloncewicz B and Żukowski M 2021 *New J. Phys.* **23** 073042

[28] Banaszek K and Wódkiewicz K 1999 *Phys. Rev. Lett.* **82** 2009
[29] Loudon R 2000 *The Quantum Theory of Light* (Oxford: Oxford University Press)
[30] Reid M D and Walls D F 1986 *Phys. Rev.* A **34** 1260
[31] Clauser J F, Horne M A, Shimony A and Holt R A 1969 *Phys. Rev. Lett.* **23** 880
[32] Santos E 1992 *Phys. Rev. Lett.* **68** 894
[33] Żukowski M, Wieśniak M and Laskowski W 2016 *Phys. Rev.* A **94** 020102
[34] Greenberger D M, Horne M A and Zeilinger A 1995 *Phys. Rev. Lett.* **75** 2064
[35] Peres A 1995 *Phys. Rev. Lett.* **74** 4571
[36] Brask J B, Chaves R and Brunner N 2013 *Phys. Rev.* A **88** 012111
[37] Vaidman L 1995 *Phys. Rev. Lett.* **75** 2063
[38] Aharonov Y and Vaidman L 2000 *Phys. Rev.* A **61** 052108
[39] Gerry C C 1996 *Phys. Rev.* A **53** 4583
[40] Ashhab S, Maruyama K and Nori F 2007 *Phys. Rev.* A **75** 022108
[41] Ashhab S, Maruyama K and Nori F 2007 *Phys. Rev.* A **76** 052113
[42] Abiuso P, Kriváchy T, Boghiu E-C, Renou M-O, Pozas-Kerstjens A and Acín A 2021 arXiv:2108.01726
[43] Ou Z Y and Mandel L 1988 *Phys. Rev. Lett.* **61** 50
[44] Popescu S, Hardy L and Żukowski M 1997 *Phys. Rev.* A **56** R4353
[45] Franson J D 1989 *Phys. Rev. Lett.* **62** 2205
[46] Das T, Karczewski M, Mandarino A, Markiewicz M, Woloncewicz B and Żukowski M 2022 *New J. Phys.* **24** 038001